Characterization of SHORT VEGETATIVE PHASE (SVP)

Li Dan

NATIONAL UNIVERSITY OF SINGAPORE

2010

LI DAN

A THESIS SUBMITTED

FOR THE PHD DEGREE

DEPARTMENT OF BIOLOGICAL SCIENCES

NATIONAL UNIVERSITY OF SINGAPORE

2010

Acknowledgements

I would like to truly express my deepest thanks and appreciation for the invaluable guidance, advice and inspiration of my supervisor, Dr Yu Hao and co-supervisor, Associate Professor Loh Chiang Shiong.

I sincerely thank all the current and former labmates in the Plant Functional Genomics Laboratory for creating a helpful working environment.

Lastly, I appreciate the administrative and technical supports from staffs at the Department of Biological Sciences and Temasek Life Science Laboratory. I am also grateful for the research scholarship awarded by the National University of Singapore.

LI DAN

Table of Contents

List of Tables

List of Figures

CHAPTER 1

Abstract

Floral transition is one of the most drastic changes occurring during *Arabidopsis* life cycle. Genetic analysis of flowering time mutants has led to a model describing four integrated flowering time pathways. Vernalization and photoperiod pathways mediate the response to environmental cues, while autonomous and gibberellin (GA) pathways mediate the internal signals. *SHORT VEGETATIVE PHASE (SVP)* is a MADS-box transcription factor acting as a floral repressor in flowering. In this study, we localized *SVP* in autonomous and GA pathways, and identified *SOC1* and *FT* as its direct target genes in the control of flowering time. Notably, SVP protein associates with the promoter regions of *SOC1* and *FT* where another potent repressor, FLOWERING LOCUS C (FLC), binds. We further show that the SVP protein consistently interacts with FLC in whole seedlings during vegetative growth, and their function in regulating flowering is mutually dependent. Our results demonstrate that SVP is a central flowering repressor, and that its interaction with FLC governs the expression of floral pathway integrators in response to developmental and environmental signals, thus determining the timing of floral transition.

CHAPTER 2

Literature Review

2.1 The genetic network controlling floral transition in *Arabidopsis thaliana*

Flowering is one of the most important phase changes during the life cycle of higher plants. It is-the switch from vegetative to reproductive growth. Floral transition is the timing of this developmental process and it is particularly susceptible to various factors. Previous studies suggested an intricate network of pathways integrating endogenous and environmental inputs determined the timing of the switch from vegetative to reproductive development in *Arabidopsis*. This process is quantitatively controlled by the convergence of signals from individual pathways on the transcriptional regulation of several floral pathway integrators including *FLOWERING LOCUS T* (*FT*), *LEAFY* (*LFY*), and *SUPPRESSOR OF OVEREXPRESSION OF CONSTANS 1* (*SOC1*) (Blazquez and Weigel, 2000, Kardailsky et al., 1999, Kobayashi et al., 1999, Lee et al., 2000 and Samach et al., 2000). The genetic pathway underlying flowering time of *Arabidopsis thaliana* is further refined in recent years. Natural variation ecotypes of *Arabidopsis* showing various flowering time and genetically engineered early- or late-flowering mutants have been used to elucidate the genes involved in the control of flowering time and the interactions among them. It has been shown that these flowering time genes respond to both internal and environmental cues. Depending on the signals received

by the plant, the flowering genetic pathways can be divided into the vernalization pathway, autonomous pathway, photoperiod pathway and Gibberellin (GA) pathway (Levy and Dean, 1998; Boss *et al.*, 2004; Buski and Frenkel, 2004; Jack, 2004; Putterill *et al.*, 2004).

2.1.1 Photoperiod pathway

Arabidopsis flowers more rapidly under long days (LDs) condition than short days (SDs) condition. This phenomenon suggests that some genes in *Arabidopsis* are involved in recognizing the light signal. Photoreceptors in *Arabidopsis* comprise five phytochromes (*PHYA* to *PHYE*) and two cryptochromes (*CRY1* and *CRY2*) (Thomas and Vince-Prue, 1997). Studies suggested that the red and far-red light are perceived by *PHYs* (Briggs et al., 2001; Quail et al., 1994), while blue light and ultraviolet-A are perceived by CRY1 and CRY2 (Briggs et al., 2001; Ahmad et al., 1993; Lin et al., 1998). The mechanism of ultraviolet-B perception is still unknown. The signal of the photoperiod pathway enters a circadian cycle only after initiation by *PHYA*, *CRY1* and *CRY2*. Downstream genes will be activated if the length of the dark period decreases below a critical level (Levy and Dean. 1998). Interestingly, light quality also affects flowering time, with far-red and blue light promoting flowering while red light inhibiting it (Martinez-Zapater et al., 1994; Guo et al., 1998).

Among the genes located downstream of photoreceptors, *GIGANTEA* (*GI*) and *CONSTANS* (*CO*) have been thoroughly investigated. Mutations of these two genes

result in late flowering phenotype under LDs but have little effect under SDs. *CO* is probably the most important target of *PHYs* and *CRYs*. The *CO* gene has homology to the Zinc-finger domain transcription factor (Putterill et al., 1995). It is regulated by photoreceptors precisely through the light cycle. Previous studies showed that the circadian rhythm of *CO* mRNA was critical for control of flowering via the photoperiod pathway (Valverde et al., 2004), while flowering activation through *CO* is a dosage-dependent process (Putterill et al., 1995). On the other hand, *GIGANTEA* (*GI*) encodes a membrane located protein with six putative membrane-spanning domains, and its expression is also regulated by the circadian clock. It is shown that GI is essential for the maintenance of circadian rhythm. The expression of *LHY* and *CCA1*, which are two other circadian clock-associated genes, is low in the *gi* mutant (Fowler et al., 1999; Park et al., 1999).

2.1.2 Autonomous pathway

Plants require both external environmental factors and internal developmental factors to promote flowering. It is shown that the mutants of *LUMINIDEPENDENS* (*LD*), *FVE*, *FY* and *FCA* cause delay flowering under both LDs and SDs, hence they are placed in the autonomous pathway. The *LD* gene encodes a protein of 953 amino acids with two bipartite nuclear localization motifs. The LD protein contains a glutamine-rich domain, which is homologous to certain transcription factors in other species. Moreover, *LD* may involve in light quality perception, since *ld* mutant plants

are insensitive to light with a high red/far-red ratio (Lee et al., 1994). The FCA protein includes two RNA-recognizing motifs and a WW (two conserved tryptophan [W]) protein interaction domain. This structure strongly suggests that *FCA* may function in the posttranscriptional process (Macknight et al., 1997). The *FCA* self-regulates its expression through alternatively splicing, which will generate α, β, γ and δ variants. However, only γ mRNA encodes functional FCA protein. This is consistent with the fact that only the constitutive expression of γ mRNA causes early flowering in transgenic plants (Macknight et al., 2002). FVE is a putative retinoblastoma-associated protein. It has bee reported that FVE is part of a protein complex performing histone deacetylation function in order to repress *FLOWERING LOCUS C* (*FLC*), which is a key factor integrating autonomous and vernalization signals (Israel et al., 2004). Additionally, *FPA* and *FY* genes act redundantly to repress *FLC*, through which plants ensure the developmental switch-on of flowering (Yushibumi, 2004; Schomburg et al., 2001).

2.1.3 Vernalization pathway

Arabidopsis winter annual ecotypes flower earlier after extreme cold treatment (vernalization), which helps plants flower in time after prolonged cold in winter. This pathway performs redundantly with the autonomous pathway. Both of them activate flowering mainly through the repression of *FLOWERING LOCUS C* (*FLC*), a member of MADS-domain protein family. *FLC* is expressed predominantly in shoot

and root apices but is also detectable in leaf tissues (He et al., 2003; Michaels and Amasino, 1999). An expression study of *FLC* with tissue-specific promoters demonstrated that *FLC* expression is required in both leaf and shoot apical meristem tissues for the full repression of flowering (Searle et al., 2006). The abundance of *FLC* mRNA is reduced by vernalization (Michaels et al., 1999), whereas *FLC* is not necessary for vernalization response since other *FLC*-independent vernalization pathways that may regulate *AGL24* and *AGL19* have been reported in recent years (Michaels et al., 2003; Schonrock et al., 2006). The *FRIGIDA* (*FRI*) gene is a powerful positive regulator of *FLC*. The coiled-coil domains of FRI protein may be the regulatory component. Allelic variation at the *FRI* locus confers the flowering differences among *Arabidopsis* ecotypes (Johanson et al., 2000). Moreover, mutation of *FLC* is epistatic to dominant alleles of *FRI*. Similarly, overexpression of *FLC* showed late flowering phenotype in the absence of an active *FRI* allele (Michaels et al., 1999).

There are several genes which have been specially located in the vernalization pathway, namely *VRN1*, *VRN2* and *VRN3* (Chandler et al., 1996). VRN1 protein may bind DNA in a non–sequence-specific manner and functions in constant repression of *FLC*. Overexpression of *VRN1* also reveals a vernalization-independent function for *VRN1*, mediated mainly through the floral pathway integrator *FT* (Levy et al., 2002). *VRN2* encodes a nuclear-localized zinc finger protein with homology to Polycomb Group (PcG) proteins in *Drosophila* and maintains *FLC* repression after vernalization (Gendall et al., 2001). In addition, another PcG protein, *VIP4* has been found to be an

activator of *FLC* (Zhang et al., 2002).

The observation that *FLC* repression is maintained through mitotic cell divisions in plants experiencing the cold treatment suggests an epigenetic mechanism of vernalization. Many components in vernalization pathways have been found to cause remodeling of *FLC* chromatin structure and histone modifications related to heterochromatin formation. These regulators includes *VRN2*, *LIKE HP1* (*LHP1*) and *VERNALIZATION INDEPENDENTS3 (VIN3*). *LHP1* encodes a protein showing high homology to HETEROCHROMATIN PROTEIN1 (HP1) in animals, which is able to stabilize the histone repressive methylation and recruit other complexes for heterochromatin formation (Bannister et al., 2001; Mylne et al., 2006). VIN3 is a plant-specific DNA-binding protein involved in histone deacetylation at *FLC*. However, *VIN3* itself is not sufficient to initiated the vernalization response since it is expressed only after an extended cold treatment (Sung and Amasino 2004).

2.1.4 Gibberellin (GA) pathway

Gibberellin (GA) is a major flowering promoter for *Arabidopsis* under SDs. Besides flowering, this class of plant hormones participates in seed germination and cell elongation during plant development, including (Finkelstein and Zeevaart, 1994). The *ga1-3* mutant, which is severely defective in gibberellin synthesis, never flowers under SDs, while it only slightly delays flowering under LDs (Wilson et al., 1992). GA promotes flowering partly through the activation of *LFY* because the constitutive

expression of *LFY* is able to restore flowering of *ga1-3* mutants in SDs (Blazquez et al., 1998). Moreover, several negative regulators, such as *RGA* and *GAI*, are involved in the GA signal transduction. They are highly homologous and may function redundantly. The *rga gai* double mutant can completely rescue these defects in *ga1-3*, although the *gai* and *rga* single mutant have limited effect on suppressing the flowering defects in the GA-deficiency mutant *ga1-3*. This suggests that *RGA* and *GAI* are repressors of the GA pathway in the control of flowering time. These genes also participate in feedback-control of GA biosynthesis. *SPY* is another repressor of the GA pathway, which is acting upstream of *RGA* and *GAI*. *SPY* activates these two genes probably through the GlcNAc modification because *SPY* is predicted to encode an *O*-linked N-acetylglucosamine (GlcNAc) transferase.

Thus the photoperiod and vernalization pathways respond to environmental signals, such as the duration of light periods and low temperatures. The autonomous pathway mediates flowering by monitoring developmental stages of plants, while the gibberellin (GA) pathway accelerates flowering in short days (SDs). In addition, another genetic pathway has been suggested to monitor the environmental cues relevant to the change of light quality and ambient temperature (Blazquez et al., 2003, Cerdan and Chory, 2003, Halliday et al., 2003 and Simpson and Dean, 2002).

2.2 Floral integrators

Previous research work provides evidence that the above mentioned four genetic

pathways converge on some key genes in order to integrate inputs from the different flowering cascades, and they are called floral pathway integrators. *LEAFY* (*LFY)*, *FLOWERING LOCUS T* (*FT*), *FLOWER LOCUS C (FLC)* and *SOC1* have been identified as such integrators in *Arabidopsis* (Simpson and Dean, 2002).

2.2.1 *LEAFY* (*LFY*)

The *LFY* gene encodes a plant specific transcription factor, which is localized primarily in the nucleus. *LFY* has dual roles in flower development, as a flowering time promoter and a floral meristem identity gene (Parcy et al., 1998; Weigel et al., 1992). The LFY protein can be transferred to different layers of floral meristem through plasmodesmata. The cell-cell movement provides a potential mechanism to ensure complete conversion of a meristem into a flower (Sessions et al., 2000). The confirmed functions of *LFY* protein are positive regulation of *AGAMOUS* (*AG*) and *APETALA1* (*AP1*) through *cis*-elements binding (Busch et al., 1999; Lohmann et al., 2001). Constitutive expression of *LFY* causes early flowering while *lfy* mutants shows slightly delay flowering and produce a flower-like shoot structure, which is related with the role of *LFY* on floral meristem specification (Weigel et al., 1992). The overexpression of *LFY* partially rescues the *co* mutant phenotype suggests that *LFY* might be the downstream target of *CO*-mediated photoperiod pathway. This has been further proven by the finding that the increase of *CO* (using inducible CO-GR transgenic plants) promotes *LFY* mRNA expression. Moreover, *CO* may not be a

direct activator of *LFY* because the *LFY* induction by *CO* takes more than 24 hours (Samach et al., 2000). As mentioned in part 2.1.4, *LFY* expression is dramatically reduced in *ga1* mutant under SD condition. GA signals upregulate *LFY* possibly through a *cis*-element in the *LFY* promoter (Blazquez and Weigel 2002). It is noteworthy that this regulatory region does not affect *LFY* induction by the photoperiod pathway. Therefore, GA and photoperiod pathway signals integrate independently at *LFY* (Blazquez and Weigel 2002; Parcy 2005).

2.2.2 *FLOWERING LOCUS T* (*FT*)

The *FT* gene has been simultaneously isolated by activation-tagging and T-DNA insertion screening. *FT* transcripts are detectable in seedlings before floral transition, increasing gradually with vegetative growth. The mRNA expression patterns under LD and SD conditions are subtly different, though both reach a maximum around the period of floral transition. *FT* encodes a 20KDa protein with similarities to phosphatidylethanolamine binding protein (PEBP) and Raf kinase inhibitor protein (RKIP) in animals (Kardailsky et al.; 1999; Kobayashi et al., 1999). FT protein is not able to regulate transcription process unless assembled with FD, a bZIP transcription factor (Abe et al., 2005; Kardailsky et al., 1999). The *FT::GUS* reporter gene shows that *FT* is primarily expressed is the vasculature, while *FD* is found at the shoot apex, suggesting that *FT* mRNA or protein need move from leaf to shoot apical meristem, where it interacts with *FD* to activate *AP1* (Abe et al., 2005; Baurle and Dean, 2006;

Takada and Goto, 2003). This assumption has been partly proven by a recent paper that *FT* fusion protein can move from phloem cells to the apex, acting as a florigen (Corbesier et al., 2007).

FT constitutive expression causes extremely early flowering under both LD and SD conditions, while the *ft* mutant is late flowering under LDs and has slight effect under SDs, implying that *FT* is regulated by the photoperiod pathway. *CO* seems to directly upregulate *FT* expression (Samach et al., 2000). The early flowering of overexpression *CO* transgenic plants can be repressed by mutations in the *FT* gene. The interaction between *CO* and *FT* is also validated by expression of *CO* with different localized promoters. *CO* triggers early flowering in the leaf phloem but not in the shoot apex, indicating that the activation signals of *CO* in leaf need to be transmitted into the apex through a florigen factor, which is possibly *FT* (An et al., 2004; Ayre and Trugeon, 2004). Another well-known regulator of *FT* is *FLC*, which is the convergence point of the autonomous and vernalization pathways. Elevated *FT* expression is found in *flc* mutant. *FLC* represses *FT* transcription mainly in the leaf phloem and delays *FD* upregulation in shoot apex. Chromatin immunoprecipitation demonstrates that *FLC* protein physically binds to the first intron of *FT* and to the promoter region of *FD* (Baurle and Dean, 2006; Searle et al., 2006). GA might also play a role in *FT* induction since the GA-dependent *ebs* mutant derepresses *FT* to promote early flowering phenotype (Gomez-Mena et al., 2001; Pineiro et al., 2003).

2.2.3 *FLOWER LOCUS C (FLC)*

The signals from the vernalization and autonomous pathways converge on a potent repressor of flowering, *FLOWERING LOCUS C* (*FLC*) (Michaels and Amasino, 1999 and Sheldon et al., 1999). *FLC* encodes a MADS-box transcription factor and is widely expressed in the meristem and leaves (Noh and Amasino, 2003and Sheldon et al., 2002). Regulation of *FLC* expression involves epigenetic control of the functional states of its chromatin by multiple factors (Amasino, 2004 and Baurle and Dean, 2006). High expression of *FLC* antagonizes the meristem's competence to respond to promotive floral signals by repressing at least the two floral pathway integrators *FT* and *SOC1*, while the vernalization and autonomous pathways promote flowering by repressing *FLC* expression (Hepworth et al., 2002, Lee et al., 2000, Michaels and Amasino, 1999, Michaels et al., 2005, Sheldon et al., 1999 and Sheldon et al., 2000). Spatial and temporal analysis of FLC regulation has revealed its dual roles in repressing flowering. FLC represses *FT* expression in the leaves and blocks the transport of the systemic flowering signals that contain FT protein from the leaves to the meristem, and FLC also impairs the meristem's response to the flowering signals by inhibiting the expression of *SOC1* and the *FT* cofactor *FD* (Abe et al., 2005, Corbesier et al., 2007, Searle et al., 2006 and Wigge et al., 2005).

2.2.4 *SUPPRESSOR OF CO OVEREXPRESSION 1* (*SOC1*)

SOC1, formerly named *AGAMOUS-LIKE 20* (*AGL20*), consists of seven exons

and six introns. It encodes a typical MADS-domain transcription factor of 214 amino acids, showing 96% identity to a mustard ortholog *MADSA*, which responds to inductive long-day signals (Borner et al., 2000; Lee et al., 2000). Phylogenetic analysis indicates that the most homologous proteins of SOC1 in *Arabidopsis* are AGAMOUS-LIKE 14 (AGL14) and FLC (Lee et al., 2000). *SOC1* was contemporaneously identified as a floral activator using activation tagging and cDNA screening for suppressors of *CO* overexpression (Lee H et al., 2000; Samach et al., 2000). Expression studies showed that *SOC1* transcripts are present in most tissues of *Arabidopsis* seedlings, including root, leaf, shoot apex, etc. The mRNA abundance is temporally upregulated after seed germination. During floral transition, there is a sharp increase of *SOC1* mRNA and strong *SOC1* expression could be found in the inflorescence meristem, after which it was absent from the stage 1 floral meristem, then reappeared in the center of older floral meristem, overlapping the spatial expression pattern of *AG* (Borner et al., 2000; Samach et al., 2000). However, floral organs of the *soc1* mutant normally develop, suggesting that *SOC1* might be a redundant co-factor in floral organogenesis (Borner et al., 2000).

2.2.4.1 *SOC1* is a flowering promoter in *Arabidopsis*

It has been suggested that *SOC1* is a major factor in determination of flowering time. Overexpression of *SOC1* causes extremely early flowering under both LD and SD conditions. Similarly, constitutive expression of the orthologous gene *MADSA* in

the short-day tobacco (*Nicotiana tabacum* Maryland Mammoth) can overcome the photoperiodic barrier of floral induction (Borner et al., 2000). On the other hand, the *soc1* mutant demonstrates significantly delayed flowering, especially under LDs. In the *soc1* mutant without any detectable *SOC1* transcripts, the leaf number is twice as that of wild-type. Whereas, the *soc1* mutant is still responsive to the photoperiod pathway since the mutant flowers earlier under LDs than under SDs (Borner et al., 2000; Lee et al., 2000).

2.2.4.2 *SOC1* integrates all the four flowering pathways in *Arabidopsis thaliana*

Expression studies confirm that *SOC1* mRNA level is promoted after a shift from SDs to LDs, mainly in the shoot apical meristem and leaf primordia (Borner et al., 2000; Samach et al., 2000). *CO* seems to play an essential role in the photoperiodic response of *SOC1*. *SOC1* expression has been examined in a 35*S::CO:GR* inducible system. *SOC1* appears to be one of the immediate targets of *CO*. The translational inhibitor cycloheximide (*CYC*) was also applied to demonstrate that regulation from *CO* to *SOC1* does not require any intermediate protein synthesis (Samach et al., 2000). This result is consistent with the study of the *SOC1::GUS* reporter gene, showing that a 351bp fragment in *SOC1* promoter region is necessary for activation by CO. Although the CO protein might not directly bind to the *SOC1* promoter, CO could recruit other DNA binding co-factors to perform transcriptional regulation through its zinc fingers and CCT domain, which mediate protein-protein

interaction (Hepworth et al., 2002). Genetic data are helpful to further clarify the relation between *CO* and *SOC1*. The *soc1* and *ft* mutants partially suppress the early flowering of overexpression of *CO*, while *ft soc1* double mutations completely eliminate the phenotype, and cause *ft soc1 35S::CO* plants to flower as late as the *co* mutant. Therefore, *SOC1* and *FT* are two major outputs of *CO*-mediated signals and partly independently perform their functions (Hepworth et al., 2002). However, some researchers proposed that *SOC1* may be regulated by *CO* through *FT* since *FT* has a positive effect on *SOC1* expression (Yoo et al., 2005). Additionally, a separate experiment indicates that *FT* is required in phloem for the early activation of *SOC1* at meristem under LDs, possibly in a *FD*-dependent manner (Searle et al., 2006). This interesting idea still needs to be further validated.

One expression study also suggested that *SOC1* expression is more dependent on the autonomous pathway since the autonomous pathway mutants, *fca-1*, *fve-1*, and *fpa-1*, show more reduction of *SOC1* transcripts compared with the photoperiod pathway mutants, *co-2*, *gi-3*, and *ft-1* (Lee et al., 2000). Nevertheless, there is no evidence supporting the direct interaction among *SOC1* and these autonomous pathway factors. As previously mentioned, *FLC* is a key gene which integrates vernalization and autonomous pathways in *Arabidopsis*. It seems that *FLC* acts as an intermediate factor involved in *SOC1* regulation by these two pathways. The investigation of *FLC* and *SOC*1 mRNA levels in each other's loss-of-function mutants show that *FLC* is an upstream repressor of *SOC1* (Lee et al., 2000). *SOC1* is quantitatively induced by vernalization in a *FLC*-dependent manner (Sheldon et al.,

2006). Independent ChIP analysis using different tagging systems indicate that *in vivo* binding of *FLC* protein to the *SOC1* genomic sequence occurs through a CArG box motif, which is recognized specifically by MADS-domain transcription factors (Helliwell et al., 2006; Searle et al., 2006). This result is consistent with the *SOC1::GUS* study and in vitro assay (Hepworth et al., 2002). Moreover, it is believed that *FLC* participants in a protein complex to perform its function as more than one *FLC* polypeptide can be detected in the complex *in vivo*. In support of this finding, *in vitro* gel shift experiments indicate that *FLC* needs to form a homodimer to interact with the CArG box motif in the *SOC1* promoter (Helliwell et al., 2006; Hepworth et al., 2002).

GA treatment accelerates *Arabidopsis* flowering under SDs, and this process is correlated with the increase of *SOC1* expression, implying that GA might be another upstream signal of *SOC1* (Borner et al., 2000; Moon et al., 2003). This regulation is not mediated by *FLC* since GA treatment does not affect *FLC* expression under SDs. In the GA-biosynthetic defective mutant *ga1-3*, *SOC1* expression is lower than in wild-type plants, and exogenous GA treatment promotes both *SOC1* expression and flowering. On the contrary, although *SOC1* expression is reduced in GA-insensitive mutant *gai-1*, exogenous GA treatment can recover neither *SOC1* expression nor the normal flowering phenotype (Moon et al., 2003). In addition, overexpression of *SOC1* is able to bypass the block to flowering in *ga1-3* mutant and the *soc1* mutant is less sensitive to *GA*, suggesting that *SOC1* integrates the *GA* pathway signals although other additional downstream factors may exist (Moon et al., 2003).

2.3 Interaction between floral integrators

2.3.1 *LFY* and *FT*

There is some evidence showing that *LFY* expression is regulated by *FT*, although this regulation might be indirect. *LFY* is ectopically expressed in the apical meristem of transgenic plants overexpressing *FT*, and its expression is reduced in *ft* mutant under LD and SD conditions (Schmid et al., 2003; Kardailsky et al., 1999). However, the *LFY::GUS* reporter gene is normally expressed in leaf primordia of the *ft* mutant (Nillson et al., 1998). The relation between *FT* and *LFY* therefore requires further investigation. In wild-type plants, *LFY* mRNA is not detectable in the shoot apical meristem due to repression by *TERMINAL FLOWER1* (*TFL1*) (Ratcliffe et al., 1998). TFL1 protein is highly homologous to *FT*, but performs the opposite function in flowering time control. These two proteins are functionally exchangeable with a single amino acid conversion (Hanzawa et al., 2005).

2.3.2 *LFY* and *SOC1*

The direct interaction between *LFY* and *SOC1* has been proposed in recent years. It is believed that *LFY* may act at least partially downstream from *SOC1*. The constitutive expression of *SOC1* activates *LFY* in the shoot meristem, producing

solitary flowers from axillary inflorescences (Lee et al., 2000; Mouradov et al., 2002; Parcy 2005). Nevertheless, *LFY* expression is not abolished in the *soc1* mutant, indicating that there are other upstream factors activating *LFY.* Consistent with this hypothesis, overexpression of *SOC1* and *LFY* have additive effects on flowering (Lee et al., 2000). Because *AGL24* also affects *LFY* expression, it has been suggested that *AGL24* is another upstream regulator of *LFY* (Yu et al., 2002). Since *AGL24* and *SOC1* mutually regulate each other's expression (Yu et al., 2002; Michaels et al., 2003), they may function together to control *LFY* expression.

2.3.3 *FT* and *SOC1*

Currently it is widely accepted that *FT* and *SOC1* acts on independent pathways. Although *SOC1* upregulation after a shift from SD to LD conditions is decreased in the *ft* mutant, this difference could be a side effect of the whole flowering-regulatory network (Schmid et al., 2003). Nevertheless, a recently published paper mentioned that FT may recruit FD in order to promote *SOC1* expression at the shoot apical meristem during floral transition (Searle et al., 2006). Moreover, some evidence also implies that *FT* may perform as an intermediate factor between *SOC1* and *CO* (Yoo et al., 2005).

2.4 Floral meristem identity (FMI) genes

Once floral integrators are activated, they regulate downstream floral meristem identity (FMI) genes, which determine the apical meristem fate to produce floral meristems that further develop into flowers with four whorls of floral organs. The appearance of floral meristem identity genes in floral primordia symbolizes the completion of floral transition. In *Arabidopsis*, *APETALA1* (*AP1*), *LFY* and *CAULIFLOWER* (*CAL*) are well studied FMI genes.

2.4.1 *APETALA1* (*AP1*)

Like *LFY*, *AP1* has dual functions during floral development, namely the determinations of floral meristem identity and floral organ identity. *AP1* encodes a MADS-domain transcription factor, which specifies the identity of floral meristem and determines sepal and petal development as a class A gene in *Arabidopsis* (Gustafson-Brown et al., 1994). The *ap1* mutant shows the defects in the floral meristem specification, and constitutive expression of *AP1* results in early flowering (Bowman et al., 1993). *LFY* has been confirmed to act as a direct transcriptional regulator of *AP1* (Wagner et al., 1999). *In situ* data shows that *AP1* is expressed in a sub-domain of the region expressing *LFY* (Mandel et al., 1992). Overexpression of *LFY* significantly promotes *AP1* expression, and *AP1* mRNA can be found in leaf primordia, which is the expression region of *LFY* in wild-type plants. Correspondingly, *AP1* expression is delayed in the *lfy* mutant (Liljegren et al., 1999; Parcy et al., 1998; Ruiz-Garcia et al., 1997; Weigel and Meyerowitz, 1993). In addition, the *LFY:GR*

inducible system and chromatin immunoprecipitation (ChIP) have been applied to demonstrate that *LFY* activates *AP1* through protein binding to the *AP1* promoter region, and this regulation does not require any intermediate translational process (Wagner et al., 1999; William et al., 2004). However, *LFY* is not the only upstream regulator of *AP1* as *FT* is also able to activate *AP1* as mentioned in Section 2.2.2. The *ft lfy* double mutant abolishes *AP1* expression as seen in the *lfy* mutant, suggesting that *FT* and *LFY* controls *AP1* in parallel pathways (Ruiz-Garcia et al., 1997).

2.4.2 *CAULIFLOWER* (*CAL*)

CAL also encodes a putative MADS-domain transcription factor. Phylogenetic analysis indicates that *CAL* and *AP1* are paralogous to each other (Purugganan and Suddith, 1998). The expression patterns of these two genes are quite similar. As expected, the activity of *CAL* appears to be redundant to that of *AP1*. The *CAL* promoter also contains a *LFY* protein binding site (William et al., 2004). However, the meristem identity functions of *CAL* and *AP1* are not entirely equivalent, because *ap1* mutants show signficant flower meristem defects even in the presence of *CAL* while *cal* mutants have no obvious floral phenotypes (references?).. Some studies support that *CAL* and *AP1* act redundantly to upregulate *LFY* to control inflorescence architecture, implying the reciprocal interactions among all the three FMI genes (Ferrandiz et al., 2000).

2.5 Overview of the clarified regulatory network controlling floral transition in *Arabidopsis thaliana*

As mentioned above, four genetic pathways have been found in mediating floral transition in *Arabidopsis*. These flowering signals would converge to several floral integrators, which further activate floral meristem identity genes and finally determine flower formation in the shoot apex (Figure 1).

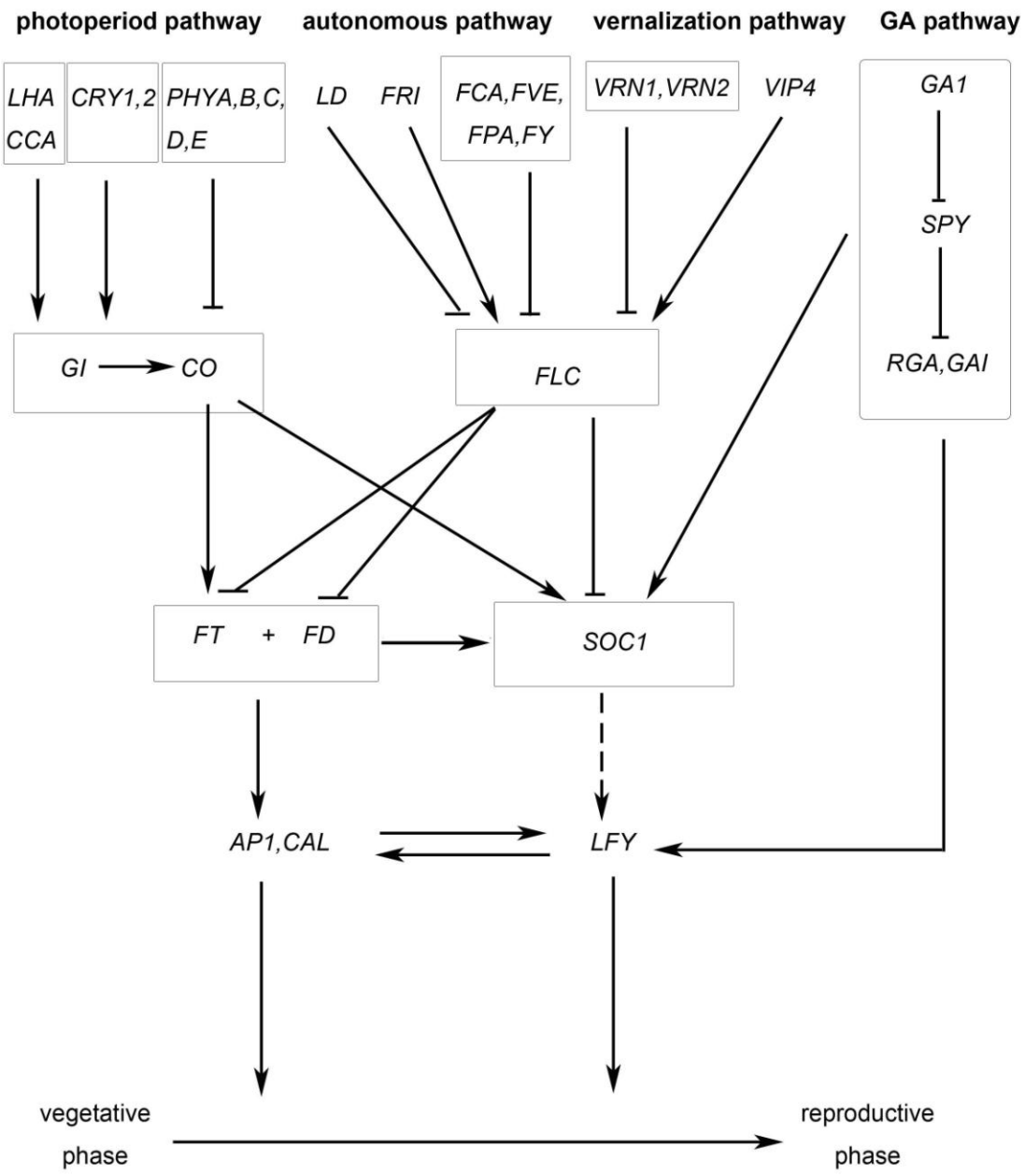

Figure 1. The schematic flowering pathways in *Arabidopsis thaliana*. Arrows and T-lines indicate positive and negative regulations, respectively. Dotted line is a possible interaction.

2.5 *AGL24* and *SVP* – Emerging new floral integrators

2.5.1 *AGL24*

Like *SOC1*, *AGL24* also encodes a putative MADS-domain transcription factor. *AGL24* protein is translocated from the cytoplasm to the nucleus to perform its transcriptional function through phosphorylation by a meristematic receptor-like kinase (MRLK) (Fujita et al., 2003). In the past few years, studies on *AGL24* have mainly focused on two stages of plant growth: flowering time control and flower development.

2.5.1.1 *AGL24* is an activator of flowering

Constitutive expression of *AGL24* causes early flowering while *agl24* mutant and RNAi transgenic plants delay flowering. Further studies demonstrated that *AGL24* is a dosage-dependent flowering promoter (Michaels et al., 2003; Yu et al., 2002), and suggests that *SOC1* is involved in the floral activation of *AGL24*. Both *SOC1* and *AGL24* transcripts are found in the shoot apical meristem an the vegetative growth phase and highly accumulated in the inflorescence during floral transition. When overexpressed, *SOC1* and *AGL24* significantly upregulate each other's expression especially in autonomous pathway mutant or *FRI*-dominant plants (Michaels et al., 2003). Furthermore, expression results showing that *AGL24* is

downregulated in most late flowering mutants (except *ft -1*) can be explained by the hypothesis that *AGL24* acts partially downstream of *SOC1*, which is a key floral signal integrator in *Arabidopsis*. This opinion is also supported by the genetic data. Overexpression of *AGL24* is able to partially rescue the late flowering phenotype of the *soc1* mutant and the mutation of *AGL24* suppresses the early flowering of overexpression of *SOC1*, indicating that *AGL24* is one of the downstream target genes of *SOC1* (Yu et al., 2002). Nevertheless, *SOC1* and *AGL24* act differently in the vernalization pathway. Although both of them are activated through vernalization, *AGL24* is regulated in a *FLC*-independent manner while *SOC1* is predominantly affected by *FLC* (Michaels et al., 2003).

2.5.1.2 *AGL24* regulates floral meristem formation

AGL24 overexpression plants also display some floral alterations, including the reversion of floral meristem to inflorescence meristem, which is similar to the *ap1* mutant. Besides, *AGL24* is found to be repressed in both *AP1* and *LFY* inducible systems, implying that *AGL24* might determine the inflorescence identity and it is regulated by floral meristem identity genes, including *AP1*, *LFY*, etc. In accordance with that, *in situ* studies show that *AGL24* is ectopically expressed in the whole zone of floral meristems in *ap1-1* and *lfy-6* mutants while in wild-type, *AGL24* is expressed mainly in the inflorescence meristem and downregulated in young floral meristems. Moreover, the mutation of *AGL24* is able to reduce the excess inflorescence apices of

ap1-1 and *lfy-6* mutants (Yu et al., 2004). In conclusion, *AGL24* maintains the inflorescence fate in *Arabidopsis* and repression of *AGL24* is required for normal floral meristem development.

2.5.2 *SVP*

SHORT VEGETATIVE PHASE (*SVP*), which encodes a MADS-box transcription factor, is another negative regulator of flowering in *Arabidopsis* (Hartmann et al., 2000). Like *FLC, SVP* also acts as a floral repressor and encodes a MADS domain protein (Hartmann *et al.,* 2000). *SVP* acts in a dose-dependent manner to delay flowering and may work synergistic with *FLOWER LOCUS M (FLM),* which is another floral repressor and close homolog of *FLC*. *svp* mutations overcome the late-flowering phenotype conferred by over-expression of *FLM,* and *svp flm* double mutants behave like single mutants (Scortecci *et al*., 2003).

In accordance with its function in maintaining the duration of the vegetative phase, *SVP* is expressed in whole vegetative seedlings, but is barely detectable in the main inflorescence apical meristem (Hartmann et al., 2000 and Liu et al., 2007). It has been recently reported that SVP mediates ambient temperature signaling within the thermosensory pathway by regulating *FT* expression (Lee et al., 2007). However, since *FT* mRNA is mainly expressed in the leaf (, Takada and Goto, 2003 and Wigge et al., 2005), the biological significance of downregulation of *SVP* at the shoot apex during the floral transition remains unknown.

SVP was first identified from early flowering mutants with the En-1 transposon (Baumann et al., 1998). *SVP* encodes a typical MADS-box protein, which has high sequence homology to AGL24 except for the C-terminal region. However, it has an antagonistic effect on flowering compared with *AGL24*. The *svp* mutant plants accelerate flowering under both LDs and SDs and the plants are still photoperiod-sensitive. Obvious morphological alterations are not observed in the *svp* mutant, although the potential effect of *SVP* overexpression on floral organogenesis needs further investigation. In accordance with its physiological functions, *SVP* expression is repressed in the apical meristem during floral transition, while the expression is maintained in young floral meristems at stages 1 and 2. Additionally, *SVP* represses flowering in a dosage-dependent manner because of the different flowering time between homozygous and heterozygous *svp* mutants (Hartmann et al., 2000). Another interesting finding is that the *SVP* genomic sequence produces several transcripts with different molecular size. It seems that the longer transcript is able to produce the entire protein while the function of the shorter ones remains to be clarified (Hartmann et al., 2000). It is possible that *SVP* is regulated via a post-transcriptional process, which is regulated by the function of *FCA*, another floral regulator in the autonomous pathway.

In conclusion, the four distinct flowering time pathways converge through several integrators to control the flowering time in *Arabidopsis*. The function of *SVP*, a novel component of flowering pathways, remains to be characterized. Further investigations

are needed to elucidate the molecular mechanism of *SVP* and its position and role in the flowering network.

2.6 The MADS protein family

2.6.1 The domain structure and function of MIKC type MADS protein

SVP belongs to a family of transcription factors that are found in species from all over the eukaryotic kingdoms and are mainly involved in developmental processes. They are collectively classified as MADS-box proteins because they share a highly conserved MADS domain, a DNA-binding domain that binds to a $CC(A/T)_6GG$ (CArG box) motif in the regulatory region of their target genes. The biological functions of MADS-box proteins and their discrete domains, the interactions between MADS-box proteins (or between MADS proteins and other cofactors), and the evolutionary significance of these proteins have been extensively reviewed (Riechmann and Meyerowitz, 1997; Messenguy and Dubois, 2003). It has been suggested that in general, the N-terminal of MADS protein is essential for DNA binding while the C-terminal is required for dimerization (Riechmann and Meyerowitz, 1997).

MADS-box genes in *Arabidopsis* are necessary for floral transition, flower morphogenesis, fruit development, as well as vegetative development. According to phylogenetic studies of MADS domains, *Arabidopsis* MADS-box genes can be

divided into two lineages, one resembling human *SERUM RESPONSE FACTOR* (*SRF)* gene and the other resembling Drosophila *MYOCYTE ENHANCE FACTOR* (*MEF)* gene and they are designated Type I and Type II, respectively (Alvarez-Buylla *et al.*, 2000). Type II MADS-box genes have been extensively studied during the last decade and are best known for their role in flower development, while the type I subfamily has remained largely unexplored (De Bodt *et al.*, 2003a). All characterized type II MADS-box genes, including *SVP*, encode proteins that share a typical MIKC structure (Figure 2). They have conserved MADS-box (M) and keratin-like box (K) domains, as well as the less conserved intervening region (I) and carboxyl terminal region (C) (Martinez-Castilla and Alvarez-Buylla, 2003). Interactions between MADS proteins or between MADS proteins and DNA-binding proteins to form homo/heterocomplexes appear to be a common theme in the MADS proteins family (Shore and Sharrocks, 1995) and these complexes are essential in the formation of specific transcriptional regulatory complexes.

Structural studies of MADS proteins such as *SRF* and *MEF2* revealed that they bind to DNA as dimers, forming a core that comprises of the 56 amino acids of a

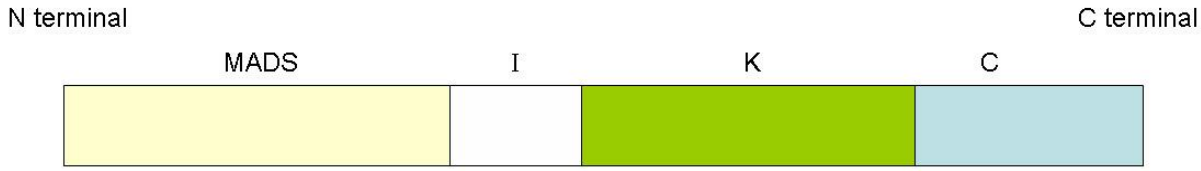

Fig 2. The four domains of MIKC-type *Arabidopsis* MADS-box protein. The MADS-box domain consists of 56 amino acids and functions as a DNA binding domain. The K box is a region that shows some similarity to the coiled coil structure of keratin and thought to be involved in protein-protein interaction. MADS-box and K box are separated by an intervening (I) region. The C region may function as a transcriptional activation domain.

MADS domain and a carboxyl-terminal extension of different length (Riechmann and Meyerowitz, 1997; Messenguy and Dubois, 2003). Crystallographic studies showed that the amino terminal of the MADS domain bind DNA while the rest of the core is involved in dimerization (Santelli and Richmond, 2000). Although similar crystal structures have not been obtained from plants, studies on *Arabidopsis* homeotic proteins *APETALA1 (AP1), APETALA3 (AP3), PISTILATA (PI)* and *AGAMOUS (AG)* have revealed their DNA-binding specificity, affinity, and DNA-binding cores that include MADS domain and its extension into the I region or K-box (Riechmann *et al.*, 1996). Significant sequence similarity among the MADS domains of MADS proteins from different organisms suggests that they probably share a similar structure and function (Riechmann and Meyerowitz, 1997). Indeed, comparison of the crystal structures of genes mentioned above showed that the conformation of the binding of MADS-box domains with DNA was well conserved (Messenguy and Dubois, 2003). It is reasonable to predict that plant MADS proteins may share a similar functional mode.

Formation of complexes between MADS proteins is another unique feature by which distinct and specific regulatory capabilities can arise (Shore and Sharrocks, 1995; Riechmann and Meyerowitz, 1997). There are several lines of evidence suggest that different floral homeotic proteins achieve combinatorial control of floral organ development through formation of complexes (Messenguy and Dubois, 2003). For example, it has been demonstrated that protein complexes PI-AP3-AP1 and PI-AP3-SEPALLATA3 (SEP3) are necessary to activate the *AP3* promoter. However,

the mechanism by which regulatory complexes determine functional specificity remains unclear. It is proposed that the components of the complexes may simultaneously recognize different sites that are caused by DNA bending on the same strand of DNA (Messenguy and Dubois, 2003).

2.6. 2 The K box

Although the crystal structure of MADS domain has been obtained, the structure and function of K domain are not clear. K-box is only unique in plant MADS-box proteins and had been postulated to form three amphipathic α-helices, namely K1, K2 and K3 respectively, which is similar in structure to the intermediate filament protein keratin (Yang *et al.*, 2003). This indicated that it may play a role in mediating the interaction between two proteins (Riechmann and Meyerowitz, 1997). Previous studies have given contradicting conclusions regarding the role of K-box as a mediator of protein-protein interaction. On one hand, K-box is dispensable for the formation of DNA-binding dimers (Riechmann and Meyerowitz, 1997, Yang *et al.*, 2003). K-box is able to mediate specific interactions among MADS domain fusion proteins in the yeast two-hybrid assays, even when the MADS domain and the I region are absent. Besides, Yang *et al.* (2003) have demonstrated that K1, K2, and the region between K1 and K2 are critical for the strength of AP3/PI dimerization. This is consistent with the finding that the regions that are required for AP3/PI complex to form a core include the MADS-box, I and K1 regions (Riechmann *et al.* 1996).

2.6. 3 The I region

Riechmann *et al.* (1996) have demonstrated that the entire or part of the I region is included in the DNA-binding core of *Arabidopsis* homeotic proteins. In fact, the crystal structure of *MEF2* showed that its MEF2 region, which is equivalent to the I region in plants is in the core for dimerization. It has been shown that the I region is located at the interaction interface between MADS proteins. This region could determine the dimerization specificity because it is more variable in length and sequence compared to the conserved MADS and K boxes. MADS proteins are possibly able to specifically dimerize with I regions of similar sequences, length or chemical properties (Riechmann and Meyerowitz, 1997). The I region is also important in determining the functional specificity for AP1, AP3, PI, and AG (Krizek and Meyerowitz, 1996), which supports the notion that dimerization specificity affects functional specificity.

2.6. 4 The C region

Unlike the MADS domain, I region and K box, the C region has never been found to be involved in protein interaction or DNA binding. However, its importance was demonstrated by a mutation in the C region, which results in functional defects (Riechmann and Meyerowitz, 1997). Domain swapping studies among AP1, AP3, PI

and AG found that C region is not important in determining their functional specificity (Krizek and Meyerowitz, 1996) and it was postulated that the C region is responsible for transcriptional activation. This was supported by the finding that the C region of AP1 and its homologues performs a transcriptional activation function (Cho *et al.*, 1999). Further studies are required to confirm the function of the C region in a MADS-box protein.

2.7 Chromatin immunoprecipitation

Interactions between protein and DNA mediate transcription, DNA replication and DNA repair, which are all central to the biology of every organism. The method of chromatin immunoprecipitation (ChIP) appears to have significant advantage over other approaches, because it allows the analysis of the interaction of transcriptional factors with DNA in living cells, thereby providing an *in vivo* picture of the native chromatin structure and its bound factors in the cells at a specific development stage (Sandoval *et al.*, 2004). In ChIP technique, biological materials are firstly fixed, where the targeted protein and DNA is crosslinked in a chromatin complex. The isolated chromatin is then sonicated to produce small fragments. Subsequently, the antibody that recognizes a protein of interest is used to purify the chromatin complex that contains the protein of interest. Finally, the crosslink between the protein and DNA is reversed, and the released DNA fragments are precipitated for further analysis (Figure 3). Although the ChIP procedure appears to be simple, a lot of parameters can

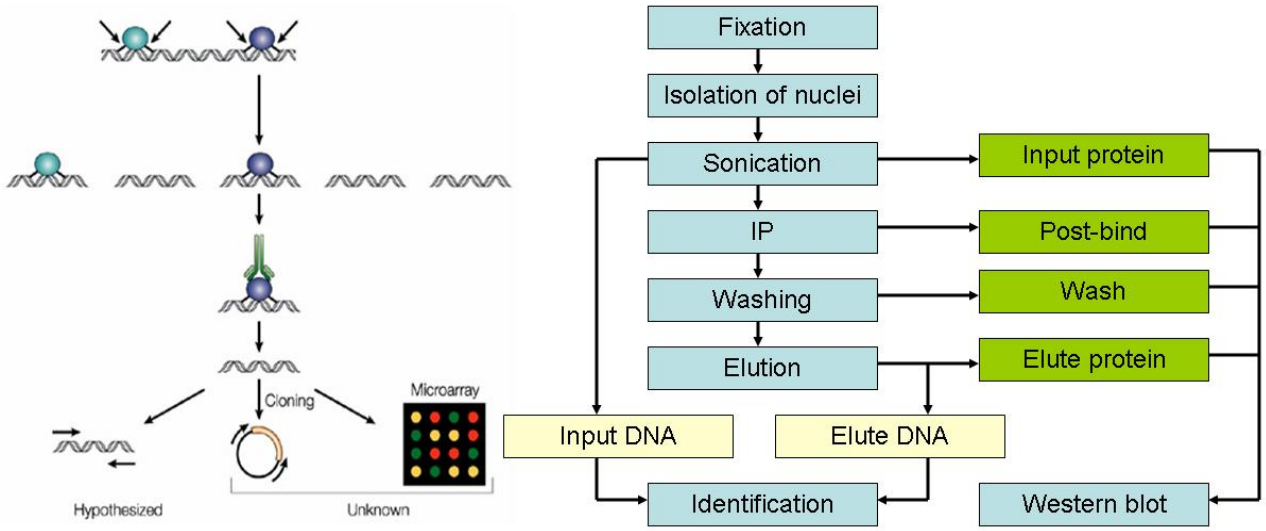

Figure 3. Flowchart of ChIP work. The plant samples were formaldehyde-crosslinked. Nuclear extracts prior to antibody incubation (input) and after ChIP (elute) were subject to PCR analysis using primers flanking putative *SVP* binding sites (CARG boxes). Western blot analysis was used to monitor the whole process.

be adjusted to achieve different levels of accuracy to determine the interaction of a protein with a specific DNA sequence. With appropriate controls, ChIP can serve as a valuable tool for studying nuclear events of protein and DNA interactions (Spencer *et al.*, 2003).

2.7.1 Fixation

In order to avoid loss of protein-DNA interaction before obtaining co-precipitated DNA, the binding between a protein and its bound DNA must be strengthened by crosslink. Formaldehyde is good candidate to serve this purpose, because it is a tight (2 Å) crosslinking reagent that can easily enter the nucleus and efficiently produce protein-nucleic acid crosslink *in vivo*. During fixation, amino and imino groups of amino acids (lysines, arginines and histidines) and of DNA (primary adenines and cytocines) readily react with formaldehyde leading to the formation of a Schiff base. This intermediate can further react with a second amino group and condense to give the final DNA-protein complex (Orlando *et al.*, 1997). In fact, the presence of formaldehyde can induce the formation of DNA-protein, protein-protein, and RNA-protein complexes. Therefore, it results within minutes in the formation of a wide crosslinked network of biopolymers, and preventing any large-scale redistribution of cellular components (Solomon and Varshavsky, 1985). In some cases, other crosslinking agent such as dimethyl adipimidate (DMA) has been used in combination with formaldehyde (Kurdistani and Grunstein, 2003). DMA is a

homobifunction imidoester with spacer arm length of 8.6 Å that possesses two identical groups that can react with primary amine group to form stable covalent bonds. Thus, large protein complex that are located relatively distant from DNA and that would not be efficiently crosslinked to chromatin by formaldehyde alone could be fixed by DMA. Also, cisplatin (Spencer *et al.*, 2003) and UV irradiation methods have been successfully employed as alternative crosslinking techniques (O'Neil and Turner, 2003). However, formaldehyde remains the most commonly used fixative because of its advantages mentioned above. Moreover, crosslinking by formaldehyde is fully reversible under a mild condition, which can beachieved by incubating the crosslinked sample at 65°C for at least 6 hours without any other chemicals. Besides doing fixation before chromatin extraction in the ChIP experiment (XChIP), there is another method designated as NChIP (native ChIP) that dose not include the fixation step. As epitope disruption and fixation of fortuitous protein-DNA could lower ChIP's efficiency during fixation process, NChIP is suitable for the investigation of those proteins that can bind DNA with high affinity, or histones and their modified isoforms (O'Neil and Turner, 2003).

An efficient fixation of a protein to chromatin *in vivo* is crucial for the XChIP technique. Therefore, the extent of crosslinking should be determined carefully. There are two major problems concerning the subsequent immunoprecipitation step that should be taken into account. Firstly, excessive crosslinking can result in reduced antigen availability. Secondly, an excess of crosslinking can result in the loss of material in chromatin (Orlando, 2000). The fixation time varies from 1 minute to

several hours according to different cell types. It has been found that prolonged exposure to formaldehyde leads to a loss of immunoprecipitation materials, although the underlying mechanisms are not fully understood (Orlando, 2000). There are several possible explanations (Orlando, 2000; Spencer *et al.*, 2003). Firstly, it is possible that the epitopes could react with formaldehyde, or the 3 dimensional structure of the protein of interest might be altered as formaldehyde is a moderately denaturing agent. Thus, in the following immunoprecipitation step, the desired antibody-antigen binding will be affected. Secondly, over-fixed cells are refractory to chromatin fragmentation treatment, and thus the chromatin complex could not be recovered for immunoprecipitation process. Thirdly, during crosslinking, soluble cellular components become more insoluble as they are crosslinked with each other and/or to the insoluble cellular material. Therefore, extensively crosslinking a cell may decrease the solubility of any target DNA-protein complex as it may be trapped in the insoluble nuclear material. Therefore, a time-course experiment is still strongly recommended to find out the duration of fixation to achieve the most efficient crosslinking, though most proteins are readily crosslinked after fixation for 30 min to one hour (Orlando, 2000).

*2.7.**2 Chromatin fragmentation***

Since fixed cells are found to be highly resistant to restriction enzyme digestion or DNase I treatment, the fragmentized chromatin can only be produced efficiently by

mechanical shearing (Orlando *et al.,* 1997). It is noteworthy that materials that are over-cross-linked do not produce small chromatin fragments under the shearing force (Orlando *et al.*, 1997). The extent to which one can fine-map the location of a specific protein along a genomic sequence depends on the extent of DNA fragmentation. For example, it has been suggested that if the average size of chromatin fragment is controlled at 600 bp, theoretically a 1,200-bp region where the binding site sits in the middle will be enriched (Kadosh and Struhl, 1998). Therefore, it is difficult to detect the exact location of a binding site if the sonicated chromatin is too large. On the other hand, chromatin fragments that are too small in size pose a difficulty in the enrichment of co-precipitated DNA. Normally, the chromatin fragment that obtained after sonication is engineered to below 1,000 bp in size.

*2.7.**3 Purification of chromatin complex***

DNA fragments crosslinked to a protein of interest can be enriched by one of these three standard ways (Buck and Lieb, 2004): firstly, immunoprecipitation with a protein-specific antibody; secondly, immunoprecipitation of a tagged protein using an antibody specific to the tag, such as Myc, HA (Hemagglutinin), StrepII; thirdly, affinity purification using a tag that obviates the need for antibodies, such as the TAP (tandem affinity purification) tag. Comparatively, immunoprecipitation by protein-specific antibodies is more established than affinity purification. Since the fixative agents could potentially modify the epitope of a protein of interest during the

fixation step, polyclonal antibodies were preferred compared to monoclonal antibodies in order to avoid this epitope masking problem. However, it should be emphasized that the specificity of polyclonal antibodies should be confirmed before doing ChIP, because the antibodies may recognize other proteins that are homologous to the proteins of interest. Alternatively, the strategy of labelling proteins of interest with a tag could be adopted to solve this problem. Fusion proteins that carry Myc/HA/StrepII/TAP tag can be generated, and anti-Myc/HA/StrepII/TAP antibodies that are commercially available could be used in the subsequent purification step. A disadvantage of this strategy is that the fused tag may perturb the structure of the protein of interest, and hence the engineered protein has altered or no biological function. Therefore, a test must be conducted to make sure that these chimeric proteins still maintain their biological function.

*2.7.**4 Analysis of co-precipitated DNA and identification of binding sites***

Depending on whether a target sequence is known or not, there are two potential ways in the analysis of immunoprecipitated DNA. If there is a known target sequence, the efficiency of ChIP can be tested by using quantitative PCR or slot blot experiment. For quantitative PCR, an optimized real-time PCR is the most reliable study as it could give direct information on the amount of target sequence that is present in the co-precipitated DNA compared to the one that is not targeted. For slot blot analysis, the immunoprecipitated DNA and mock DNA are immobilized on a nylon membrane

by slot blot. The relative enrichment for a target sequence can be determined by comparing the hybridization of a specific probe to immunoprecipitated DNA and mock DNA or genomic DNA (Orlando *et al.*, 1997).

It will be more difficult if the sequences of the downstream targets of the protein of interest are unknown, mostly because of the uncertainty regarding the overall ChIP efficiency, or even its feasibility. Three methods including southern analysis, microarray, and conventional sequencing are used to identify the first batch of target sequence (Buck and Lieb, 2004; Orlando *et al.*, 1997).

In southern blot analysis, co-precipitated DNA is used as a probe to scan genomic regions. Typically genomic DNAs are digested with restriction enzymes, blotted onto membrane, and hybridized with the immunoprecipitated DNA. Microarray method, also named as ChIP-chip, is a high-throughput scheme that utilizes the same principle as southern blot analysis. The genomic DNA that contains the binding template is printed on a chip. Co-precipitated DNA and mock DNA are labelled differently and hybridized with the prepared chip, enabling their signals to be compared and the highly enriched regions to be identified. In conventional sequencing method, DNA sequences purified from a ChIP experiment are cloned and sequenced, and the sequences that appear at a higher frequency are selected as candidates for further tests.

Sometimes due to the small size, the co-precipitated DNA is below the detection level. To circumvent this problem, the immunopurified chromatin DNA is ligated to a synthetic linker and amplified by PCR before it is used for further analysis (Orlando, 2000). One method is to digest the co-precipitated DNA with restriction enzymes and

amplify it by PCR after being ligated to a sticky-ended linker. The risk in this method is the irregular distribution of restriction enzyme sites within the genome region, which could lead to the loss of enriched fragments. In comparison, the introduction of unbiased ligation of a blunt-ended linkers to undigested co-precipitated DNA represent a significant improvement (Orlando, 2000), despite the fact that blunt end ligation has a lower efficiency.

CHAPTER 3

Materials and Methods

3.1 Plants growth conditions

Wild-type and transgenic *Arabidopsis* plants of the Columbia, Landsberg *erecta* (L*er*), or C24 ecotype were grown on soil at 22^{o}C under long days (16 h light/8 h dark) or short days (16 h dark/8 h light). Seeds were stratified on soil at 4^{o}C for 4-5 days before being transferred to a growth room in order to ensure synchronized germination. Basta selection was conducted twice within 10-20 days after seed germination to screen transgenic plants. The mutants *co-1*, *gi-1*, *ft-1* (Ler *ft-1* introgressed into Col), *fve-3*, *soc1-2*, *svp-41*, and *agl24-1* are in the Col background, and *co-2*, *ft-1*, *fve-1*, *fca-1*, *fpa-1*, and *ga1-3* are in the L*er* background.

For plant growth on Murashige and Skoog (MS) agar medium, sterilization of seeds was first performed: Seeds were initially incubated in sterile water for 20-30 min until precipitation. Then they were washed with 70% ethanol and rinsed with sterile water three times. After incubation in 15% Clorox® for 20 min, seeds were rinsed with sterile water again and sequentially sowed in Petri dishes containing autoclaved MS agar medium, which was adjusted to pH 5.8. The plates were maintained in a tissue culture room under LDs (16 h light/ 8 h dark). In addition, the successful *pER22-SVP* transgenic plants in MS agar medium were obtained with hygromycin selection (15μg/ml).

3.2 GA treatment

For GA treatment of plants grown in SDs, the treatment was started with seedlings grown in SDs at 1 week after germination, and weekly application of 100 μM GA_3 was performed. To break dormancy, *ga1-3* seeds were imbibed in 100 μM GA at 4℃ for 7 days, and then rinsed thoroughly with water before sowing.

3.3 Vernalization treatment

Seeds were first sown on MS agar plates and germinated in the tissue culture room. 2-3 day-old seedlings were then transferred to a 4^{o}C cold room for 6-week vernalization treatment (without light), after which plants were transferred to soil growth conditions under a short-day photoperiod.

3.4 β-Estradiol Induction of pER22-SVP

To observe the phenotype of pER22-SVP and wild-type plants upon β-estradiol induction, the plants were grown on solid MS medium supplemented with 1% sucrose at 22℃ in LDs before being applied with various treatments. For continuous treatment, 10 μM β-estradiol was applied and replaced every two days once treatment started. For testing induced *SVP* expression, 5-day-old pER22-SVP seedlings grown

on solid MS medium were transferred into MS liquid medium supplemented with 10 μM β-estradiol. These seedlings incubated in the liquid medium were harvested at different time points until 48 hr. Mock treatment of transgenic plants was also performed for the above experiments, in which β-estradiol was replaced with an equal amount of dimethyl sulfoxide which was used to dissolve β-estradiol.

3.5 Molecular cloning

3.5.1 cDNA amplification

cDNA for the *SVP* were previously generated by reverse-transcription polymerase chain reaction (RT-PCR) and cloned into a pGEM®-T Easy Vector (Promega) subsequently. cDNAs were amplified from the above mentioned template by polymerase chain reaction (PCR). To perform PCR, 200 ng of deoxyribonucleic acid (DNA) template was added to a reaction mix containing 1 X PCR buffer [10 mM Tris-hydrochloric acid (pH 8.8), 50 mM, potassium chloride (KCl), 1.5 mM magnesium sulphate (MgSO4), 1% Triton-X100 and 0.02 mM deoxyribonucleotide triphosphate (dNTP) mix], 10 pmol each of forward and reverse primers with restriction sites at the 5’ ends and 1U Pfu Turbo® DNA polymerase (Stratagene). The procedure was performed in the Peltier thermo cycler-200 (MJ Research) as follows: denaturation at 94°C for 5 min, followed by 40 cycles of denaturation at 94°C for 30 sec, primer annealing at 58°C for 45 sec, extension at 68°C for 1 min. At the end of 40 cycles, a final extension of PCR products was carried out for 10 min at 72°C.

3.5.2 Gel extraction

The PCR products were separated on 1% Tris-Acetate-ethylenediaminetetraacetic acid (EDTA) (TAE) agarose gel. The expected DNA fragment was cut out from the agarose gel and purified using the QIAquick® Gel Extraction Kit (Qiagen, Hilden, Germany). An appropriate amount of Buffer QG (3 volumes of buffer to 1 volume of gel) was added to the excised gel in a microfuge tube and vortexed for 30 sec. The mixture was incubated at 50°C for 10 min to help dissolve the agarose, after which 1 gel volume of isopropanol was added. The sample was passed through the QIAquick column and washed twice with Buffer QG. The bound DNA was eluted with 30 µl of H2O.

3.5.3 Restriction digestion

Purified DNA and plasmid were digested in double digestion mixtures with the appropriate enzymes at 37°C. The 50 µl digestion mixture consisted of 1 X buffer (1 X BSA if necessary) 10 U of each restriction enzyme and approximately 1 µg of DNA. Restriction enzymes were purchased from New England Biolabs. After digestion, plasmid reaction mixtures were dephosphorylated by Alkaline Phosphatase (CIP).

3.5.4 Ligation

After digestion, the purified PCR amplified DNA fragment was cloned into the digested plasmids. To do this, 20 ng DNA was mixed with 50 ng vector in the reaction

mix containing 1 X of T4 DNA ligase Buffer and 3 U of T4 DNA ligase. The ligation mixture was incubated overnight at 16°C. The recombinant plasmid was subsequently transformed into competent *E.coli* DH5α cells as described below.

3.5.5 Competent cell preparation

Prior to cell transformation, competent DH5α cells were prepared. Bacterial culture that was grown overnight at 37°C was transferred to 250 ml of SOB medium [2% (w/v) bacto tryptone, 0,5% (w/v) yeast extract, 10mM MgSO4, pH6.7] in a 2 L Erlenmeyer flask and grown with vigorous shaking at 18°C until an OD600 reached 0.6. The bacterial culture was kept on ice for 10 min and spun down by centrifugation at 4,500 rpm for 10 min at 4°C. The bacterial pellet was resuspended in 80 ml ice-cold Tris-Borate (TB) buffer [10 mM pipes, 55 mM manganese chloride (MnCl2), 15 mM calcium chloride (CaCl2) and 250 mM KCl, pH 6.7], incubated on ice for 10 min, and spun down as previously described. Subsequently, the pellet was resuspended in 20 ml of ice-cold TB buffer, and dimethyl sulfoxide (DMSO) was added to a final concentration of 7%. After incubation on ice for 10 min, the cell suspension was stored in aliquots of 100 µl in 1.8 ml Eppendorf tubes that were further snap-frozen in liquid nitrogen and stored at -80°C until ready to use.

3.5.6 Transformation into E.coli competent cells

Ligation mixture was added to 100 µl of *E.coli* DH5α competent cells, incubated on ice for 30 min and subjected to heat shock at 42°C for 90 sec. The mixture was

then incubated in 1 ml LB broth at 37°C for 1 h. Subsequently, the bacteria cells were pelleted by centrifugation at 10,000 rpm for 4 min. The pellet was resuspended in approximately 100 μl LB broth and spread onto an LB agar medium containing 100 μg/ml kanamycin.

3.5.7 Screening for putative colonies

Colonies which survived selection with kanamycin were dissolved in 5 μl water and 1 μl of the bacterial suspension was used as template for PCR. PCR was performed with DyNAzyme™ II DNA polymerase on the Peltier thermo cycler (MJ Research), using a forward primer located on the vector and a reverse gene-specific primer. The reaction profile was as follows: denaturation at 94°C for 5 min, followed by 35 cycles of denaturation at 94°C for 30 sec, primer annealing at 57°C for 30 sec, extension at 72°C for 1 min. At the end of 35 cycles, a final extension of PCR products was carried out for 10 min at 72°C. The PCR products were separated by electrophoresis on a 1% agarose gel and colonies which gave the right size were cultured at 37°C overnight in LB broth supplemented with 50 μg/ml kanamycin.

3.5.8 Plasmid DNA isolation

Plasmid DNA was purified using Wizard® Plus SV Minipreps DNA Purification System (Promega). The bacterial cells cultured for 12-16 h were first centrifuged for 5 min at 14,000 rpm and the pellet was resuspended in Cell Resuspension solution. The Cell Lysis solution was then added to the culture, after which the solution was

neutralised by Neutralization Solution. The lysate was centrifuged to remove the cell debris and the clear lysate was then added to the spin column for the binding of plasmid DNA to the resin. After the lysate had passed through the column by centrifugation, the column was rinsed with Wash Buffer to clean the plasmid DNA. The Wash Buffer was thoroughly removed from the resin by a second brief centrifugation and the plasmid DNA was eluted with 50 µl of sterile distilled water.

3.5.9 DNA sequencing

The nucleotide sequences were determined using the ABI PRISM® Big Dye and dRhodamine Terminator Cycle Sequencing Ready Reaction Kit (Perkin-Elmer, Applied Biosystems, California, USA). Prior to sequencing, the reaction was prepared by mixing 200 ng of double-stranded DNA with 1.6 pM of appropriate primers and 4 µl of Terminator Ready reaction mix, and the final volume was adjusted to 10 µl with deionised water. Sequencing PCR was performed by denaturation at 96°C for 10 sec, annealing at 52°C for 5 sec, and extension at 60°C for 4 min. The reaction was repeated for 25 cycles and held at 4°C. Sequencing was performed using the ABI PRISM® sequencer (Applied Biosystems). The identity of the DNA sequences was determined by BLAST nucleotide homology search on National Centre for Biotechnology Information (NCBI, http://www.ncbi.nlm.nih.gov) website.

3.6 Plant transformation

The recombinant DNA constructs were firstly introduced into *Agrobacterium tumefaciens,* which were used to transform *Arabidopsis thaliana* by floral dipping.

3.6.1 Electroporation

Electroporation-competent *Agrobacteria tumefaciens* GV3101 were electroporated with the plasmids constructs in 1 mm Gene Pulser® cuvettes (Bio-Rad). The electroporated bacteria were cultured in 1 ml of LB broth for 3 h at 28 °C, after which the cells were precipitated at 4,000 rpm for 3 min and plated on the LB agar medium supplemented with 25 μg/ml gentamycin, 10 μg/ml tetracycline and 50 μg/ml kanamycin. The plates were incubated overnight at 28 °C. Successful transformants were screened via PCR.

3.6.2 Floral dipping

Transformed *Agrobacteria* carrying the desired recombinant DNA were cultured in LB broth containing 25 μg/ml gentamycin, 10 μg/ml tetracycline, and 50 μg/ml kanamycin at 28 °C until OD_{600nm} of 0.8 was reached. *Agrobacteria* were then precipitated at 4,000 rpm for 15 min and resuspended thoroughly in a same volume of 5% sucrose with 0.03% Silwet L-77. Flower buds of wild-type plants were dipped into the bacteria suspension for a few seconds. The inoculated plants were then covered in a black plastic bag overnight to improve transformation efficiency. The

treated plants were grown under normal growth conditions after removing the cover the next day.

3.7 Plant screening

In T1 generation, transgenic plants grown on soil were sprayed with 0.3% Basta at the 2-rosette-leaves stage and 5-10 lines that have shown late-flowering phenotypes were selected for further studies. In T2 generation, the genetic segregation for the seeds from a T1 line was observed. The lines that show the ratio of death to surviving with or more than 1:3 were the plant with single transgene insertion and they were selected for further study. In T3 generation, a T2 line has all of its T3 progenies resistant to antibiotics was the homozygous plant with single transgene insertion and they were used in our study.

Seeds that were sown on plate were surface-sterilized by a sequential wash with 70% ethanol (v/v) for 30-60 sec, 15% Clorox solution for 20 min, and a final rinse with sterile distilled water for 3 times. After surface sterilization, seeds were sown in Petri dishes (95x15mm) containing MS medium supplemented with 100 μg/ml hygromycin. Culture dishes were sealed and maintained in a tissue culture room at 22°C under a 8 h light/16 h dark photoperiod.

3.8 Genomic DNA isolation and Genotyping

Plant samples were ground in 500 μl Extraction Buffer (0.2 M Tris-HCl, pH 9.0, 0.4 M LiCl, 25 mM EDTA, and 1% SDS) using micropestles. The homogenized sample was centrifuged at 14,000 rpm for 5 min at 4°C and 350 μl. The supernatant was transferred into new eppendorf tubes and mixed, by inversion, with an equal volume of isopropanol. After spinning for 10 min at 14,000 rpm at 4°C, the pellet was washed twice with 70% ethanol. The pellet was dried and dissolved in 100 μl TE buffer (10 mM Tris, pH 8, 1 mM EDTA).

For PCR genotyping, 2 μl of the extracted genomic DNA was added into a buffered PCR reaction system containing 0.2 mM dNTP, 1 U of Dynazyme® thermostable DNA polymerase, and 0.2 mM primers. PCR was performed by denaturation at 94°C for 5 min, followed by 30 cycles of denaturation at 94°C for 30 sec, annealing at 58°C for 30 sec, and extension at 72°C for 1 min, and final extension at 72°C for 7 min. About 5 μl of the PCR products were separated on a 1% TAE agarose gel by electrophoresis.

3.9 RNA isolation

Total RNA was isolated using the RNeasy® Mini Kit (Qiagen). Plant tissue was pulverized in liquid nitrogen with mortar and pestle, after which the appropriate amount of lysis buffer RLT (450 μl/100 mg plant tissue) was added. The sample was

shaken vigorously and the lysate was transferred to the QIA shredder spin column and centrifuge for 2 min at 14,000 rpm. The supernatant was transferred to a new tube, and the RNA in the aqueous solution was precipitated with 0.5 volume of 100% absolute ethanol. The mixed sample was transferred to an RNeasy mini column and centrifuged at 10,000 rpm for 15 sec. The final wash with 500 μl of Buffer RPE was performed at 14,000 rpm for 2 min. The column was dried by centrifuging at 10,000 rpm for 1 min, followed by elution of RNA for 1 min at 10,000 rpm with 30 μl of RNase-free water.

3.10 Reverse Transcription PCR (RT-PCR)

Two-step RT-PCR was carried out using the Thermoscript® RT-PCR System (Invitrogen Life Technologies). The DNase I (Ambion, Inc.) treated total RNA (1.5 μg) was mixed with 1 μl 50 μM Oligo(dT)20 and 2 μl of 10 mM dNTP mix, topped up to 12 μl with diethyl-pyrocarbonate (DEPC)-treated water, and incubated at 65°C for 5 min. The reaction mix comprising 4 μl of 5 X cDNA Synthesis Buffer, 1 μl each of 0.1 M DTT, RNaseOUT® (40 U/μl), DEPC-treated water, and Thermoscript® Reverse Transcriptase (15 U/μl) was added to the RNA mixture. The total reaction mixture was incubated at 50°C for 1 min for Oligo (dT)20 priming and terminated at 85°C for 5 min followed by incubation with 1 μl of RNase H at 37°C for 20 min. About 1 μl of synthesized cDNA was added in the PCR reaction system followed by 28 cycles of PCR amplification with denaturation at 94°C for 30 sec, annealing at 58°C for 30 sec,

and extension at 72°C for 1 min, and the final extension step at 72°C for 10 min. About 5 μl of the PCR products were separated on a 1% TAE agarose gel by electrophoresis.

3.11 Real-time PCR

Quantitative real-time PCR was performed in triplicates on 7900HT Fast Real-Time PCR system (Applied Biosystems) with SYBR Green PCR Master Mix (Applied Biosystems). Efficiency of each pair of primers was determined based on its standard curve obtained from a series of 10-fold diluted template DNAs. The difference between the cycle threshold (Ct) of target genes and the Ct of control primers ($\Delta Ct = Ct_{target\ gene} - Ct_{control}$) was used to obtain the normalized expression of target genes. Semiquantitative PCR was performed as previously described (). The relative fold change was eventually calculated based on both Ct value and primer efficiency according to a published protocol (Pfaffl, 2001). A constitutively expressed gene, *β-TUBLIN* was used as an internal control. Primer sequences used for gene expression analysis are listed in Table 1. Nonradioactive in situ hybridization and synthesis of RNA probes were carried out as previously published (Liu et al., 2007). GUS staining was performed as previously described (Jefferson et al., 1987). For analysis of GUS activity, T3 homozygous seedlings from independent lines were used for transformants with a single insertion of transgenes, while both T2 and T3 lines were analyzed for transformants with multiple insertions.

Primer pairs used for quantitative real-time PCR

Gene	Sequence
AGL24	5′-GAGGCTTTGGAGACAGAGTCGGTGA-3′
	5′-AGATGGAAGCCCAAGCTTCAGGGAA-3′
SOC1	5′-AGCTGCAGAAAACGAGAAGCTCTCTG-3′
	5′-GGGCTACTCTCTTCATCACCTCTTCC-3′
AP1	5′-CATGGGTGGTCTGTATCAAGAAGAT-3′
	5′-CATGCGGCGAAGCAGCCAAGGTT-3′
SVP	5′-CAAGGACTTGACATTGAAGAGCTTCA-3′
	5′-CTGATCTCACTCATAATCTTGTCAC-3′
FT	5′-CTTGGCAGGCAAACAGTGTATGCAC-3′
	5′-GCCACTCTCCCTCTGACAATTGTAGA-3′
TUB2	5′-ATCCGTGAAGAGTACCCAGAT-3′
	5′-AAGAACCATGCACTCATCAGC-3′

Primer pairs used for semi-quantitative PCR

Gene Amplified	Primer Pair
SOC1	5′-GAAGATATGGTGAGGGGCAAAACTC-3
	5′-GGGCTACTCTCTTCATCACCTCTTCC-3′
FT	5′-CCCTGCTACAACTGGAACAACCTTT-3′
	5′-TAGGCATCATCACCGTTCGTTACTC-3′
SVP	5′-GTGACAAGATTATGAGTGAGATCAG-3′
	5′-GAATTCACTACTTAGACATTGTCTC-3′
TUB2	5′-ATCCGTGAAGAGTACCCAGAT-3′
	5′-TCACCTTCTTCATCCGCAGTT-3′

Table 1. Primer Pairs Used for Gene Expression Analysis

3.12 GUS histochemical assay and expression analysis

Prior to staining, tissues were incubated in cold 90% acetone and washed thrice with rinse solution containing 50 mM NaPO4 pH 7.2, 0.5 mM K3Fe(CN)6, 0.5 mM K4Fe(CN)6 on ice. The samples were placed in the staining solution [50 mM NaPO4 pH 7.2, 0.5 mM K3Fe(CN)6, 0.5 mM K4Fe(CN)6 and 2 mM X-Gluc], and infiltrated under vacuum condition for 20 min and incubated for 24 h at 37℃. The stained samples were subjected to a serial wash with 20% ethanol, 35% ethanol, FAA fixative (50% ethanol, 5% acetic acid, 3.7% formaldehyde), and 70% ethanol at room temperature for 30 min each. The samples were examined under a dissection microscope.

For the examination of *GUS* transcription, RNA was extracted from transgenic plants harboring different reporter genes, reverse-transcribed into cDNA, and further detected for *GUS* gene expression with a specific primer pair (Table 2) by quantitative real-time PCR.

3.13 Mutagenesis

Mutagenesis of the third CArG box on *SVP* genomic sequence was done by using QuikChange® II XL Site-Directed Mutagenesis Kit (Stratagene). 50 ng of P2::GUS plasmid was added to a reaction mixture containing 5 µl of 10 X reaction buffer, 125 ng of forward primer, 125 ng of reverse primer, 1 µl of dNTP mix, 3 µl of **Table 2.**

Primer name	Sequence
SOC1-P4-*Xma*I	5’-AACCCGGGATCGTATTTACTAGTGGTATACG-3’
SOC1-R1-*Xma*I	5’-GTCCCGGGCTTTCTTGAAGAACAAGGTAA-3’
SOC1-M1-F2	5’-GGGATGGAAAGATATTATAAAAATTGATTAAAAGGA ATATACCTGTATTACTCACAGGTAAG-3’
SOC1-M1-R2	5’-CTTACCTGTGAGTAATACAGGTATATTCCTTTTAATCA ATTTTTATAATATCTTTCCATCCC-3’
SOC1PM3-F	5’-GTCCATATGTATCAAAATATGGGATTTTTCCTCTTTCT TAAGGCTTTTTTCC-3’
SOC1PM3-R	5’-GGAAAAAAGCCTTAAGAAAGAGGAAAAATCCCATAT TTTGATACATATGGAC-3’
SOC1PM4-F	5’-GGTCTTTCTTAAGGCTTTTTTGGAAAATACCTAAAGG ATGAGGTTTCAGACGTCCATC-3’
SOC1PM4-R	5’-GATGGACGCTTGAAACCTCATCCTTTAGGTATTTTCC AAAAAAGCCTTAAGAAAGACC-3’

Table 2 Primers for GUS constructs

QuickSolution, and 2.5 U of PfuUltra HF DNA polymerase. The mixture was put through 18 cycles of PCR amplification with denaturation at 95°C for 1 min, annealing at 60°C for 45 sec, and extension at 68°C for 10 min, and the final extension step at 68°C for 10 min. Finally, after incubating with 1 μl *DpnI* for 1 h at 37°C, DNA was transformed into the *E.coli* as described in 2.2.6.

3.14 Plasmid construction and plant transformation

The *35S:SVP-6HA* constructs were constructed by co-workers in the lab (Li et al., unpublished data). Single insertion transgenic lines were used in our experiments. To construct pER22-SVP, the *SVP* cDNA was amplified and cloned into a derived pER22 vector. The pER8 vector (Zuo et al., 2000) was cut with ApaI and SpeI, filled in the cohesive ends, and self-ligated to produce pER22. To construct *35S:SVP-6HA*, the *SVP* fragment was cloned into the pGreen-35S-6HA vector to obtain an in-frame fusion of *SVP-6HA* under the control of 35S promoter. The pGreen-35S-6HA vector was generated by cloning six repetitive HA epitopes into the SpeI site of pGreen-35S (Yu et al., 2004). To construct *SVP:SVP-6HA*, the 5.1 kb *SVP* genomic fragment was amplified and cloned into the pGreen-6HA vector to obtain an in-frame fusion of *SVP*:*SVP-6HA*. The pGreen-6HA vector was generated by cloning six repetitive HA epitopes into the SpeI site of pHY105 (Liu et al., 2007). To construct *SVP:GUS*, the *SVP* genomic sequence of 3.6 kb in length was amplified and cloned into pHY107 (Liu et al., 2007).

SOC1:GUS was constructed as previously reported (Liu et al., 2008). This construct was further mutagenized to produce the M1 and M2 mutations (Figure 4) using the QuikChange II XL-Site-Directed Mutagenesis Kit (Stratagene). For the complementation test, the *SOC1* genomic fragment consisting of 1.97 kb of the promoter region and the full gene coding region plus introns was amplified and cloned as previously reported (Liu et al., 2008). The genomic constructs containing the M1 and M2 mutations were further generated using the QuikChange II XL-Site-Directed Mutagenesis Kit (Stratagene).

For the construction of *ProSOC1:GUS*, the *SOC1* genomic sequence of 4.4 kb was amplified with the primers SOC1-P4-*Xma*I and SOC1-R1-*Xma*I (Table 2). The amplified products were digested by *Xma*I and cloned into the corresponding site of pHY107. This construct was further mutagenized to produce the mutated AGL24 and SVP binding sites by using the QuikChange® II XL-Site-Directed Mutagenesis Kit (Stratagene). For generation of the mutated CArG box for AGL24 binding, the primers SOC1-M1-F2 and SOC1-M1-R2 (Table 2) were used. For generation of two mutated CArG boxes for *SVP* binding, two pairs of primers, SOC1PM3-F and SOC1PM3-R and SOC1PM4-F and SOC1PM4-R (Table 2), were used, respectively.

A derivative pGreen-35S vector (Yu et al., 2004) was cut by *Kpn*I and *Xho*I to remove the 35S promoter, filled in the ends by T4 DNA polymerase, and self-ligated to generate a promoterless pGreen vector pHY105. A GUS fragment was then amplified from pBI101 and cloned into the *Xba*I site of pHY105 to generate pHY107.

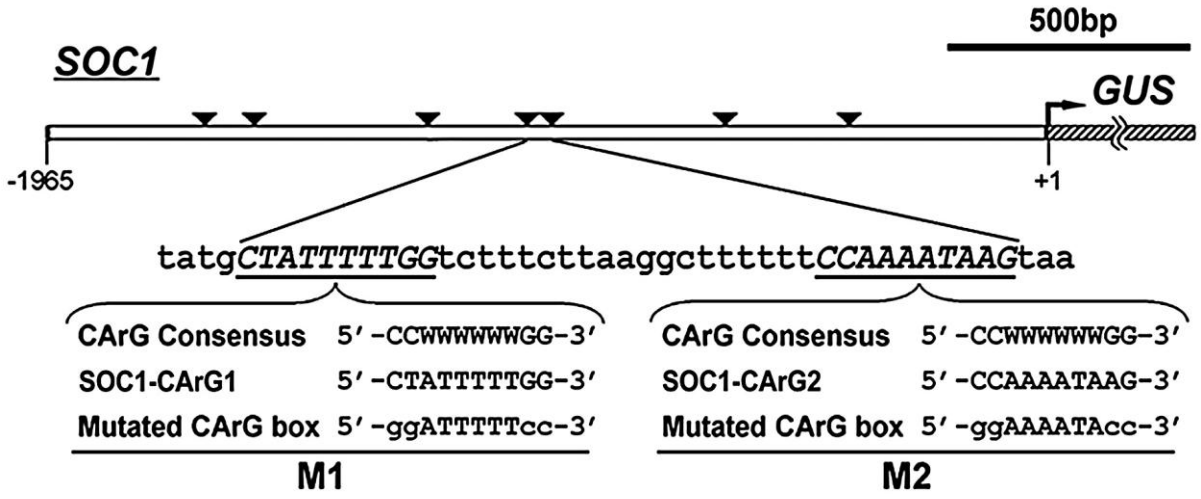

Figure 3. Schematic diagram of the SOC1:GUS construct. 2 kb SOC1 5′ upstream sequence was transcriptionally fused with the GUS gene. Two native CArG boxes within fragment 5 were mutated as indicated.

These constructs were introduced into wild-type Columbia plants using the *Agrobacterium*-mediated floral dip method (Clough and Bent, 1998). The T3 homozygous lines with single insertion of transgenes were isolated for most studies, while both T2 and T3 plants were used for GUS expression analysis.

3.7 Gel Shift Assay

The full-length SVP cDNA was cloned into PQE-30 vector (QIAGEN), which was subsequently transformed into *E. coli* strain Rosetta (DE3) (Novagen). 6×His-SVP was induced using sopropyl 1-thio-β-D-galactopyranoside (IPTG) and affinity-purified using Ni-NTA Agarose (QIAGEN) according to the manufacturer's protocol. DNA binding assays were performed using LightShift Chemiluminescent EMSA Kit (Pierce).

3.8 In Vitro Pull-Down Assay

The full-length *SVP* and *FLC* cDNA sequences were cloned into the pGEX-4T-1 vector (Pharmacia). *E. coli* strain Rosetta (DE3) (Novagen) transformed with the plasmids was induced by IPTG. *E. coli* cells were then harvested and lysed. After centrifugation, the supernatant was used to incubate with Glutathione sepharose beads (Amersham Biosciences). The beads with the bound GST-SVP and GST-FLC proteins were subsequently washed and used in GST pull-down assays.

For synthesis of myc-tagged SVP and HA-tagged FLC proteins, the full-length *SVP* and *FLC* cDNA sequences were cloned into the pGBKT7 and pGADT7 vectors (Clontech), respectively. Following the manufacturer's instructions, the plasmid DNA templates were added to the TNT T7 Quick Coupled Transcription/Translation Systems (Promega) to synthesize proteins. GST-FLC or GST-SVP proteins prebound to Glutathione sepharose beads were mixed with the in vitro translated myc-tagged SVP or HA-tagged FLC proteins. The beads were washed, and the eluted proteins were separated by SDS-PAGE. Myc-tagged SVP and HA-tagged FLC proteins were detected using anti-Myc antibody (Sigma) and anti-HA antibody (Santa Cruz biotechnology).

3.9 Chromatin Immunoprecipitation (ChIP) Assay

3.9.1 Nuclear fixation

Seven-day-old *35S:SVP-6HA* and *svp-41 SVP:SVP-6HA* seedlings were immediately soaked in MC buffer (10 mM potassium phosphate, pH 7.0, 50 mM NaCl, and 0.1 M sucrose) with 1% formaldehyde that was freshly added. The materials were then infiltrated under vacuum pressure for 45 min at 4℃. When vacuum pressure was released, the formaldehyde was quenched by incubation in 0.15 M glycine for 60 min at 4℃. This was followed by washing the fixed tissues with fresh MC buffer three times at 4℃ for 20 min. After these treatments, the fixed materials were either stored at -80℃ for future use or applied immediately into the following procedures.

3.9.2 Homogenization and sonication

About 1.0 g of fixed materials were ground with mortar and pestle using liquid nitrogen, and mixed thoroughly with M1 buffer (10 mM potassium phosphate, pH 7.0, 0.1 M NaCl, 10 mM β-mercaptoethanol, 1M 2-methyl 2, 4-pentanediol, and 1mM PMSF). The slurry was centrifuged at 14,000 rpm for 10 min at 4℃. After discarding the supernatant, the pellet was resuspended in M2 buffer (10 mM potassium phosphate, pH 7.0, 0.1 M NaCl, 10 mM β-mercaptoethanol, 1 M 2-methyl 2, 4-pentanediol, 10 mM $MgCl_2$, and 0.5% Triton X-100), and subsequently centrifuged

at 14,000 rpm for 10 min at 4℃. The above step was repreated thrice to ensure that the pellet was thoroughly washed. The resulting pellet was resuspended in M3 buffer (10 mM potassium phosphate, pH 7.0, 0.1M NaCl, and 10 mM β-mercaptoethanol), and centrifuged at 14,000 rpm for 10 min at 4 ℃. The supernatant was discarded and the pellet was subjected to the sonication step.

For sonication, the crude nuclear extract was resuspended in 0.5 ml sonication buffer (10 mM potassium phosphate, pH 7.0, 0.1 mM NaCl, 0.5% sarkosyl, and 10 mM EDTA). The nuclear extract was then sheared with a probe sonicator (Misonix, XL-2020 Sonicator®). The output power was controlled at about 65 W with each pulse lasting for 4 min and repeated 3 times. Between two continuous pulses, the chromatin solution was cooled on ice for 1 min. After sonication, the solution was centrifuged at 14,000 rpm for 5 min at 4℃ and the supernatant was transferred into a new microcentrifuge tube. About 1/10 of the sonicated sample was set aside as "input", which was used for Western blot analysis and PCR enrichment test, while the remaining samples were subjected to immunoprecipitation.

3.9.3 Immunoprecipitation (IP)

Before incubating the sheared chromatin with the immunoprecipitation column, 25 μl of anti-HA antibody conjugated with agarose beads was washed three times with sonication buffer. After incubation with the antibody for 2 h at 4℃ on a shaker, the mixture was centrifuged at 3,000 rpm for 1 min. The supernatant was retained as the post-bind sample, while the remaining anti-HA beads were washed 4 times with IP

buffer (50 mM Tris, pH 8.0, 1% SDS, and 10 mM EDTA) lasting 5 min each. To elute, the anti-HA antibody beads were incubated with 400 μl of elution buffer (50 mM Tris, pH 8.0, 1% SDS, and 10 mM EDTA) at 65 °C for 30 min on a shaker. The beads were precipitated at 14,000 rpm at room temperature for 1 min and the supernatant was collected. An additional 100 μl of elution buffer (50 mM Tris, pH 8.0, 1% SDS, and 10 mM EDTA) was incubated with beads at 65°C for 5 min. Of the total volume of 500 μl eluant, 20 μl was retained for Western blot analysis, while the remaining was subjected to the DNA recovery step.

3.9.4 Western blot

For Western blot, 20 μl of protein sample was mixed with 4.5 μl of 6 X SDS-PAGE loading buffer (300 mM Tris-HCl, pH 6.8, 12% SDS, 0.6% bromophenol blue, and 60% glycerol) and 2.7 μl of 1 M β-mercaptoethanol and denatured in boiling water for 5 min. The protein sample was then separated on denaturing 12.5% (w/v) polyacrylamide gels and blotted onto immun-Blot^{TM} PVDF membrane (Bio-Rad). The membrane was blocked with 5% non-fat dry milk (dissolved in PBS buffer) for 1 hour, and incubated with 1:10000 (v/v) anti-HA or anti-TAP alkaline phosphatase conjugate antibody (Sigma) (diluted with PBS buffer supplemented with 0.05% Tween 20) at room temperature for 1 h. The membrane was subsequently washed three times with PBS buffer containing 0.05% Tween 20 for 15 min each. Finally, the membrane was treated with CDP-Star (Roche) and exposed to CL-X Posure X-ray film (Pierce).

3.9.5 DNA recovery

The eluted chromatin complex and the input DNA were first incubated with 1 μl of RNase A (1 mg/ml) at 37°C for 30 min, and then treated overnight with 0.5 mg/ml Proteinase K at 37°C. After a first round of incubation, a second aliquot of Proteinase K was added and the solution and incubated at 65°C for 6 hours to reverse the formaldehyde crosslink. The released DNA was subsequently extracted by phenol:chloroform and precipitated with standard protocols. Briefly, an approximately equal volume of extraction solution A (50% v/v Tris saturated phenol, 48% v/v chloroform, and 2% v/v isoamyl alcohol) was added and mixed with the chromatin solution. After centrifugation, the aqueous layer was collected and mixed with an equal volume of extraction solution B (96% v/v chloroform and 4% v/v isoamyl alcohol). The solution was further centrifuged. The aqueous layer was transferred into a new microcentrifuge tube and precipitated overnight at -20°C by adding 1 μl glycogen (20 mg/ml), 1/10 volume of 3 M sodium acetate, and 2.5 volumes of absolute ethanol. DNA was eventually pelleted at 14,000 rpm at 4°C for 20 min and washed twice with 70% ethanol. The DNA pellet was completely dried, and dissolved in 30 μl water. The recovered DNA was analysed for the DNA enrichment via PCR by using different gene specific primers. All primer sequences used for ChIP enrichment tests are listed in Table 4. ChIP assays were performed for at least three independent rounds. For identification of the precise binding sites of SVP, DNA enrichment was evaluated by real-time quantitative PCR in triplicates. Relative enrichment of each

fragment was calculated first by normalizing the amount of a target DNA fragment against a genomic fragment of *ACTIN* as an internal control, and then by normalizing the value for transgenic plants against the value for wild-type as a negative control using the following equation $2^{(Ct_{SVP\text{-}6HA\ Input} - Ct_{SVP\text{-}6HA\ ChIP})} / 2^{(Ct_{WT\ Input} - Ct_{WT\ ChIP})}$. All primer sequences used for the ChIP enrichment test are listed in Table 4.

3.9.6 CArG motif analysis

For the analysis of CArG motif, genomic sequences that had been identified were sent to MatInspector at the web site: http://www.genomatix.de/index.html. The CArG box motif was set as CCWWWWWWGG with maximal one mismatching base pair.

3.10 Coimmunoprecipitation Experiments

Plant material grown in LDs was harvested at different developmental stages. After the frozen samples were ground with mortar and pestle in liquid nitrogen, proteins were extracted as previously published (Sawa et al., 2007). For immunoprecipitating HA-tagged SVP protein, anti-HA agarose (Sigma) was added into the protein extract before it was incubated at 4℃ for 1 hr. For immunoprecipitating FLC protein, the protein extract was immunoprecipitated with affinity-purified anti-FLC antibody and Protein G PLUS-Agarose (Santa Cruz biotechnology). All coimmunoprecipitation experiments were performed in biological

Primer Pairs Used for ChIP Assay of SVP Binding on the *SOC1* Sequence

Primer	Sequence
1	5′-TATATCGGGAGGAGGACCACAC-3′
	5′-ATCCATACAGATTTTCGGACCT-3′
2	5′-GAGGCTAGTACAGAGACAATGG-3′
	5′-GACCAAAAATAGCAAATGCCTC-3′
3	5′-TCTCGTACCTATATGCCCCCACT-3′
	5′-TTTATCTGTTGGGATGGAAAGA-3′
4	5′-AGTTGGATGGAAATGCCTGTCA-3′
	5′-TTACAAGTGGGGGCATATAGGT-3′
5	5′-TGGACGCTTGAAACCTCATCCT-3′
	5′-GGGAGGGAAAAAGATGTGTATG-3′
6	5′-GCAAAAGAAGTAGCTTTCCTCG-3′
	5′-AGCAGAGAGAGAAGAGACGAGTG-3′
7	5′-AAAAACCTAACCAGGAGGAAGC-3′
	5′-CTTCTTCTCCCTCCAGTAATGC-3′
8	5′-GGATGCAACCTCCTTTCATGAG-3
	5′-ATATGGGTTTGGTTTCATTTGG-3′
9	5′-ATCACATCTCTTTGACGTTTGCTT-3′
	5′-GCCCTAATTTTGCAGAAACCAA-3′
10	5′-CTTTTGGTTTGAACTAATCTTTGTCTTG-3′
	5′-AATGAGCATGAAATGAAGCATGA-3′
11	5′-TGTTTCAGACATTTGGTCCATTTG-3′
	5′-AGTCTTGTACTTTTTCCCCCTATTTTAG-3′
ACTIN	5′-CGTTTCGCTTTCCTTAGTGTTAGCT-3′
	5′-AGCGAACGGATCTAGAGACTCACCTTG-3′

Table 4 Primer Pairs Used for ChIP Assays

triplicate. The immunoprecipitated proteins and the protein extract as an input were resolved by SDS-PAGE. SVP-HA, FLC, or actin protein was detected by western blot using anti-HA (Santa Cruz Biotechnology), affinity-purified anti-FLC (Helliwell et al., 2006), or anti-mouse actin antibody (Sigma), respectively.

CHAPTER 4

Results

4.1 Construction of gene tagged plasmids

4.1.1 SVP tagging systems

Although it has been reported that *SVP* functions in the control of flowering time (Hartmann *et al.*, 2000), the concrete mechanism of *SVP* in this process is not clear. To facilitate the investigation of the role of *SVP* in the relevant regulatory network, we planned to use the ChIP method to isolate its direct downstream genes. Since *SVP* antibody was unavailable, the tagging polypeptides of 12HA, 6HA, GR (glucocorticoid receptor), TAP, StrepII, and 9Myc epitopes that had commercially available antibodies were fused with the C-terminal of *SVP* under the control of the cauliflower mosaic virus 35S promoter.

The *35S::SVP-GR-12HA/35S::SVP-GR-TAP/35S::SVP-GR-9Myc* constructs were produced as follows**:** The coding region of *SVP* was amplified from pGEM®-T Easy Vector that contained the *SVP* cDNA by using primers SVP-F2 and SVP-R3 (Table 1). The PCR fragment was cloned into the *Xho*I and *Apa*I sites of pGreen0244 (with hormone binding domain GR followed by different tags, such as 12HA, TAP and 9Myc) (Figure 3). The *35S::SVP-12HA, 35S::SVP-TAP* and *35S::SVP-9Myc* constructs were further derived by excising the GR fragment with *Xma*I from *35S::SVP-GR-12HA, 35S::SVP-GR-TAP* and *35S::SVP-GR-9Myc* respectively (Figure 3).

The fusion of GR at the C or N terminal of *SVP* was produced by amplifying the *SVP* coding region with primers SVP-F1 and SVP-R2 (Table 5), and cloning into the

*Eco*RI and *Bam*HI sites of HY209 that contains a 35S promoter with tandem enhancers and multiple cloning sites (MCS) followed GR or HY106 that contains a 35S promoter with tandem enhancers and GR followed by MCS (Figure 3).

The *SVP* fragment amplified by primers SVP-F1 and SVP-R1 (Table 1) was cloned into the *Eco*RI and *Bam*HI sites of the vector LC101 (35S::StrepII) to form *35S::SVP-StrepII. 35S::SVP-6HA* was created by cloning the *SVP* fragments amplified by primers SVP-F1 and SVP-R5 (Table 1) into the *Eco*RI and *Spe*I sites of the vector OE6HA (35S::6HA) (Figure 4).

Table 5. Primers used in molecular cloning

Primer name	Sequence 5'-3'	Restriction site
SVP-F2	CCGCTCGAGCTAAGCTCTCTCTCTTGCTTCTAGG	*XhoI*
SVP-R3	ATGGGCCCACCACCATACGGTAAGCCGAGCCTA	*ApaI*
SVP-R5	GGACTAGTACCACCATACGGTAAGCCGAGCCTAA	*SpeI*
35S Pro	GACCCTTCCTCTATATAAGGAAGTTC	
PG-P4	ATGGGCCCGAGACTGGTGATTTCAGCGAA	*ApaI*
GSVP-STRF1	GATCCTGGTCTCATCCTCAATTTGAAAAATAAG	*BamHI*
GSVP-STRR1	GATCCTTATTTTTCAAATTGAGGATGAGACCAG	*BamHI*
SVP-F1	CGGAATTCGTTGTGATGGCGAGAGAA	*EcoRI*
SVP-R1	CGGGATCCTTCCATCTCTAACCACCA	*BamHI*
SVP-F3	GGACTAGTATGGCGAGAGAAAGAGTT	*SpeI*
SVP-R2	GCTCTAGACTAACCACCATACGGTAA	*XbaI*

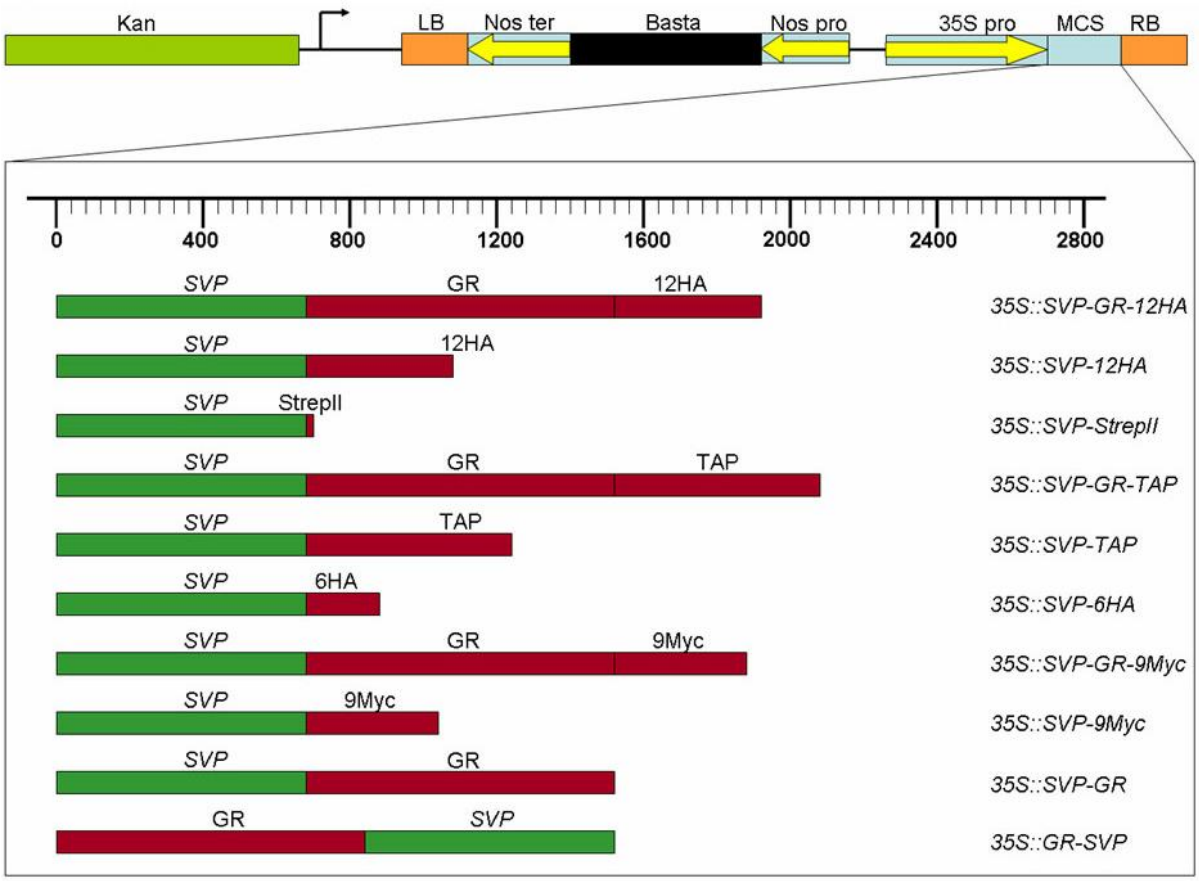

Fig 4. Construction of *SVP* tagging vectors. The pGreen vector contains the 35S promoter, multiple cloning site (MCS), selectable marker kanamycin and Basta. Different *SVP-tags* fusion genes were cloned based on this pGreen vector.

4.1.2 XVE inducible expression system

XVE system is an estrogen receptor-based chemical-inducible system in transgenic plants. This system is a reliable and efficient chemical-inducible system for regulating transgene expression in plants. The chimeric transcription activator, XVE, is assembled by the fusion of a DNA-binding domain of the bacterial repressor LexA (X), an acidic transactivating domain of VP16 (V) and a regulatory region of the human estrogen receptor (E) (Figure 4). The transactivating activity of the chimeric XVE factor is strictly regulated by estrogens. In this study, the *SVP* fragment was cloned after eight copies of the LexA operator downstream of the -46 35S minimal promoter. The estradial-activated XVE could induce *SVP* expression by VP16 when LexA was bound with its operator upstream of *SVP*. This system allowed the induction of *SVP* at a specific time point, hence facilitating the study of its immediate effect. For this reason, it can be used for microarray analysis.

XVE::SVP-6HA and *XVE:SVP-StrepII* constructs (Figure 5) were produced by cloning the SVP-6HA and SVP-StrepII fragments, which were amplified by primers 35S pro and PG-P4 (Table 1) from *35S::SVP-6HA* and *35S::SVP-StrepII,* into the *Xho*I and *Apa*I sites of pER8 vector (containing XVE promoter)

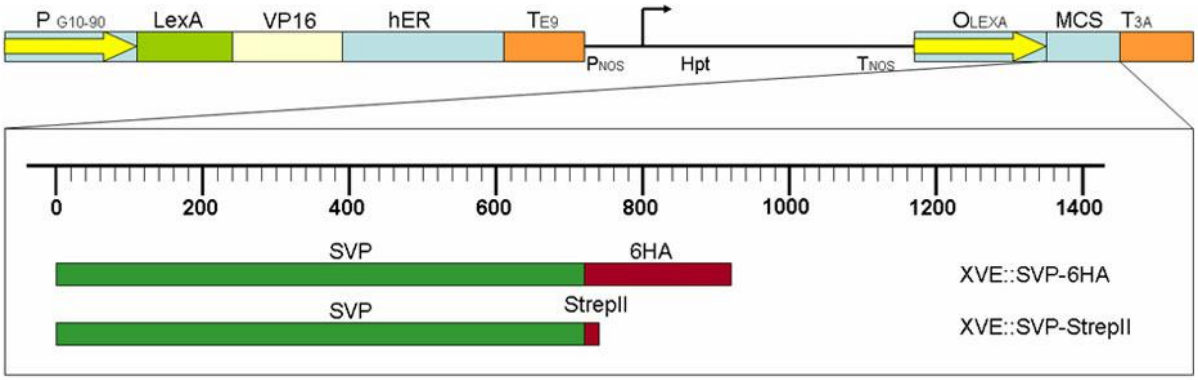

Fig 5. Construction of *SVP* inducible vectors. The XVE vector contains the DNA-binding domain of LexA, transcription activation domain of VP16, regulatory region of human estrogen receptor (hER) and eight copies of the LexA operator sequence (OLEXA). *SVP-HA* or *SVP-StrepII* fusion genes were cloned after OLEXA.

4.1.3 SVP native expression system

Both 35S over-expression system and XVE inducible system has some potential side effects to disturb endogenous development context. For example, in 35S over-expression system, constitute over-expression of *SVP* driven by the 35S promoter would lead to an ectopic expression of *SVP* in certain tissues where it is not originally expressed. Hence, changes in the spatial and temporal pattern of expression of *SVP* could mask or interfere with downstream effects. To avoid this problem, the *SVP* native promoter system was created, in which we simulated the same *SVP* expression pattern as wild-type plant by using a *SVP* genomic fragment containing the *SVP* native promoter, introns, exons and followed by an affinity tag. This system could provide more accurate information about the direct targets or protein partners of *SVP* compared with the constitutive expression systems.

To create the above constructs, the *SVP* genomic sequence was amplified from *Arabidopsis* genomic DNA using primers SVP-P1 and SVP-P5 (Table 7). The resulting fragment was then cloned into the *Pst*I and *Xma*I sites of the vector HL101 containing the 6HA tag to get the construct of *SVPG-6HA* (Figure 6). *SVPG-StrepII* was produced by replacing the 6HA fragment with StrepII fragment amplified by primers GSVP-STRF1 and GSVP-STRR1 directly (Table 6) into the *Bam*HI site of *SVPG-6HA* plasmid.

4.2 Selection of transformants with functional SVP tagging protein

Table 7. Primers used in the *SVP* promoter studies

Primer name	Sequence 5'-3'
SVP-P1 (PstI)	AACTGCAGGGGTGAGTGATACGAGCCACACTTATT
SVP-P2 (PstI)	AACTGCAGCAGCAAGTTATATGCCACATGATTGAC
SVP-P3 (BamHI)	CGGGATCCGCTGGAGCTACAGAACTCGAACAGTT
SVP-P4 (BamHI)	CGGGATCCTTCAAGGGCCTTCTCTAGCTGCTGAAG
SVP-P5 (BamHI)	CGGGATCCACCACCATACGGTAAGCTGCACAACAC

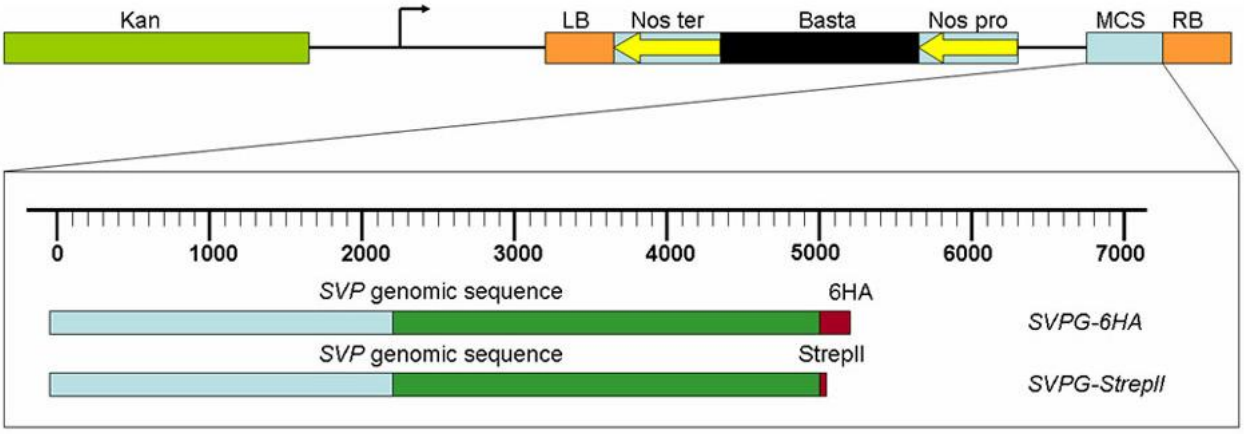

Fig 6. Construction of *SVP* native expression vectors. The pGreen vector without 35S promoter was cloned with the native *SVP* genomic sequence tagged with HA or StrepII.

The above mentioned constructs were transformed into *Arabidopsis* (Columbia ecotype) plants via Agrobacterium-mediated transformation. Transformed lines at the T1 generation that survived Basta or hyromycin selection were screened for their phenotypes, and only those lines that showed late-flowering phenotype as *35S::SVP* were selected. After genetic segregation at the T2 generation and T3 progenies' resistance to selection agents, we eventually identified the homozygous lines with single insertion of the transgene for further studies.

Among the *SVP* tagging constructs created, *35S::SVP-6HA* (T3 generation) and *SVP::SVP-6HA* (T3 generation) showed obviously late-flowering phenotype (15-18 rosette leaves) compared with wild-type plant (8-10 rosette leaves), although they still flowered earlier than strong *35S::SVP* lines (35-40 rosette leaves) (Figure 6a). RT-PCR results further showed that the late-flowering phenotype corresponded to the over-expression of *SVP* (Figure 7b, 7c). These results indicated that SVP-12HA and SVP-TAP fusion proteins had the similar biological function as SVP protein as a repressor of flowering. Thus, corresponding transgenic lines could be used for ChIP experiments to detect the *in vivo* direct targets of SVP protein.

The T2 seeds of *XVE::SVP-6HA* and *XVE::SVP-StrepII* have been harvested, and the transformed lines are being identified via hygromycin selection on MS media.

The T1 seeds for *SVPG-6HA* and *SVPG-StrepII* have been collected, and the transformed lines are being identified via Basta selection on soil.

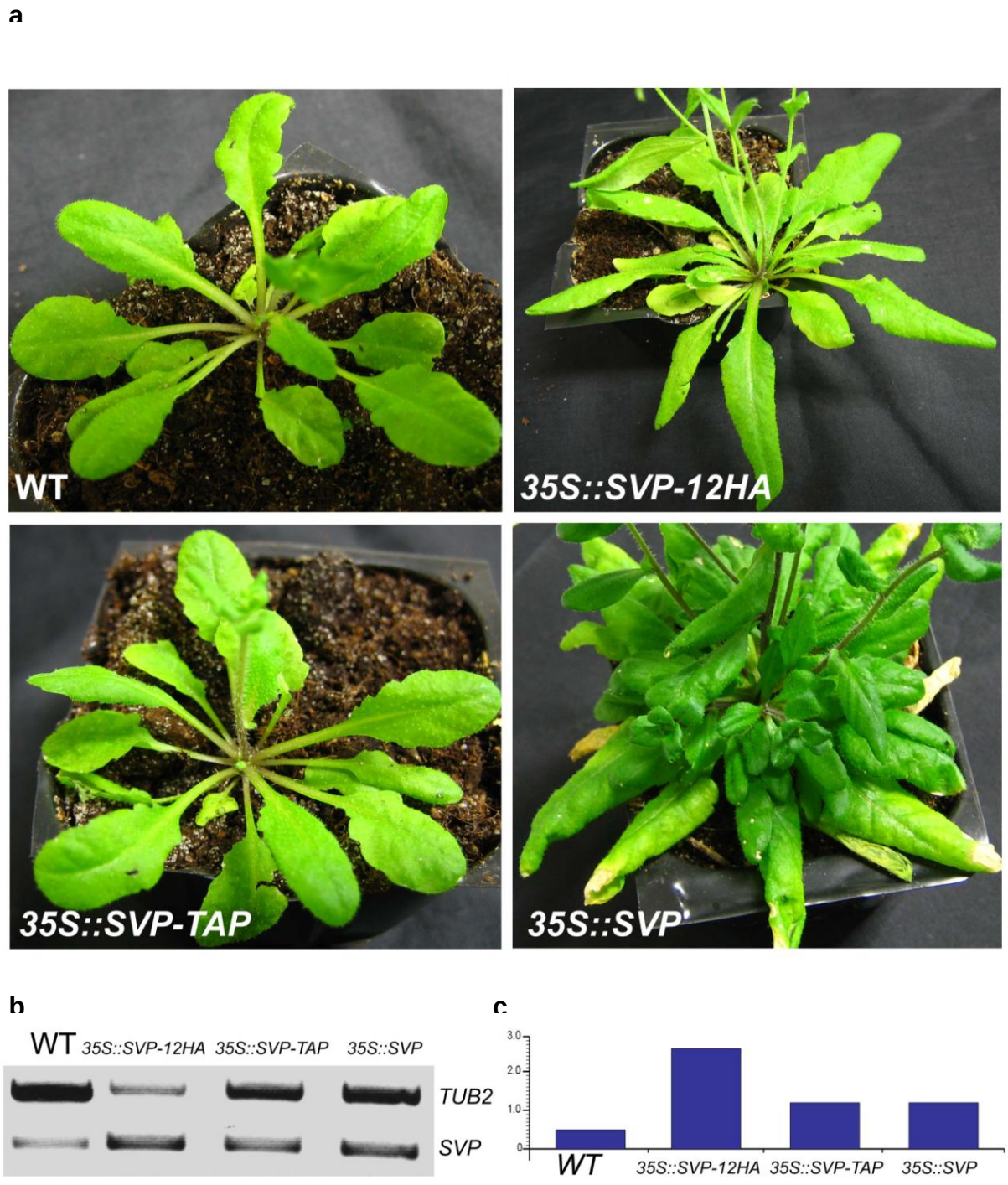

Fig 7. Functional *35S::SVP-6HA* and *SVP::SVP-6HA* tagging lines were selected for further studies. (a) *35S::SVP-6HA* and *SVP::SVP-6HA* transgenic plants show moderate late-flowering as compared with 35S::SVP and wild-type plants. (b) *SVP* expression in wild-type, *35S::SVP-6HA*, *SVP::SVP-6HA* and *35S::SVP*. *TUB2* serves as an internal control. (c) Quantitative analysis of *SVP* expression in (b).

4.3 The GA and Autonomous Pathways Regulate *SVP* Expression

To understand the role of SVP in the control of flowering time, we examined the effect of various flowering genetic pathways on its expression in whole seedlings.

4.3.1 Vernalization pathway

Genes in the vernalization pathway mainly act to promote flowering by epigenetic down-regulation of the *FLC* expression. To determine whether *SVP* might act in the vernalization pathway, the effect of vernalization on *SVP* expression was determined in *FRI*-dominant seedlings (Figure 8). The plants harvested for RNA isolation were first cold treated at 4°C for 40 days, and then grown for 2 weeks at normal growth temperatures (22°C). Wild-type and *FRI FLC* seedlings that were subjected to cold treatment for only 4 days were used as controls. From the result, *vernalization treatment of wild-type and FRI FLC plants (Michaels and Amasino, 1999), which greatly affects the expression of FLC and SOC1, did not regulate SVP expression (Figure 8).*

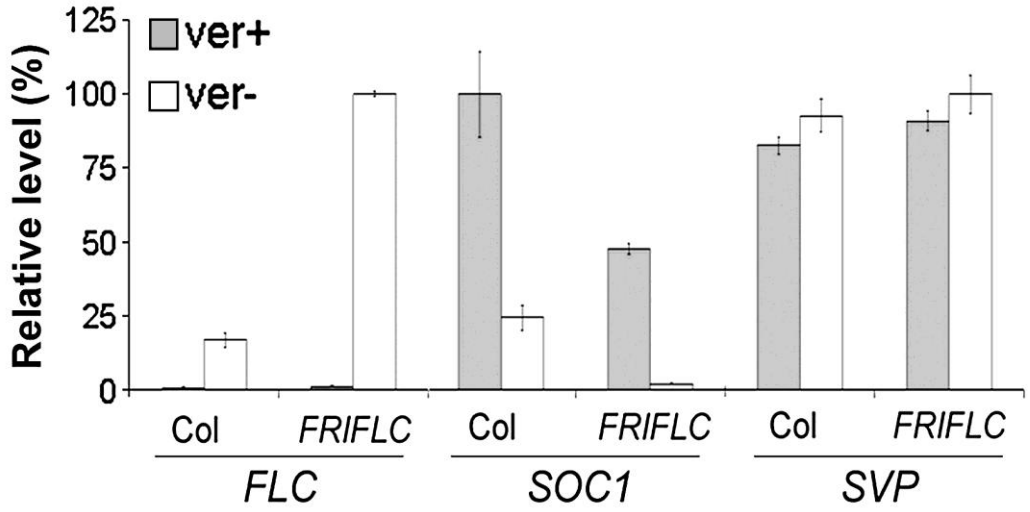

Fig 8. Effect of vernalization on *SVP* expression. For vernalization treatment, seeds were sown on Murashige and Skoog (MS) agar plates and incubated at 4℃ under low light levels for 8 weeks. The expression of *FLC*, *SOC1*, and *SVP* in 9-day-old seedlings grown in LDs was compared. The maximum expression of each gene is set as 100%.

4.3.2 Autonomous pathway

The autonomous pathway promotes flowering by suppressing *FLC* expression, and mutants in this pathway are late-flowering due to elevated levels of *FLC*. In order to study whether *SVP* plays a role in this pathway, the expression levels of *SVP* in autonomous pathway mutant *(fve)* were determined (Figure 9). The result showed that, *in long days (LDs), SVP expression was consistently upregulated in loss-of-function mutants of fve-3 (Col) and fve-1 (Ler) in the autonomous pathway (Figure 9). In addition to its role in the autonomous pathway, FVE also mediates ambient temperature effects ([Blazquez et al., 2003] and [Koornneef et al., 1991]). Thus, SVP expression is affected by both the autonomous and thermosensory pathways (Lee et al., 2007).*

4.3.3 Photoperiod pathway

A Previous study suggested that *SVP* might act downstream in the photoperiod pathway (Scortecci *et al.*, 2003). To prove this hypothesis, the *SVP* expression was examined in some photoperiod pathway mutants *(co-1, gi-1* and *ft-1*) (Figure 10a). The result suggested SVP expression remained almost unchanged in photoperiod loss-of-function mutants (Figure 10a and 10b).

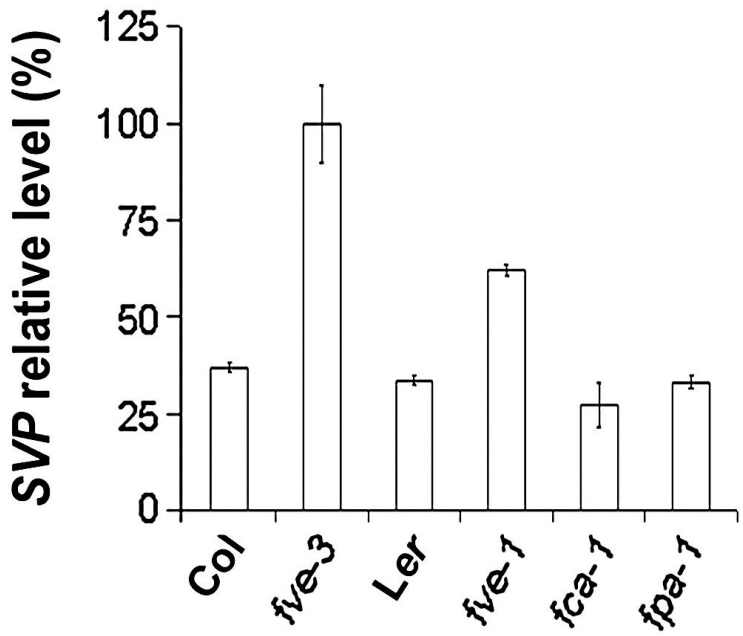

Fig 9. Quantitative real-time PCR analysis of *SVP* expression in the mutants of the autonomous pathways. *SVP* expression in 9-day-old seedlings grown in LDs was compared. Results were normalized against the expression of *TUB2*.

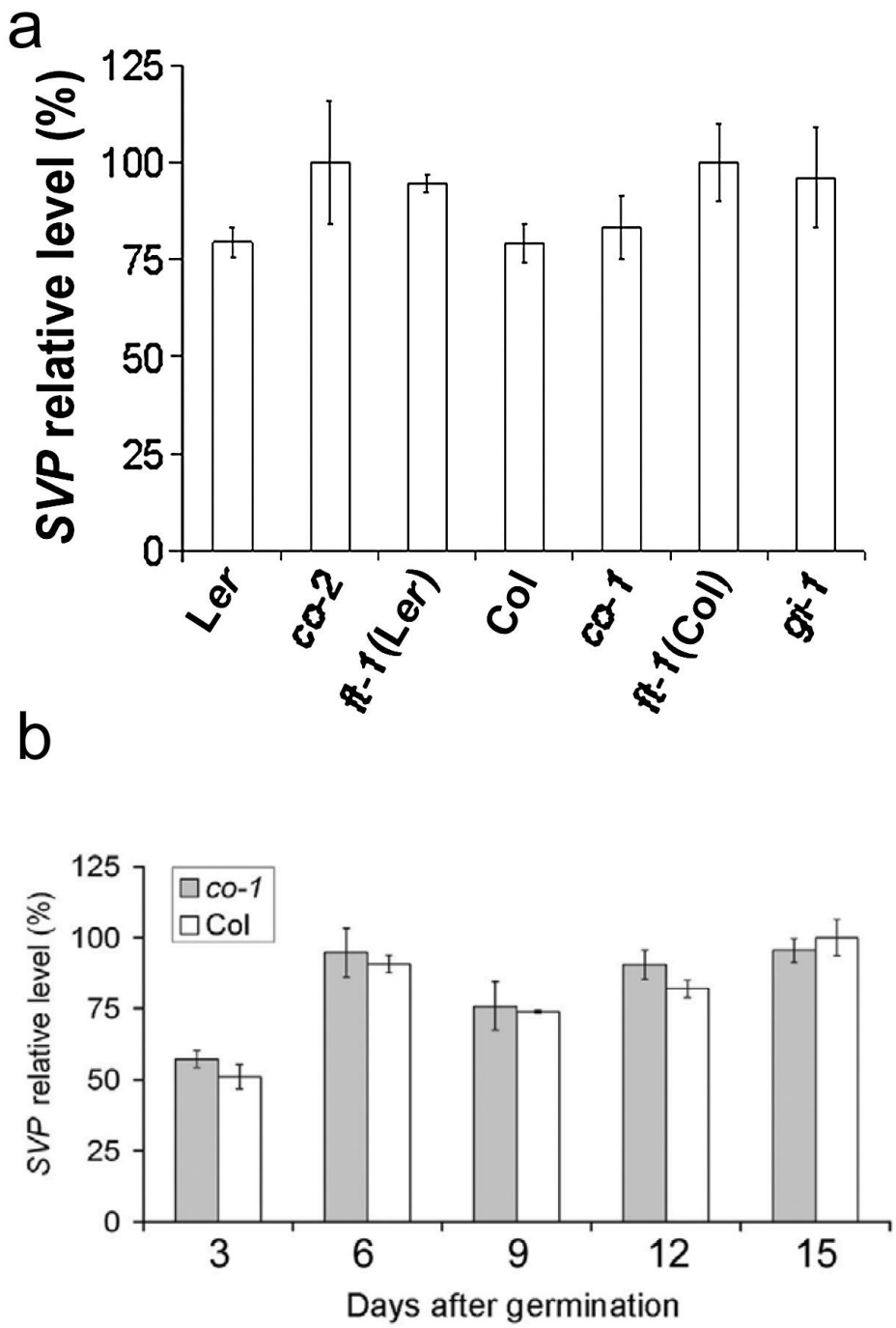

Fig 10. **Quantitative real-time PCR analysis of *SVP* expression in the mutants of the photoperiod pathways.** (a). *SVP* expression in 9-day-old seedlings grown in LDs was compared. (b). Time-course study of *SVP* expression in *co-1* from 3 to 15 days after germination. Results were normalized against the expression of *TUB2*.

4.3.4 GA pathway

To determine whether *SVP* plays a role in the GA pathway, *SVP* expression in wild-type plants with or without GA treatment grown under short day (SD) condition were compared. *GA treatment consistently reduced SVP expression in wild-type plants in SDs* (Figure 11a). *In the GA-deficient mutant ga1-3, which does not flower in SDs (Wilson et al., 1992), SVP expression was consistently higher than in wild-type plants* (Figure 11b), *implying that the GA effect on flowering is partly mediated through SVP.* These results demonstrate that *SVP* responds to the flowering signals from the GA and autonomous pathways, in addition to the thermosensory pathway.

In summary, both photoperiod and GA pathways are involved in inhibiting *SVP* expression and consequently promoting floral transition.

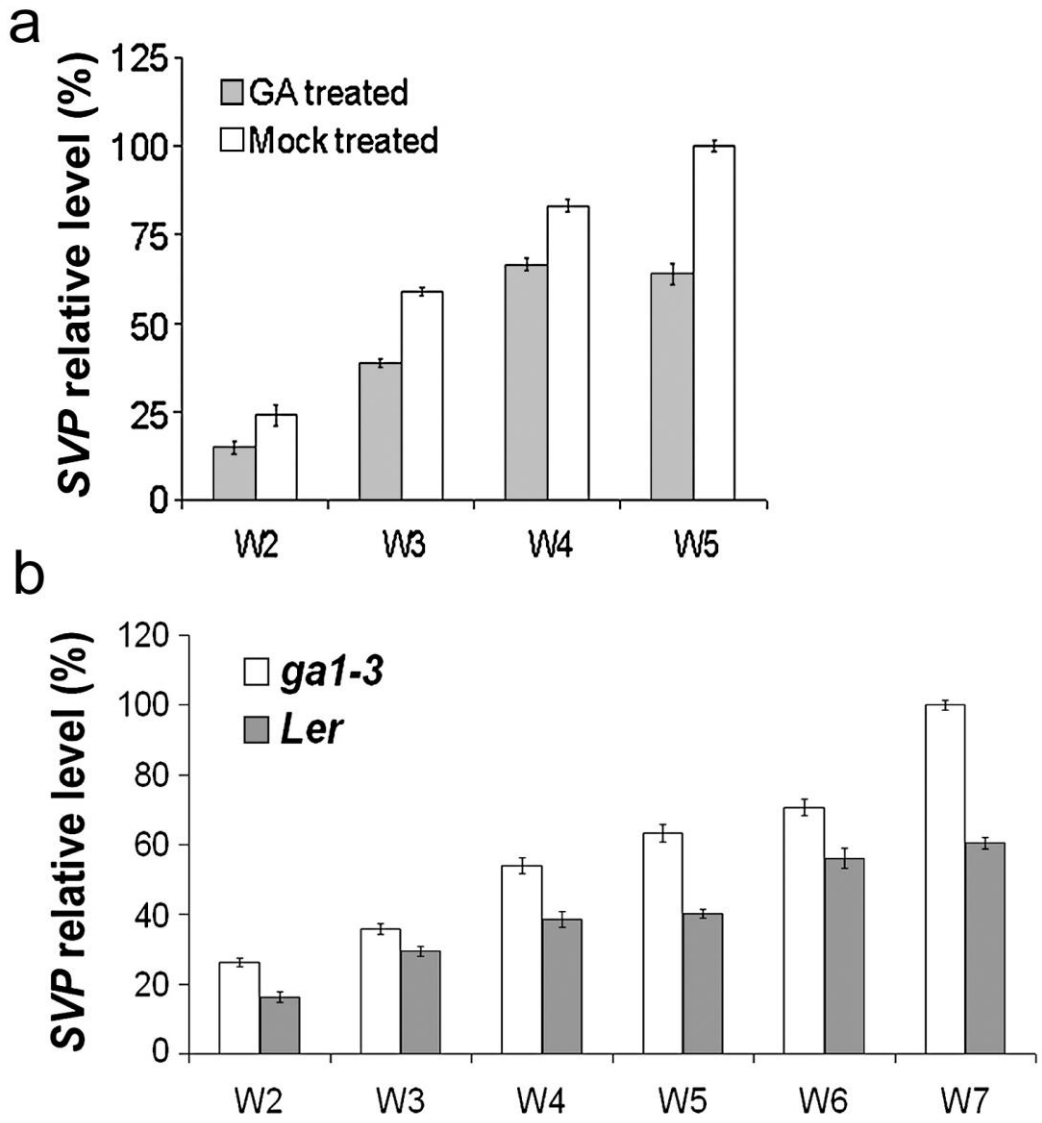

Fig 11. **Effect of GA on *SVP* expression in SDs.** (a) For GA treatment, exogenous GA (100 μM) was weekly applied onto wild-type Col plants grown in SDs. Seedlings from week 2 (w2) to week 5 (w5) were harvested for expression analysis. (b) Comparison of *SVP* expression in GA-deficient mutant *ga1-3* (L*er*) and wild-type L*er* plants. Seedlings grown in SDs from week 2 (w2) to week 5 (w5) were harvested for expression analysis.

4.4 Identification of putative regulatory domain within the *SVP* promoter

In order to localize the regulatory elements within the *SVP* genomic sequence, derivatives of a 5.4 kb fragment compassing the 5' upstream region, introns and exons, were generated and fused to the *E.coli* uidA gene encoding the beta-glucuronidase (GUS) enzyme (Figure 12).

4.4.1 Generation of GUS reporter gene constructs

The P2, P3, P4 and P5 fragments of *SVP* genomic sequences were amplified using the plant genomic DNA as a template by primer pairs SVP-P1/SVP-P4, SVP-P2/SVP-P3, SVP-P2/SVP-P5, SVP-P2/SVP-P4 (Table 8). They were directionally cloned into pGreen-GUS using the *Pst*I and *Bam*HI sites (Figure 12).

These constructs were used to define the minimal region required for endogenous expression of *SVP*. They were introduced into the *Arabidopsis* genome and at least three independent stably transformed lines were analyzed for each construct. Plant tissues from each line (T3 generation) were stained for GUS enzyme activity and analyzed for GUS localization. The distribution of GUS enzymatic activity for each construct was usually consistent for the different lines tested. A time course study was carried out for each transgenic line from Day 6 to Day 41 to characterize GUS staining patterns before floral transition (Day 6 to Day 17).

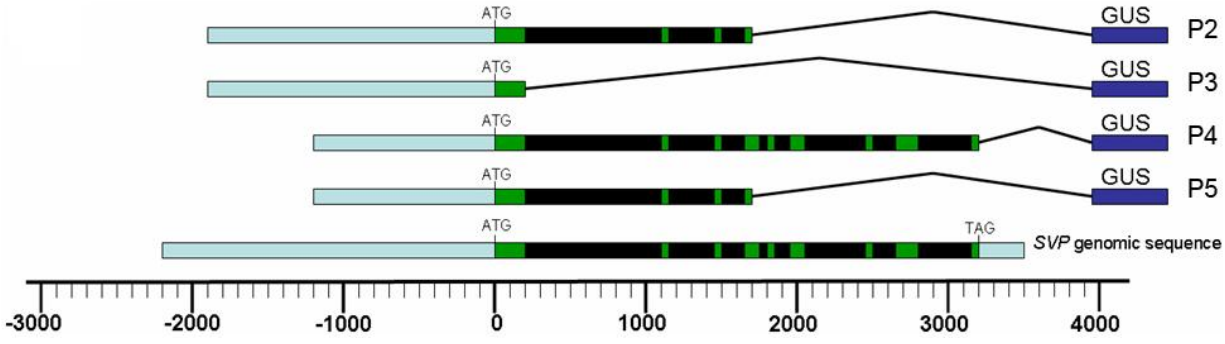

Fig 12. *SVP* promoter study constructs. The 5.7 kb *SVP* promoter region is shown. Selected regions used in the GUS fusion constructs are depicted schematically. The black regions are denoted introns and the green regions are denoted exons.

Primer name	Sequence 5’-3’
SVP-P1 (PstI)	AACTGCAGGGGTGAGTGATACGAGCCACACTTATT
SVP-P2 (PstI)	AACTGCAGCAGCAAGTTATATGCCACATGATTGAC
SVP-P3 (BamHI)	CGGGATCCGCTGGAGCTACAGAACTCGAACAGTT
SVP-P4 (BamHI)	CGGGATCCTTCAAGGGCCTTCTCTAGCTGCTGAAG
SVP-P5 (BamHI)	CGGGATCCACCACCATACGGTAAGCTGCACAACAC

Table 8. Primers used in the *SVP* promoter studies

4.4.2 GUS staining results

Plants harbouring the P2 construct containing the 3.6 kb *SVP* promoter displayed GUS expression in leaves and stems from Day 6 to Day 17 (Figure 13 A-D). The transformants containing the P5 construct also showed a similar expression pattern but with much lower enzymatic activity (Figure 13 M-P). Plants containing P3 constructs displayed almost no GUS expression (Figure 13 E-H). The differences in staining seen among P2, P3 and P5 indicate that the regions from -1,800 bp to -1,200 bp and +200 bp to +1,700 bp are important in driving normal *SVP* expression (Figure 12).

Interestingly, transformants containing the P4 construct, which is 1.4 kb longer than P5, showed little GUS activity from Day 6 to Day17 (Figure 13 I-L). This staining pattern may be caused by two possibilities: firstly, the lines selected did not reflect the expression pattern of P4 constructs due to possible transgene inactivation; secondly, the additional 1.4 kb sequence may contain important *cis*-regulatory elements that is involved in *SVP* down-regulation. The ChIP data suggest that the second possibility might be true (see below).

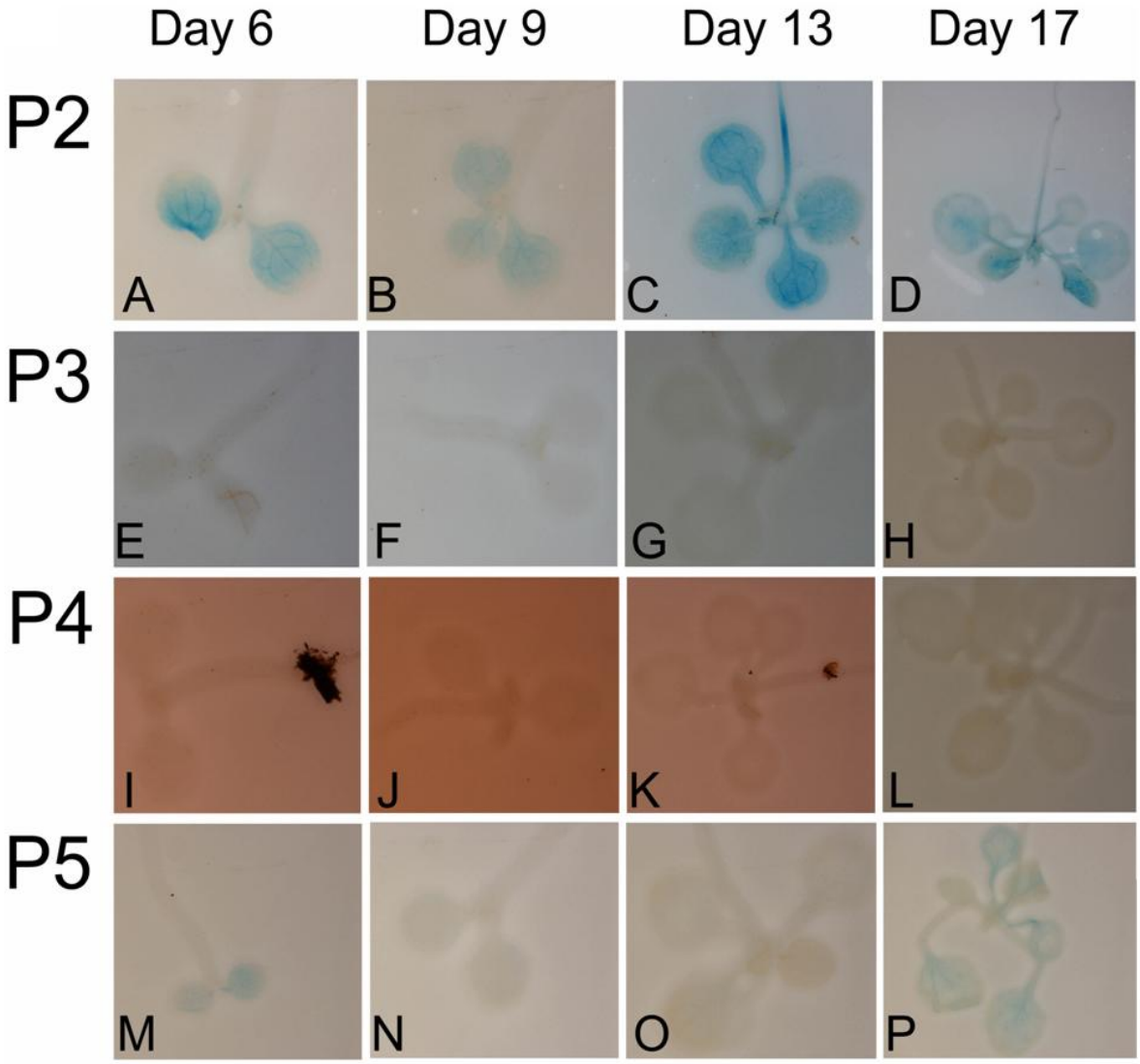

Fig 13. GUS staining pattern conferred by *SVP* promoter constructs. (A-D) GUS expression conferred by P2 construct from Day 6 to 17. **(M-P)** Lower GUS expression conferred by P5 from Day 3 to 17, compared with P2. **(E-L)** P3 and P4 display little GUS activity from Day 6 to 17.

In addition, of the six putative CArG boxes that were found within *SVP* promoter region, *AGL24* ChIP data suggested the CArG boxes 3 and 5 might be important in regulating *SVP* expression (unpublished data). Thus, mutagenesis was performed on these CArG boxes with primer pairs SVP-CARG3M1/SVP-CARG3M2 and SVP-CARG5M1/SVP-CARG5M2 (Table 9), respectively. This caused the change of CArG boxes 3 and 5 on P2 from CC(A/T)6GG into GG(A/T)6CC. The mutated constructs have been introduced into Arabidopsis plants, which are now being characterized.

4.5 *In vivo* Identification of *SVP* direct target genes

4.5.1 SVP potential targets

Next we analyzed the genetic interaction between *SVP* and other flowering time genes that act downstream of multiple floral pathways. In both LDs and SDs, single or double mutants of floral pathway integrators *SOC1* and *FT* suppressed the early flowering phenotype of *svp-41* (Figure 14), indicating that the activity of *SOC1* and *FT* may be partially responsible for early flowering of *svp-41* plants.

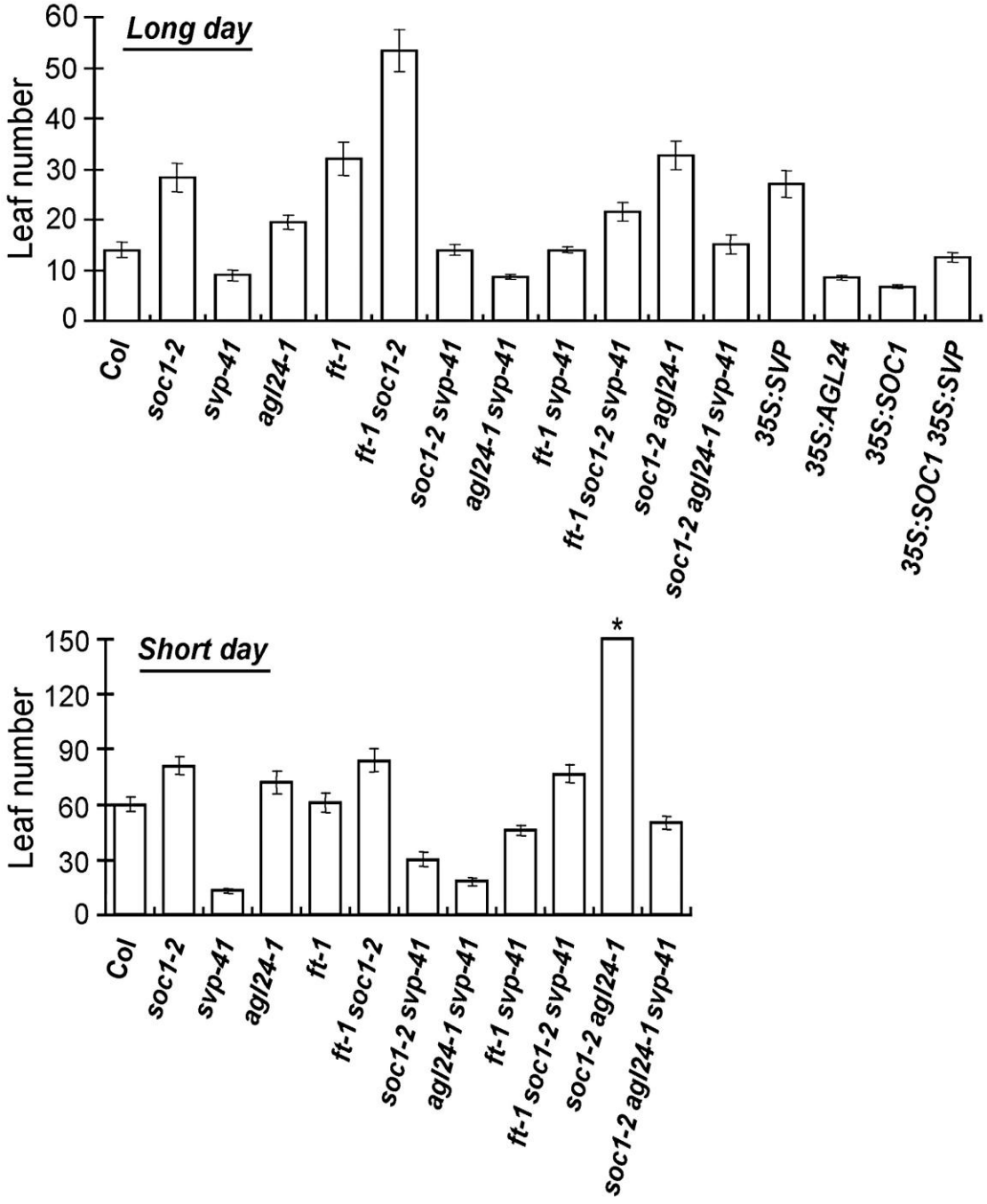

Fig 14. Flowering time of transgenic and mutant plants in LDs and SDs. The asterisk indicates that flowering was not observed in soc1-2 agl24-1 under short days. Error bars indicate standard deviation.

Primer name	Sequence 5'-3'
SVP-CARG5M1	CATTAATCATGAggATAAATccCATATATAAAGTG
SVP-CARG5M2	CACTTTATATATGggATTTATccTCATGATTAATG
SVP-CARG3M1	CACTCTCTCTCTCTTCTTAAAGTCTCggTTTTTAccAAAAATTCTCTCTCTCAC
SVP-CARG3M2	GTGAGAGAGAATTTggTAAAAAccGAGACTTTAAAGAAGAGAGAGAGAGTG

Table 9. Primers used in the Mutagenesis

To further explore the interaction between *SVP* and these genes, we examined temporal expression of these genes in developing *svp-41* and *35S:SVP* seedlings. *SOC1* expression was much elevated in *svp-41*, but almost completely suppressed by *35S:SVP* at the vegetative phase and floral transition that occurred at 9 days after germination in wild-type plants (Figure 15). On the contrary, the expression of *AGL24*, another flowering promoter that acts downstream of several floral pathways (Michaels et al., 2003 and Yu et al., 2002), was not significantly affected by *SVP* (Figure 16). *FT* was slightly upregulated in *svp-41* seedlings before the floral transition (9 days after germination) and demonstrated a comparable increased trend in expression levels in *svp-41* and wild-type plants afterwards (Figure 17). *FT* expression in *35S:SVP* was still upregulated during seedling development, although its expression was lower than that in wild-type plants at some time points (Figure 17).

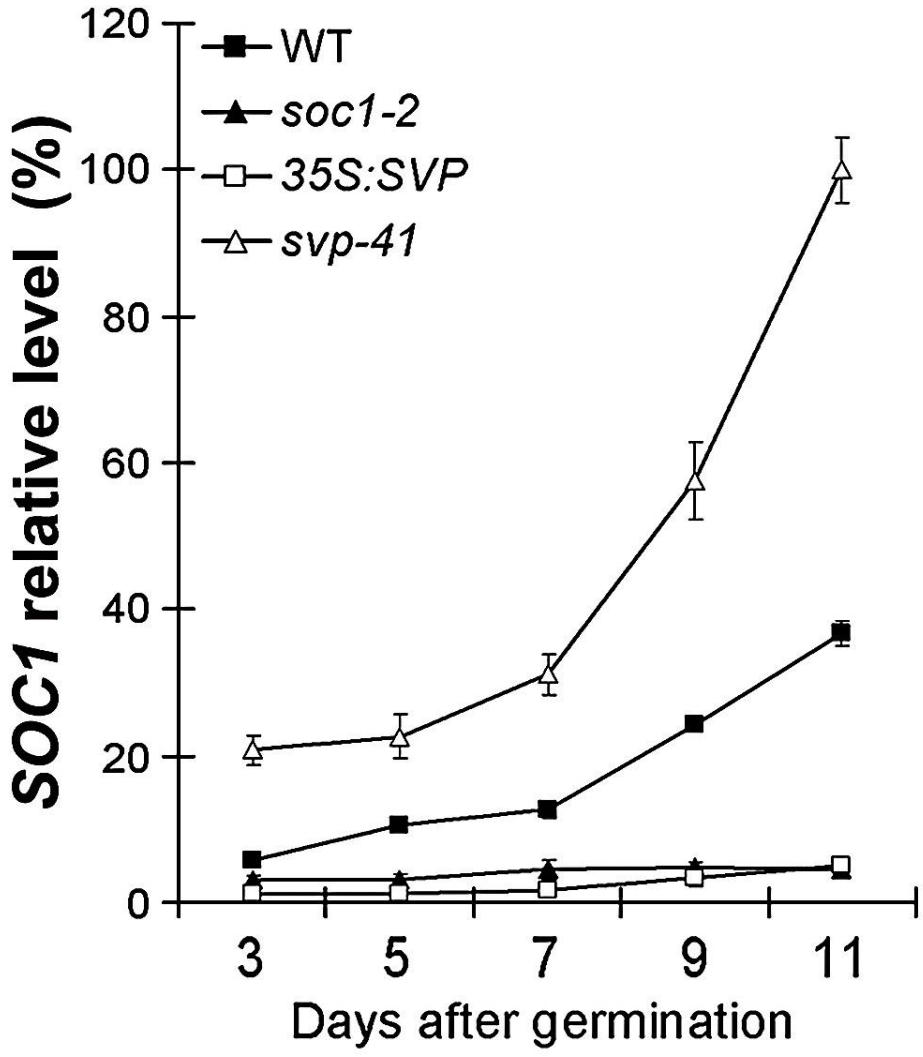

Fig 15.. *SOC1* Expression Is Closely Controlled by *SVP*. Temporal expression of *SOC1* in developing seedlings with various genetic backgrounds in LDs.

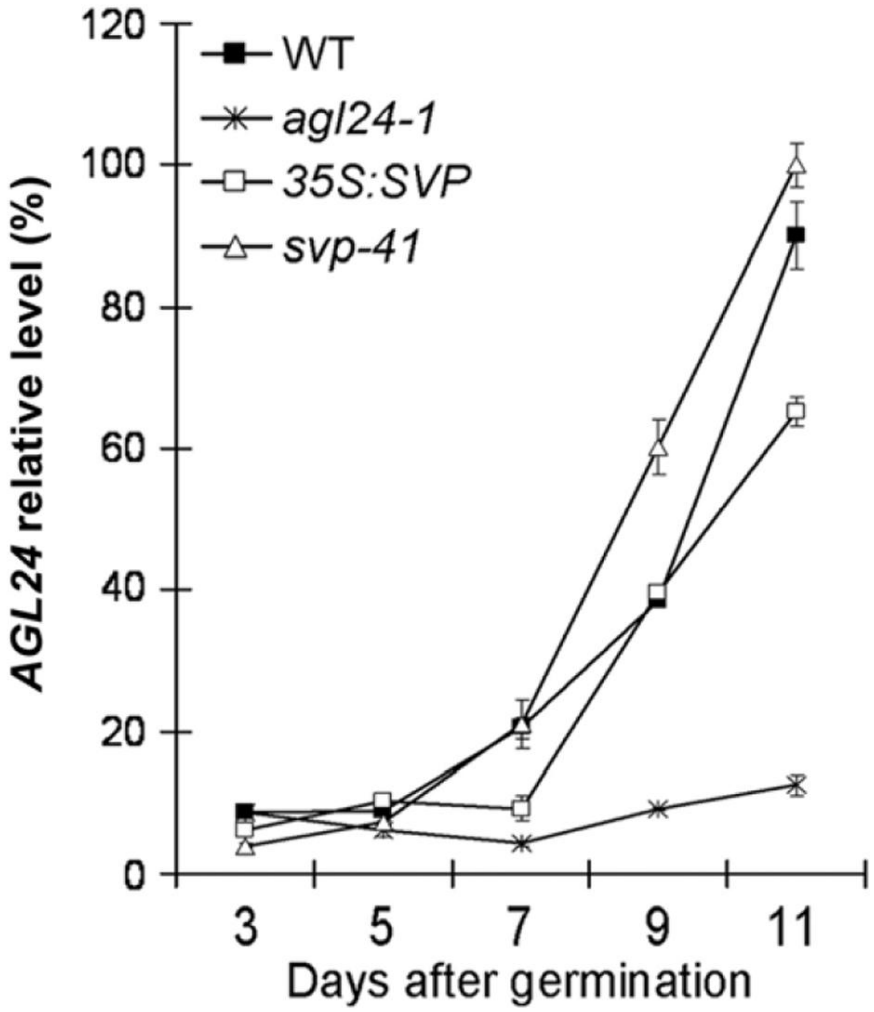

Fig 16.. Temporal Expression of *AGL24* in *svp-41* and *35S:SVP* Seedlings Grown in LDs. Transcript levels were determined by quantitative real-time PCR analyses of three independently collected samples. Results were normalized against the expression of *TUB2*. Error bars indicate SD.

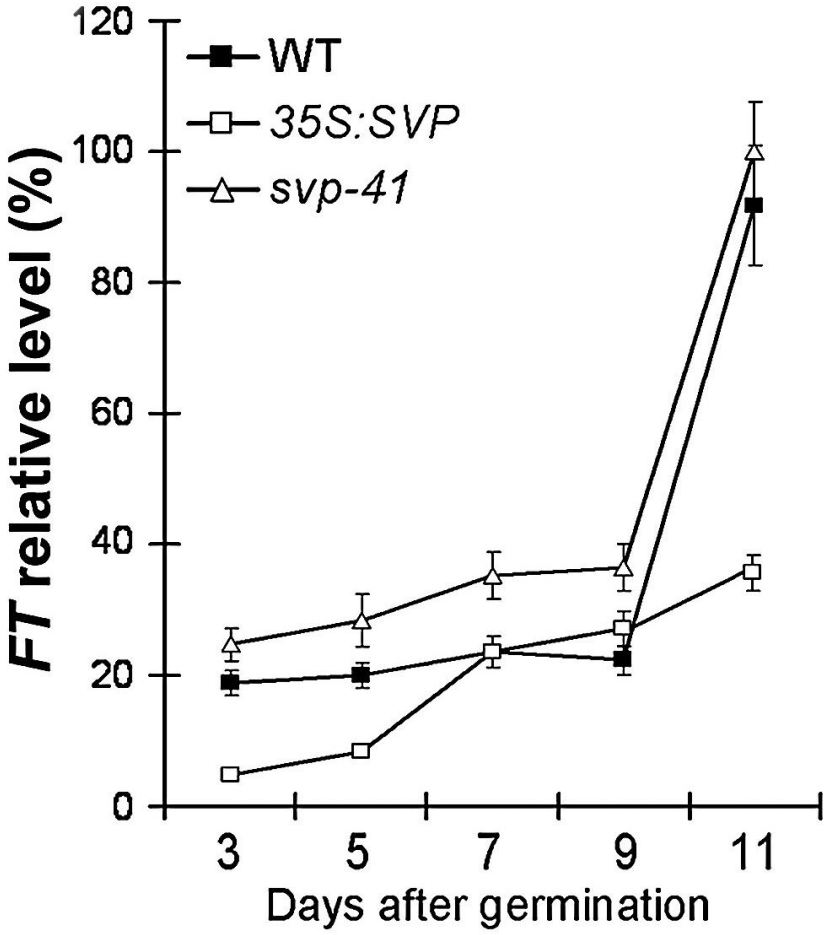

Fig 17. *FT* Expression Is Closely Controlled by *SVP*. Temporal expression of *SOC1* in developing seedlings with various genetic backgrounds in LDs.

We dissected developing young (3- to 7-day-old) seedlings before the floral transition to separately detect *SOC1* and *FT* expression in the leaves (cotyledon and rosette leaves) and the remaining aerial part without leaves, including the shoot apical meristem and young leaf primordia (Figure 18). Upregulation of *SOC1* in the leaf was about 2- to 3-fold in *svp-41* as compared to wild-type plants, while its expression in the aerial part without leaves was continuously upregulated by 4- to 6-fold in developing *svp-41* seedlings. On the contrary, *FT* was only slightly upregulated by 1.3-fold in *svp-41* leaves and was barely detectable in the shoot apex of both wild-type and *svp-41* plants (Figure 18). In situ hybridization further revealed higher *SOC1* expression in the shoot apical meristem and emerging young leaves of *svp-41* mutants than in those of wild-type (Figure 19). On the contrary, overexpression of *SVP* suppressed *SOC1* expression in the shoot apex.

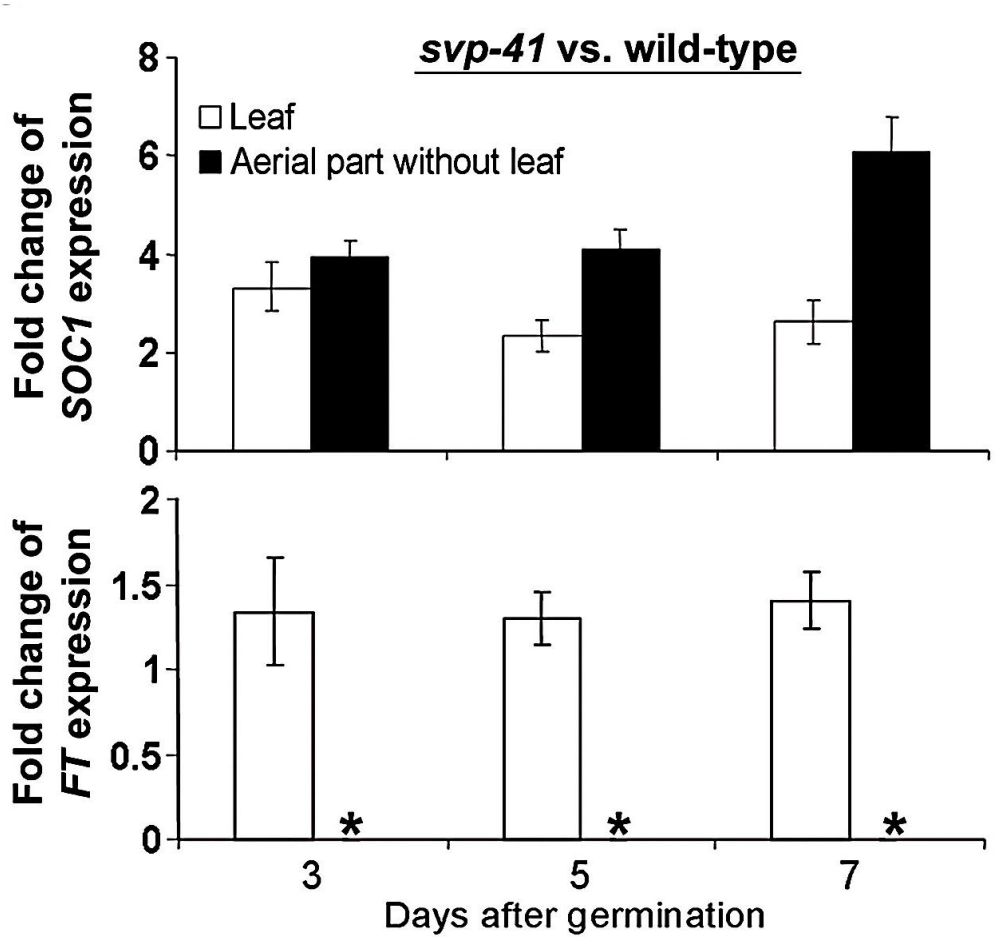

Fig 18. Fold change of SOC1 and FT expression in the aerial part without leaves and leaves of svp-41 against that in wild-type seedlings. Asterisks indicate that in the aerial part without leaves of both svp-41 and wild-type plants, quantitative real-time PCR analysis of FT RNA obtained very high Ct values because of its barely detectable level.

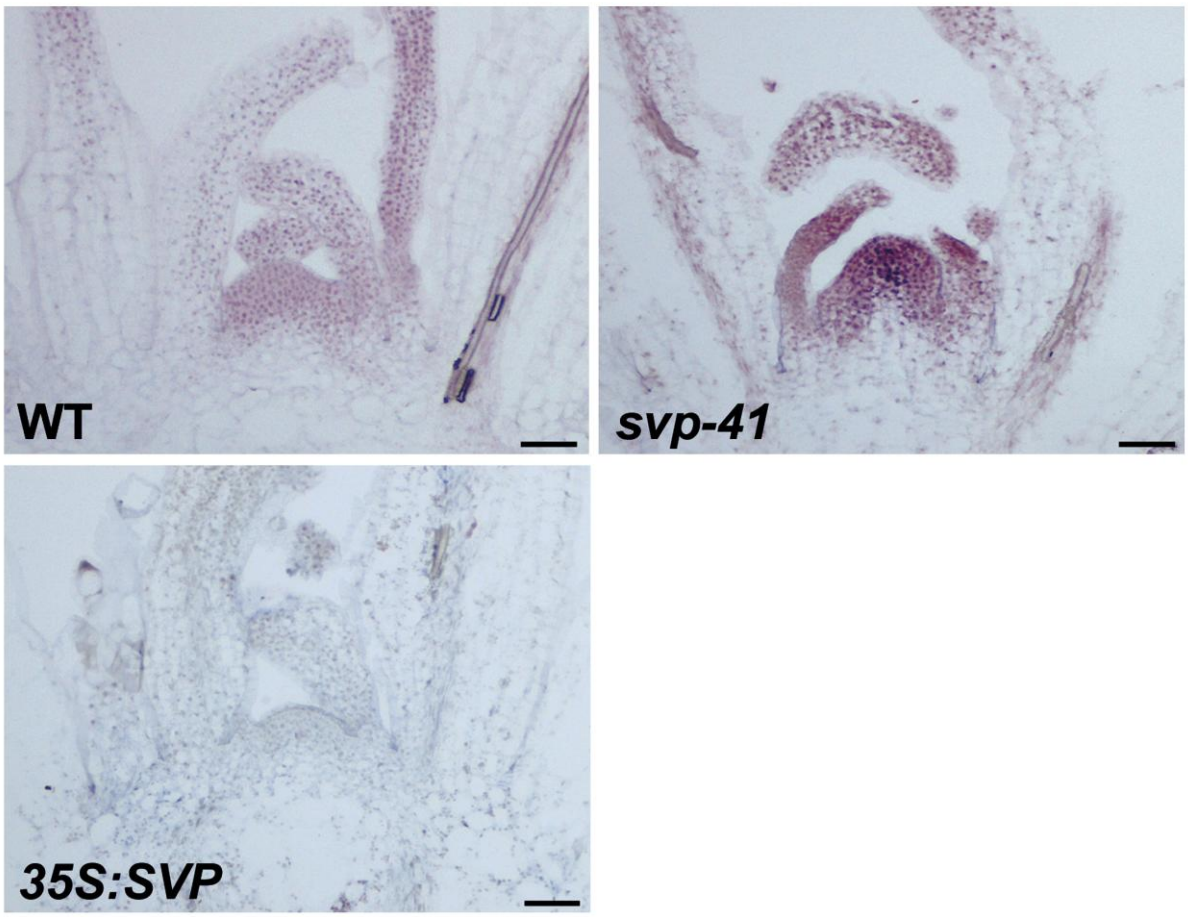

Fig 19. In situ localization of SOC1 at the shot apex of 11-day-old wild-type, svp-41, and 35S:SVP seedlings grown at 22℃ under long days. For comparing signals, sections of these plants were placed on the same slides for hybridization and detection. Scale bars, 25 μm.

4.5.2 SVP Represses SOC1 Expression

Since *SVP* likely represses *SOC1* expression, we further examined *SOC1* expression in response to *SVP* activity using a functional pER22-SVP transgenic line where *SVP* expression is controlled by an estradiol-induced XVE system (Zuo et al., 2000). We applied continuous β-estradiol treatment to pER22-SVP seedlings at different developmental stages to test the biological effects of *SVP* induction (Figure 20). The pER22-SVP seedlings initially treated with β-estradiol at the vegetative stage (1 and 5 days after germination) showed significantly delayed flowering compared with the wild-type and mock-treated transgenic seedlings (Figure 20). However, pER22-SVP seedlings initially treated with β-estradiol at the floral transitional stage (13 and 17 days after germination) showed similar flowering time as other seedlings. Thus, high levels of *SVP* expression before the floral transition were responsible for repressing flowering. In 5-day-old pER22-SVP seedlings treated with estradiol, *SVP* expression was continuously induced (Figure 21), while *SOC1* expression was immediately repressed at 2 hr of induction and continuously maintained at low levels afterwards (Figure 22). These results demonstrate that *SOC1* expression is tightly controlled by *SVP*.

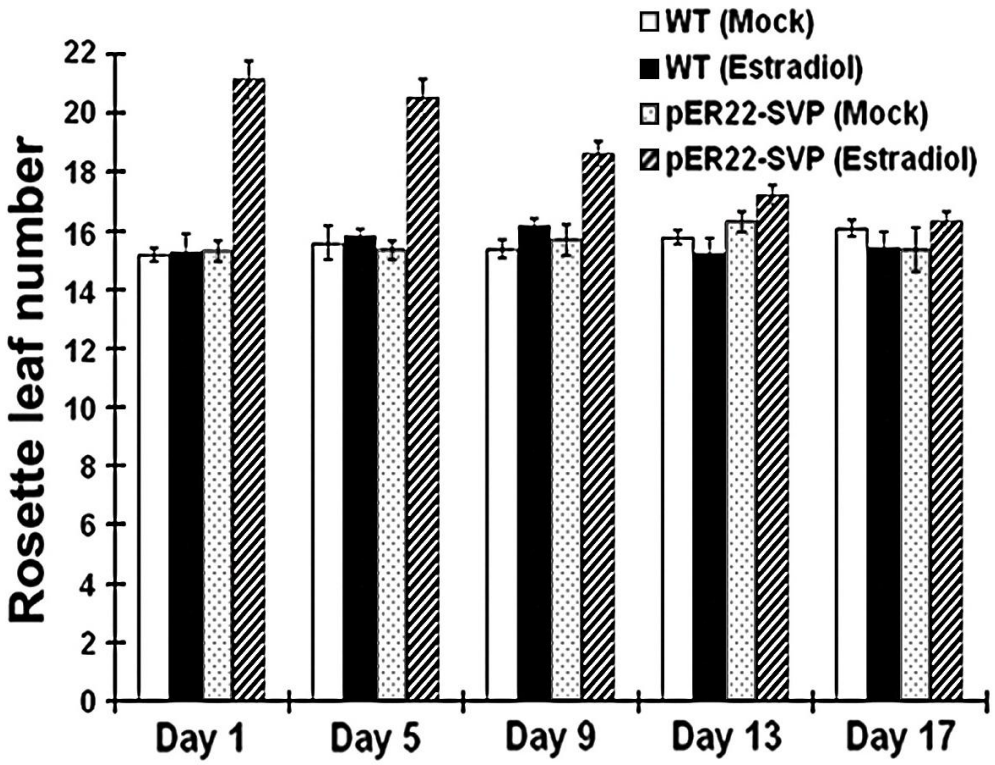

Fig 20. Generation of a functional estradiol-inducible SVP expression system (pER22-SVP). Induction of SVP expression in pER22-SVP seedlings causes late flowering as compared with mock-treated seedlings. β-estradiol treatment does not affect the flowering of wild-type plants, while its initial treatment of pER22-SVP before the floral transitional stage (1 and 5 days after germination) significantly delays flowering.

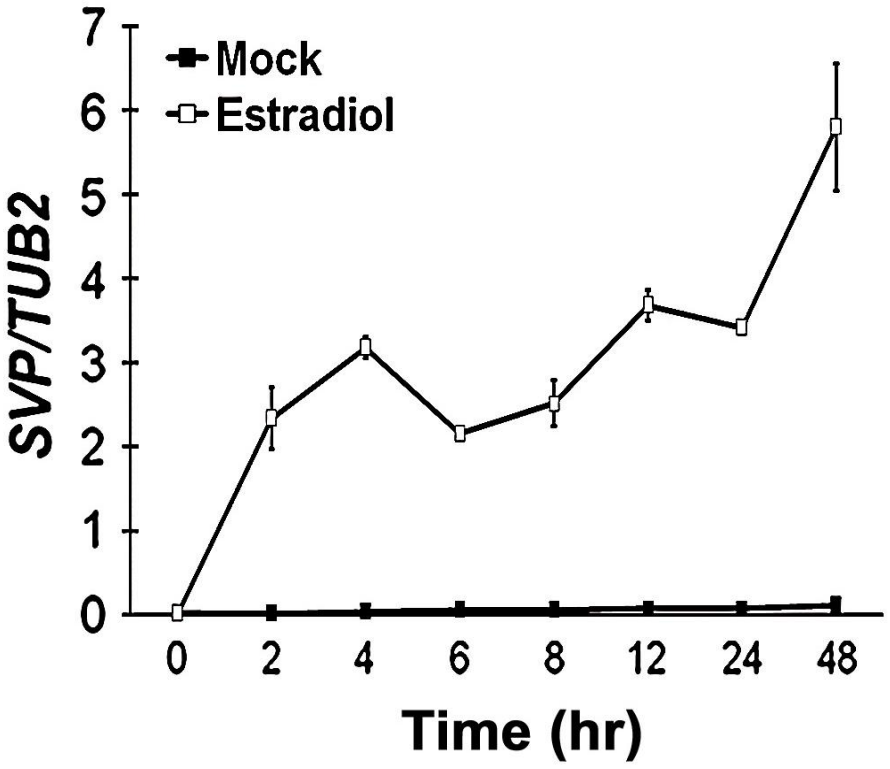

Fig 21. Time course expression of *SVP* in 5-day-old pER22-SVP seedlings. The plants were treated with 10 μM β-estradiol or mock-treated was compared. Error bars indicate standard deviation.

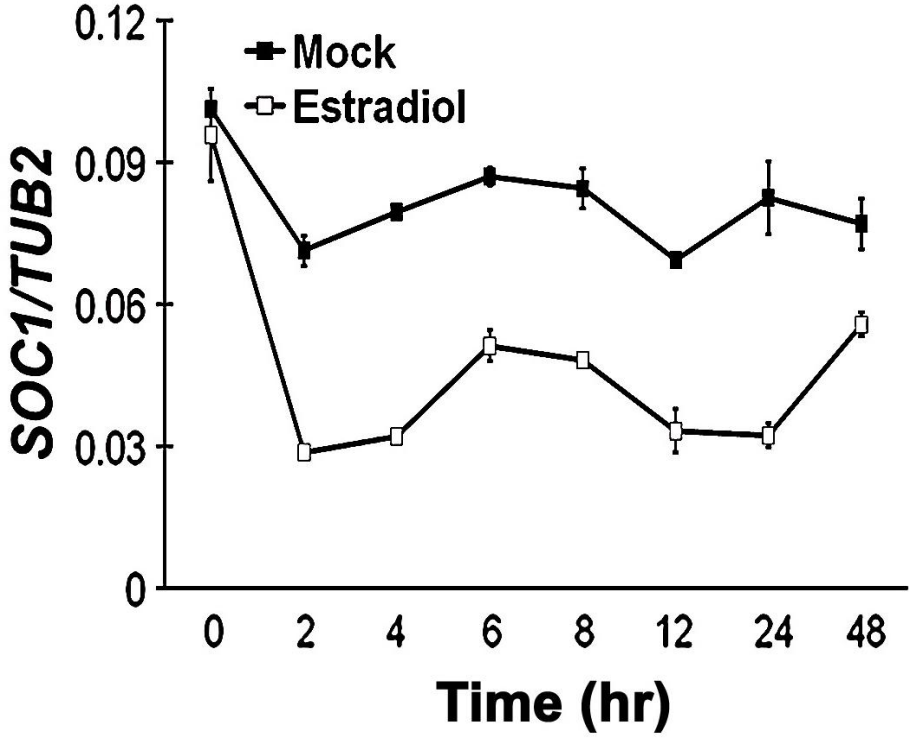

Fig 22. *SOC1* expression is repressed by *SVP*. Time course expression of *SOC1* in 5-day-old pER22-SVP seedlings. The plants were treated with 10 μM β-estradiol or mock-treated was compared. Error bars indicate standard deviation.

In contrast to *SVP*, *FT* and *AGL24* have been suggested as upstream promoters of *SOC1* expression (Liu et al., 2008, Michaels et al., 2003, Searle et al., 2006 and Yoo et al., 2005). To clarify the combined effect of these genes on *SOC1* expression, we analyzed *SOC1* expression in 9-day-old seedlings with various genetic backgrounds (Figure 23). *SOC1* expression was downregulated in *ft-1* and *agl24-1*, but upregulated in *svp-41*. Loss of *SVP* function in *ft-1* and *agl24-1* significantly elevated *SOC1* expression to levels that were much higher than those in wild-type plants. These results demonstrate that loss of *SVP* function derepresses *SOC1* expression largely independently of *FT* and *AGL24*, suggesting that *SVP* exerts a dominant effect on *SOC1* expression.

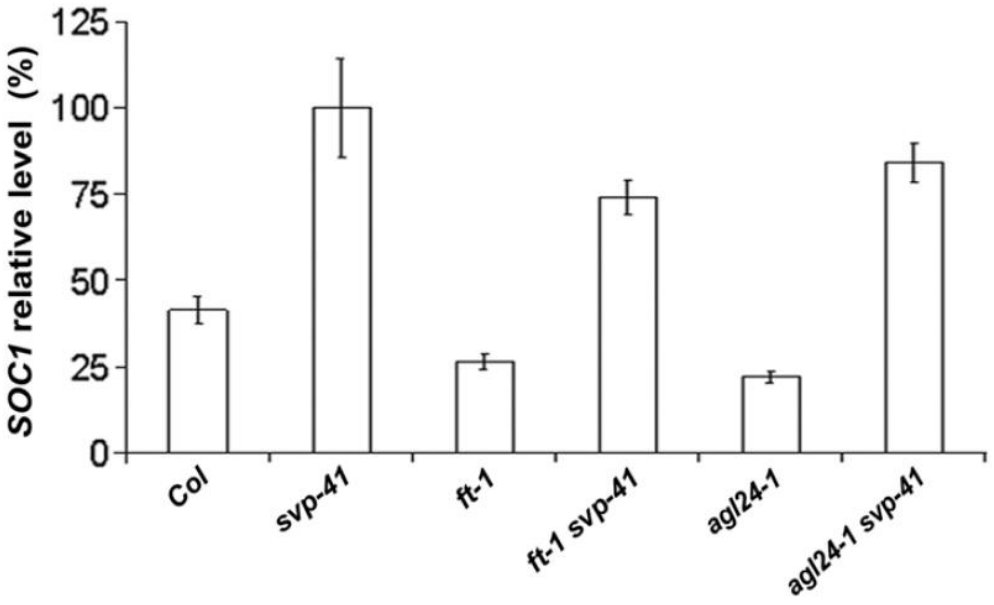

Fig 23. Loss of *SVP* Function Derepresses *SOC1* Expression Largely Independently of *FT* and *AGL24.* *SOC1* expression in 9-day-old seedlings with various genetic backgrounds in LDs was measured by quantitative real-time PCR. *TUB2* was used for normalization. Error bars indicate SD.

4.6 SVP Binds Directly to the SOC1 Promoter

4.6.1 Identification of SVP direct targets by ChIP

To test for *in vivo* binding of *SVP* to *cis*-regulatory regions, we performed ChIP assays using two functional transgenic lines. One line expressing an SVP-6HA fusion gene driven by the CaMV 35S promoter showed late flowering like 35S:SVP, and another transgenic line *svp-41 SVP:SVP-6HA* containing HA-tagged SVP regulated by its endogenous promoter showed comparable flowering time to wild-type plants (Figure 26). The SVP binding DNA sequences were isolated by ChIP. Homozygous *35S::SVP-6HA* or *svp41 SVP::SVP-6HA* plants with one transgene insertion were treated with formaldehyde in order to stabilize the *in vivo* complexes of SVP-tag and DNA. Solubilized chromatin fragments were obtained from the isolated nuclei. An aliquot of the solubilized chromatin was either retained as the input control or used for examining the size of fragmentation of DNA (Figure 24c). The rest of solubilized chromatin was used for immunoprecipitation with anti-HA beads. After the protein A-Sepharose beads were pelleted, the supernatant sample was analyzed by Western Blot as a 'post-bind' fraction. SVP-tag fusion protein has been depleted from the post-bind fraction after immunoprecipitation by anti-HA beads (Figure 24a, 24b). The protein A-Sepharose beads were further washed and the immunoprecipitated protein and its associated co-purified DNAs were eluted. An aliquot of the eluted solution was analyzed by Western Blot with anti-HA antibody to confirm that SVP-6HA were specifically precipitated during the immunoprecipitation (Figure 24a, 24b). The

proteins associated DNAs were subsequently recovered from the eluted fraction and used for subsequent enrichment test.

4.6.2 PCR enrichment test

SVP is one of MADS-box proteins that have been known to bind the CArG motifs, which have a canonical sequence of CC(A/T)6GG. Based on predictions using MatInspector (**http://www.genomatix.de**), we scanned the putative CArG boxes with a maximum of one nucleotide mismatch located in the genomic regions of the potential target genes. Gene-specific primers that could amplify a 200- to 400-bp region including one to three relevant CArG boxes were designed and used to detect the enrichment of these DNA sequences associated with SVP protein (Figure 24) (Table 10). In this project, we designed the primers to test if SVP protein could bind to the regulatory regions of SOC1, SVP itself and other SVP potential targets (e.g. AGL24 and LFY) (Figure 25).

Our results showed that *SOC1* was preferentially bound by SVP in 35-day-old plant (Figure 27) and 13-day-old seedlings (Figure 28) for both 35S*::SVP-6HA* and *svp41 SVP::SVP-6HA*. In addition, ChIP analysis with 13-day-old seedlings suggested SVP-6HA fusion protein could bind to *SVP* genomic region (Figure 29). We concluded that *SOC1* and *SVP* are direct targets of SVP protein. In contrast, *AGL24* and *LFY* did not show any enrichment in 35S*::SVP-6HA* transgenic line of 13-day-old, which suggesting that *SVP* may not affect flowering time through these two genes (Figure 30).

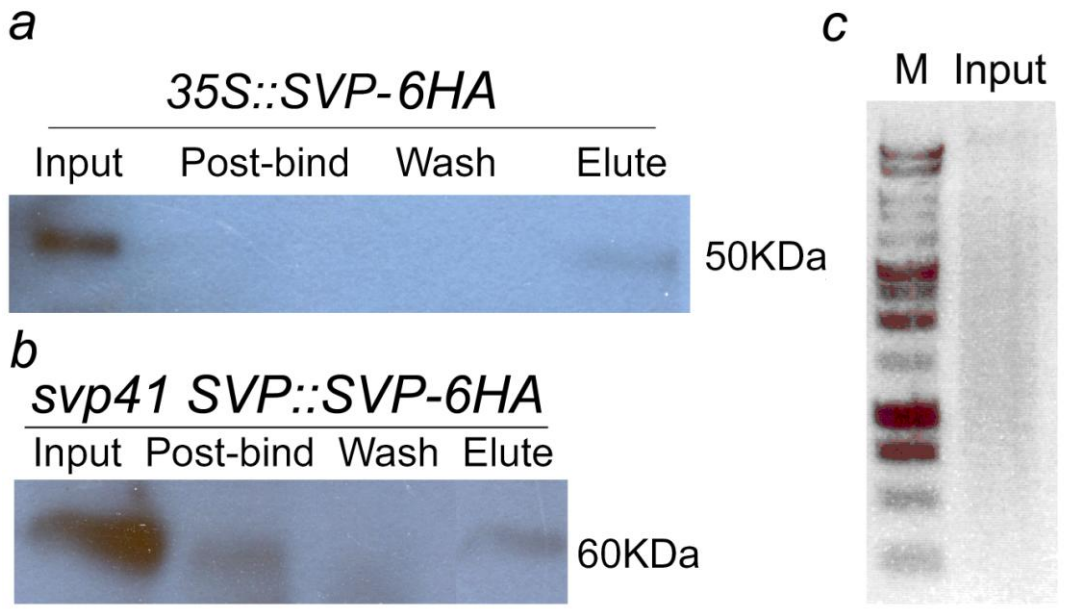

Fig 24.Western analysis of the specificity of anti-HA and anti-TAP beads in the ChIP procedure. (a) The SVP-6HA proteins is present in large amount in the *35S::SVP-6HA* transgenic plant and input mixture, but depleted from the 'post-bind' fraction after Immunoprecipitation (IP) by anti-HA beads. After wash, SVP-6HA is only present in the eluted fraction (Elute), but not in Washing Buffer (Wash). (b) SVP-6HA was detected as in (a). (c) The chromatins of both *35S::SVP-6HA* and *svp41 SVP::SVP-6HA* transgenic plants were sonicated to shear the genomic DNAs to an average size of 2,500 bp.

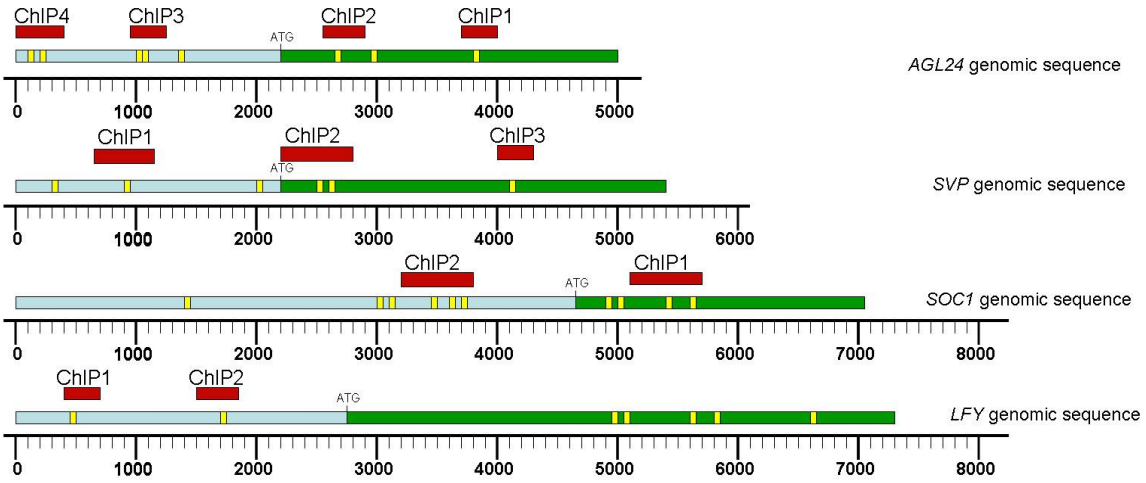

Fig 25. Primers of *AGL24, SVP, SOC1* and *LFY* for enrichment test. Putative *SVP* binding sites (CArG boxes) are marked in yellow, and the regions amplified after ChIP are shown as red rectangles. The open reading frame (ORF) of each gene is shown as green rectangles.

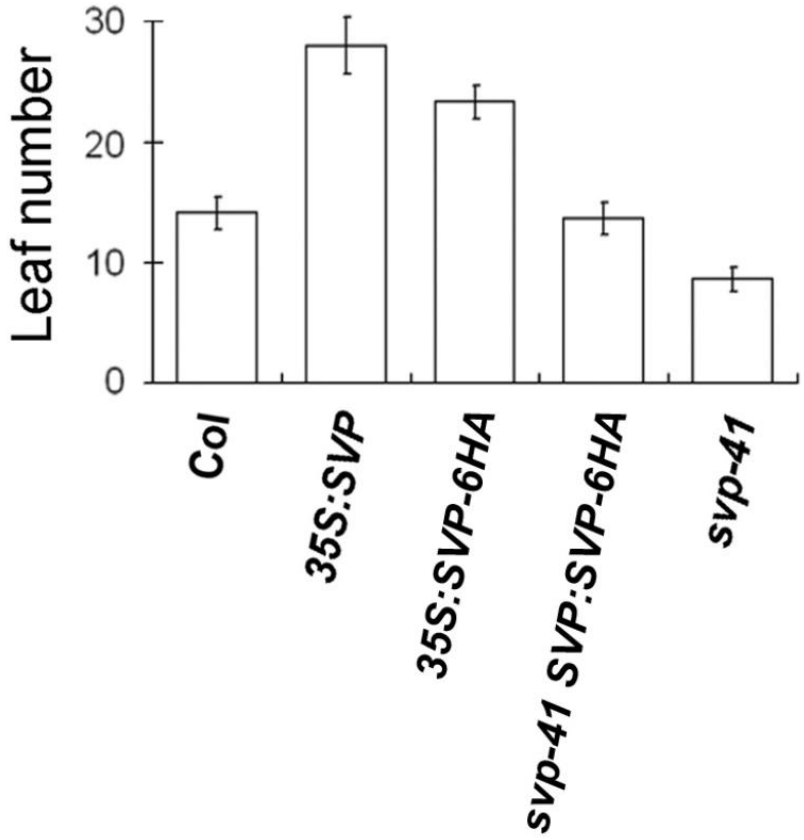

Fig 26. Figure S5. Generation of Functional *35S:SVP-6HA* and *SVP:SVP-6HA* Transgenic Lines. Flowering time of generated transgenic lines in LDs was compared by calculating the number of total leaves. Values representing the mean ±SD were scored from at least 20 plants of each genotype. *35S:SVP-6HA* and *35S:SVP* plants show late flowering as compared with wild-type plants. *svp-41* mutants show early flowering, while *svp-41 SVP:SVP-6HA* plants exhibit comparable flowering time as wild-type plants, indicating that SVP-6HA protein retains the biological function as endogenous SVP.

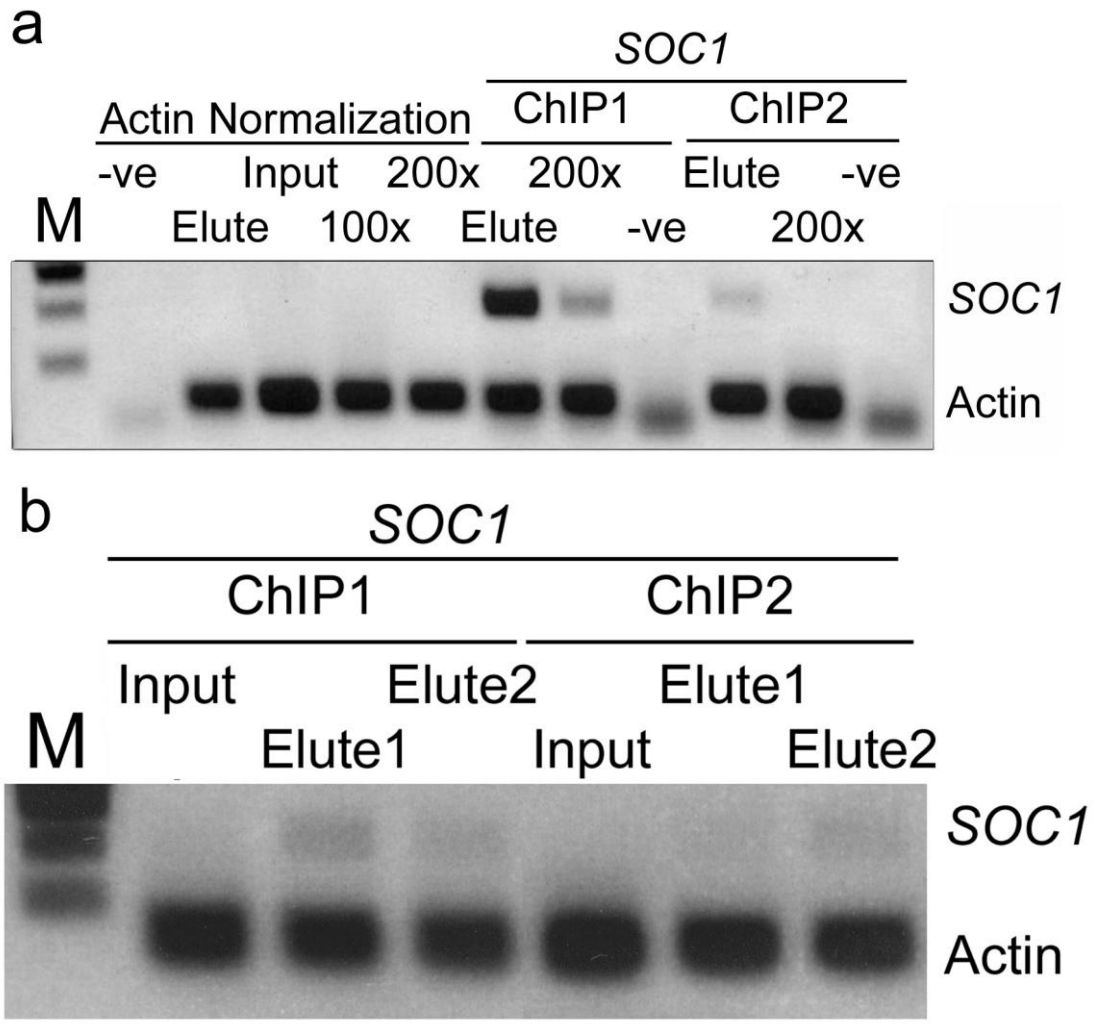

Fig 27. *SOC1* is the direct target gene of *SVP* after floral transition. (a) homozygote *35S::SVP-6HA* plants after floral transition (35-day-old) were formaldehyde-crosslinked. Nuclear extracts prior to anti-HA antibody incubation (Input) and after ChIP (Elute) were subjected to PCR analysis using *SOC1* primers described in **Fig 13**. (b) ChIP analysis of homozygote *svp41 SVP::SVP-6HA* plants after floral transition (35-day-old).

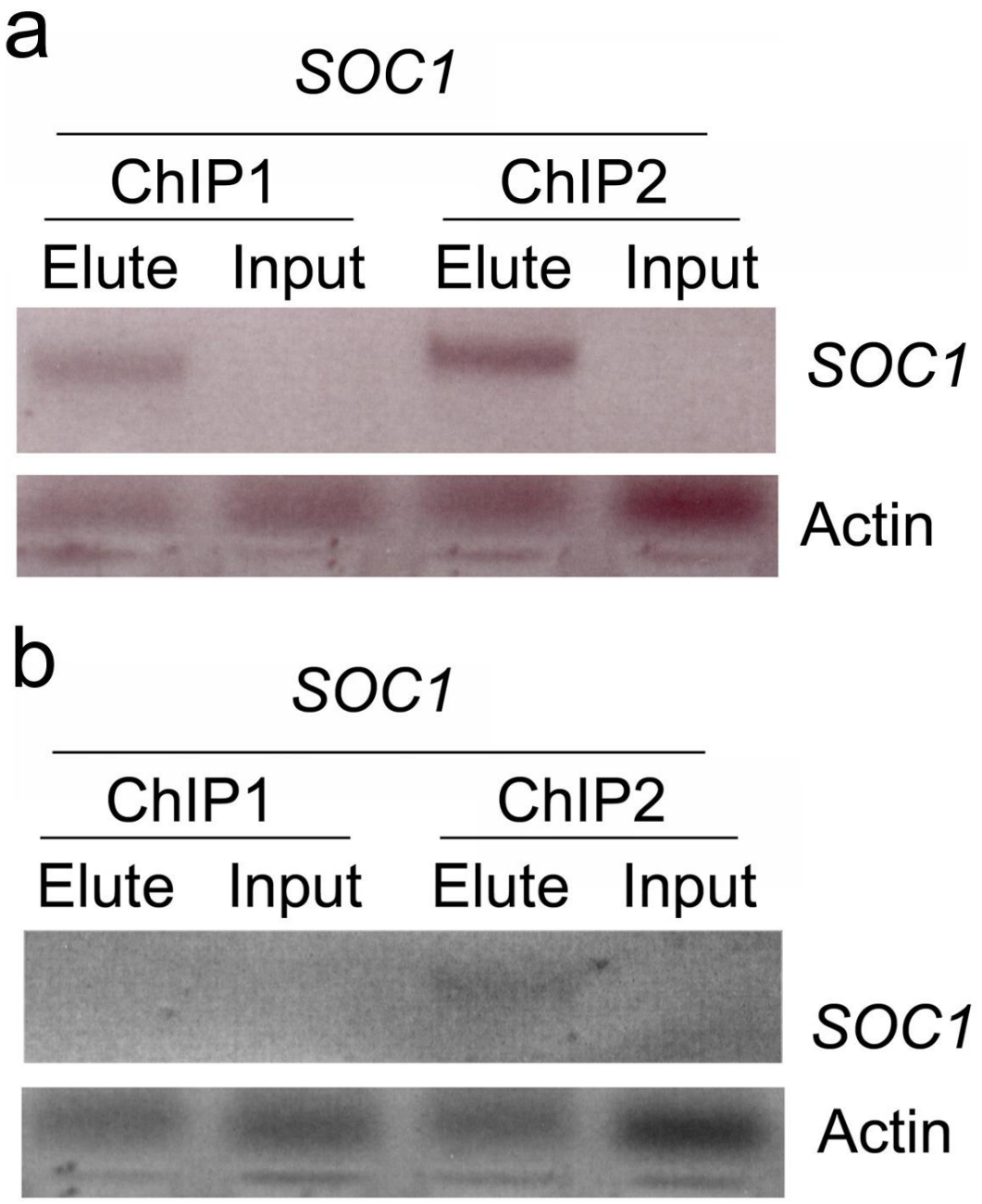

Fig 28. *SOC1* is the direct target gene of *SVP* before floral transition. (a) Homozygote *35S::SVP-6HA* plants before floral transition (13-day-old) were subjected to ChIP analysis and PCR enrichment test using *SOC1* primers described in **Fig 13**. (b) ChIP analysis of homozygote *svp41 SVP::SVP-6HA* plants before floral transition (13-day-old).

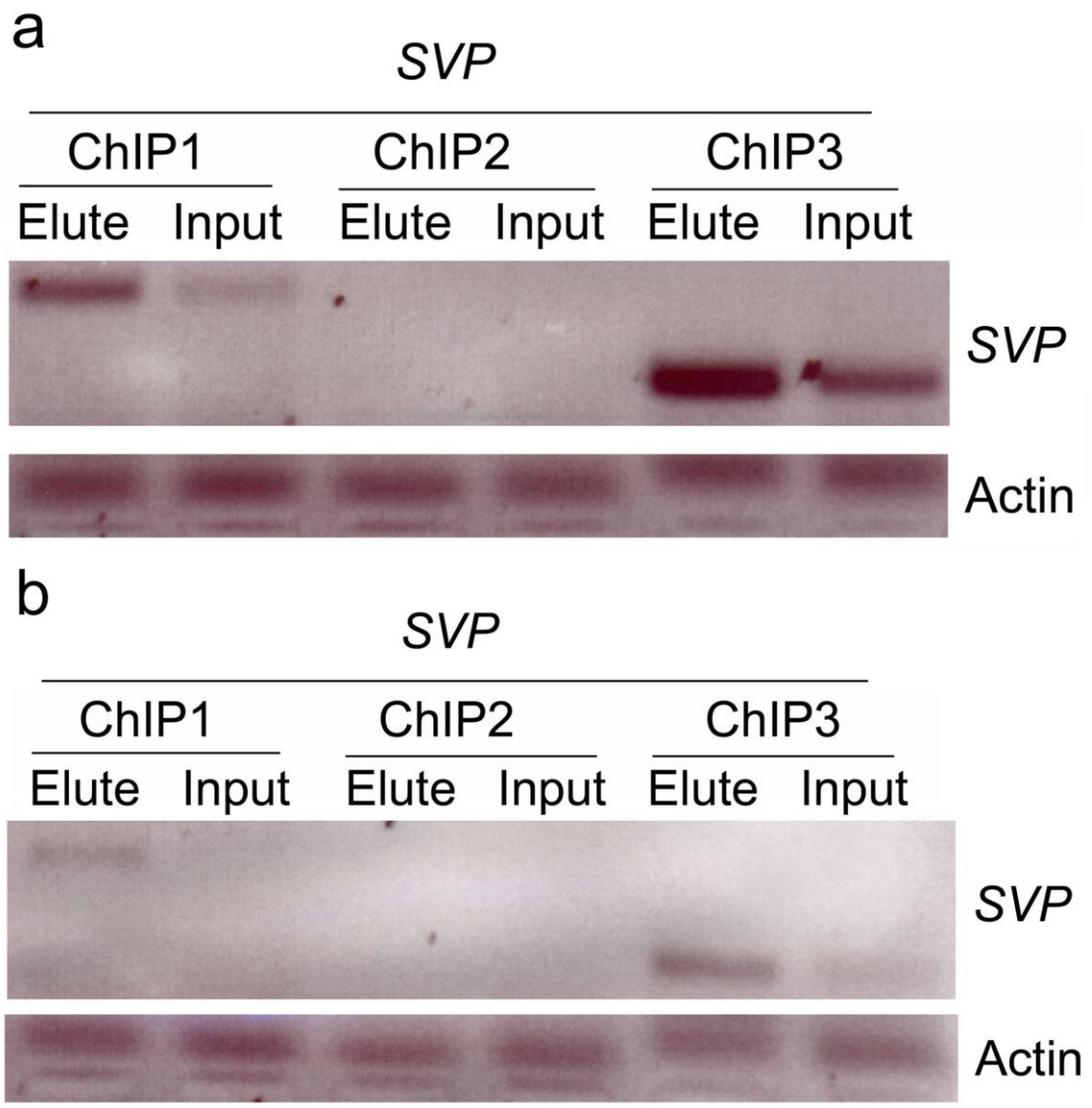

Fig 29. *SVP* itself is the direct target gene of SVP before floral transition. (a) Homozygote *35S::SVP-12HA* plants before floral transition (13-day-old) were subjected to ChIP analysis and PCR enrichment test using *SVP* primers described in **Fig 13**. (b) ChIP analysis of homozygote *35S::SVP-TAP* plants before floral transition (13-day-old).

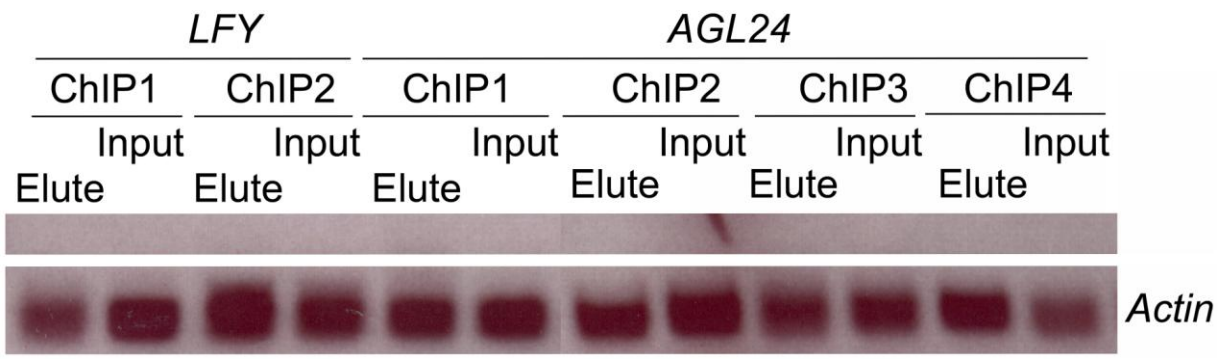

Fig 30. *LFY* and *AGL24* may not be the direct target genes of *SVP* before floral transition. Homozygote *35S::SVP-12HA* plants before floral transition (13-day-old) were subjected to ChIP analysis and PCR enrichment test using *LFY* and *AGL24* primers described in **Fig 25**.

Primer name	Sequence 5’-3’
CHIP_SVP-1F	ATATGTTTGGTTCTGTTGTTGACG
CHIP_SVP-1R	AAGAAATAAGTTTGTGAGTTCGGC
CHIP_SVP-2F	AAAAGATTCAGATCAGGAAGATCG
CHIP_SVP-2R	CGGCTTAAACATATCATACCACAA
CHIP_SVP-3F	ATGTGTTTGCAGAGTGACAAGATT
CHIP_SVP-3R	GGATTAAATTTAGGGGTGTGTACG
CHIP_AGL20-1F	TGAAAAGTCTTGTACTTTTTCCCC
CHIP_AGL20-1R	AATAAAATGTGCTCTTTCGTAGCC
CHIP_AGL20-2F	GCTAAATAGTCAGTCATATGTGTCGC
CHIP_AGL20-2R	GGATTAATGGTCACTTAGGTAATGAGG
CHIP_AGL24-1F	AGTTCAATCCATCAAGATCCTCTC
CHIP_AGL24-1R	TTTCACGTGTAAGTTCGTCAAGTT
CHIP_AGL24-2F	ATCCCCAATCATACCAAGTGAC
CHIP_AGL24-2R	CGGCATAATTTGATGACCTAAA
CHIP_AGL24-3F	TGCTGTTCATCAGTTCATCTACC
CHIP_AGL24-3R	TTTACAAGATACTTGTCGGCCA
CHIP_AGL24-4F	ATCCCGAAAGTCTTCACTAACCTT
CHIP_AGL24-4R	GTTTGGTTAAGTCTACTGATCGCC
CHIP_LFY-1F	AGTTGAAGAAGATTCGTCTATGGC
CHIP_LFY-1R	AATATACCGGATAAACAAGACCGA
CHIP_LFY-2F	TTAAAGCAAAAGAACAACTTGTGG
CHIP_LFY-2R	GCAGAAGCCCGATAAGTTACTAAA

Table10. Primers used in ChIP analysis

4.6.1 SVP binds to a region on SOC1 promoter that FLC binds to

To identify the exact SVP binding site on SOC1 promoter region, we scanned *SOC1* promoter region with eleven pairs of primers near the identified CArG boxes motifs for measurement of DNA enrichment (Figure 31). In ChIP assays of 7-day-old *35S:SVP-6HA* and *svp-41 SVP:SVP-6HA* seedlings, we consistently found the highest enrichment of the number 5 fragment associated with SVP-6HA by quantitative real-time PCR (Figure 32). This enriched genomic fragment was near two CArG motifs (SOC1-CArG1 and SOC1-CArG2), each with one nucleotide mismatch from the canonical CArG box (Figure 33).

To confirm that SVP can directly bind to that site on the *SOC1* promoter, gel shift assays were carried out using two fragments bearing SOC1-CArG1 and SOC1-CArG2 as probes (Figure 34). The recombinant 6×His-SVP protein bound strongly with SOC1-CArG1, but only very weakly with SOC1-CArG2. Formation of the complex between 6×His-SVP and SOC1-CArG1 was also inhibited by a specific competitor, unlabeled SOC1-CArG1, thus demonstrating the specific interaction between 6×His-SVP and SOC1-CArG1.

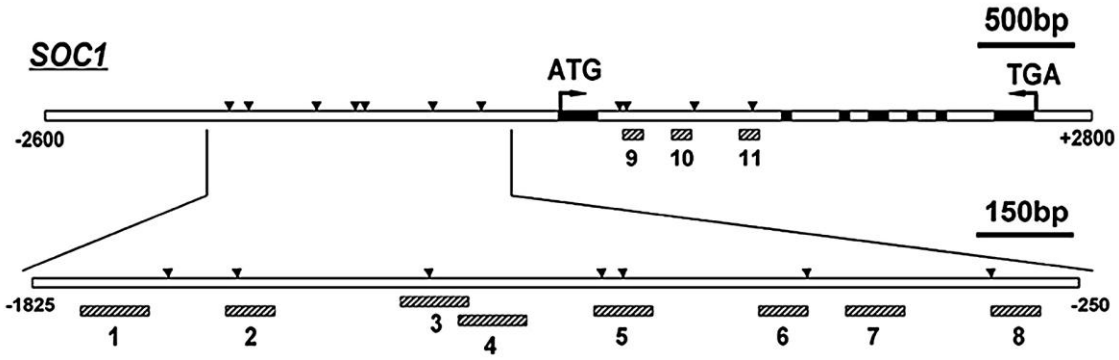

Fig 31. Schematic diagram of the *SOC1* genomic region. ***Exons are represented by black boxes, while introns and upstream regions are represented by white boxes. The arrowheads indicate the sites containing either a single mismatch or a perfect match to the consensus binding sequence (CArG box) of MADS-domain proteins. Eleven DNA fragments flanking these sites were designed for ChIP analysis of the SVP binding site.***

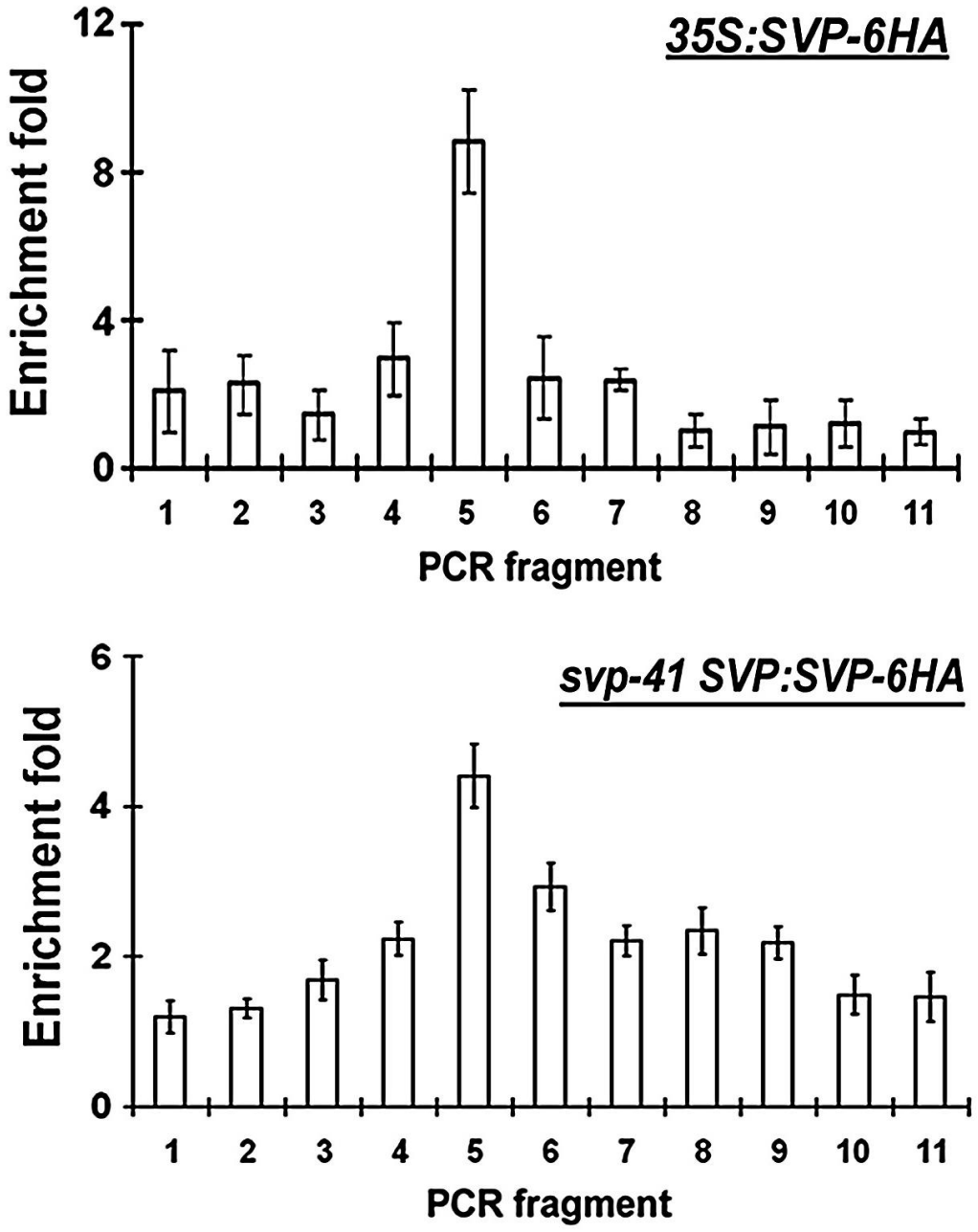

Fig 32. ChIP enrichment test showing the binding of SVP-6HA to the region near fragment 5. Seven-day-old seedlings of 35S:SVP-6HA and svp-41 SVP:SVP-6HA were harvested for ChIP analysis. Relative enrichment of each fragment was calculated first by normalizing the amount of a target DNA fragment against a genomic fragment of ACTIN, and then by normalizing the value for transgenic plants against the value for wild-type as a negative control.

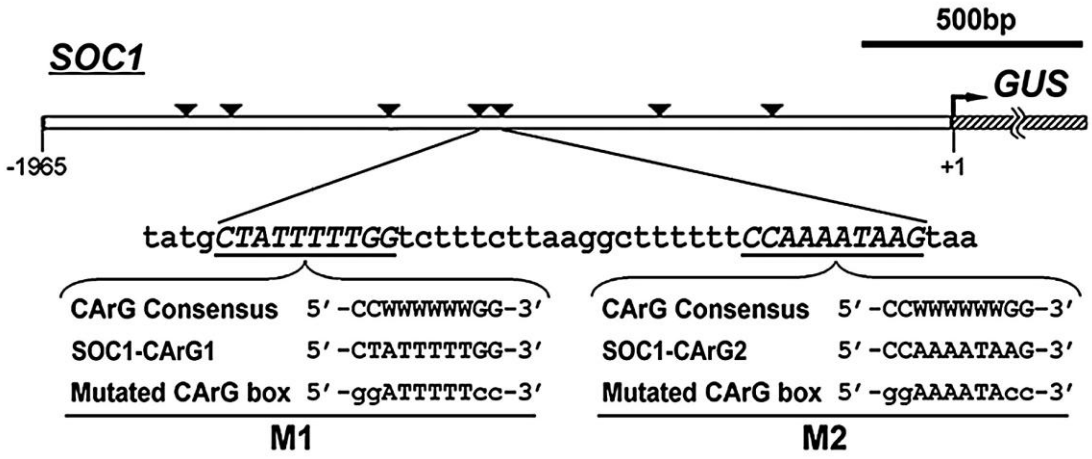

Fig 33. Schematic diagram of the SOC1:GUS construct. 2 kb SOC1 5′ upstream sequence was transcriptionally fused with the GUS gene. Two native CArG boxes within fragment 5 were mutated as indicated.

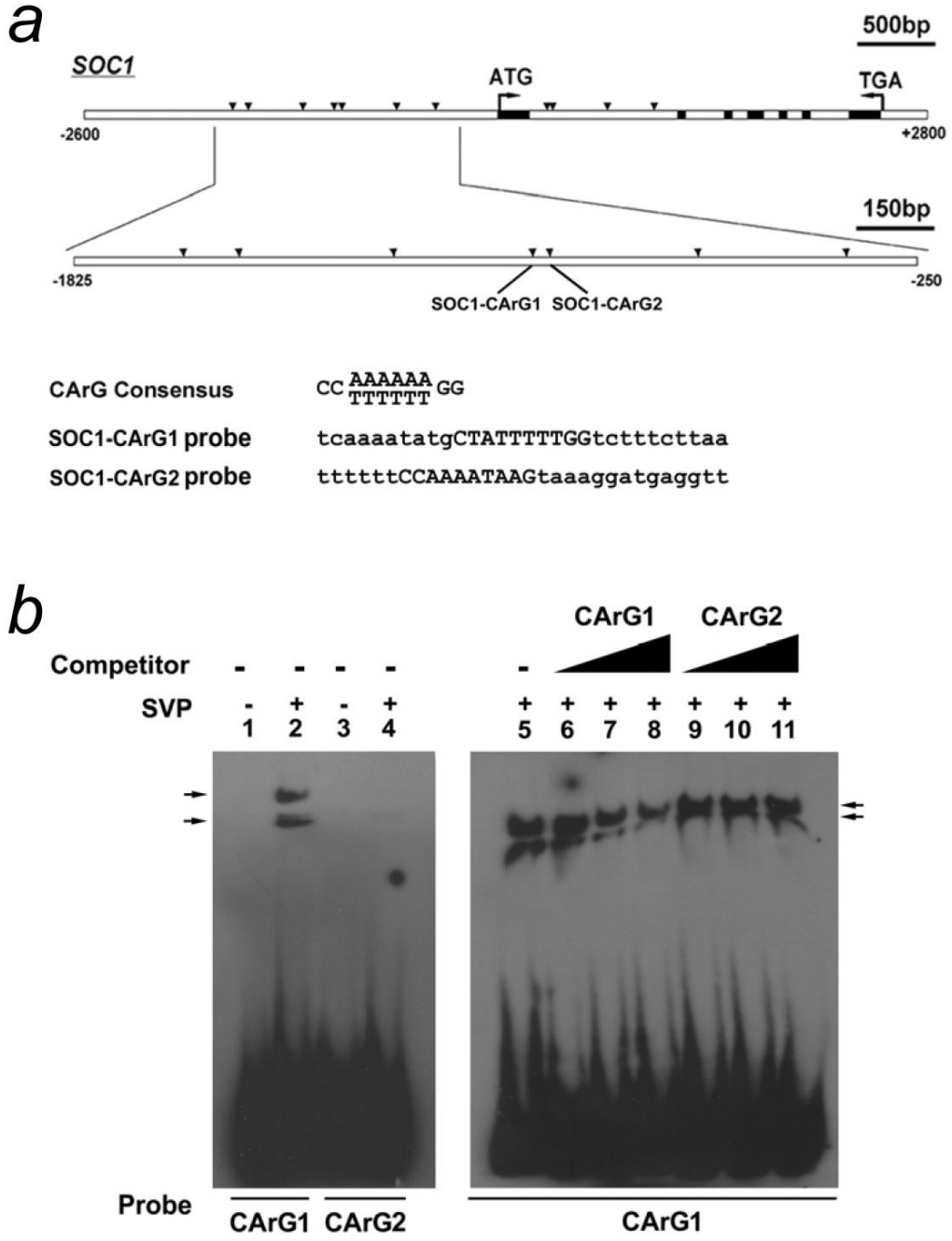

Fig 34. Specific Binding of SVP Protein to the SOC1-CArG1 Sequence. (a) List of two probes containing putative MADS-box binding sites (CArG boxes) used for gel shift assays. (b) Preferential binding of 6His-SVP protein to a 30 bp fragment containing the SOC1-CArG1 sequence (arrows). 6His-SVP protein was incubated with either SOC1-CArG1 or SOC1-CArG2 probe as indicated below the panel. The presence of 6His-SVP protein and unlabelled competitor DNA is indicated above the panels. Lanes 1 and 3, no protein and no competitor DNA; lanes 2, 4 and 5, 6His-SVP protein and no competitor DNA; lanes 6, 7 and 8, SOC1-CArG1 fragment as competitor DNA; lanes 9, 10, and 11, SOC1-CArG2 fragment as competitor DNA. Non-labeled DNA in molar excess was used as competitor in lanes 6 and 9 (50-fold), lanes 7 and 10 (200-fold), and lanes 8 and 11 (800-fold).

4.7 SVP Binding Regulates *SOC1* Function in Flowering

To test in vivo whether these CArG motifs are responsible for the regulation of *SOC1* by SVP, we applied an established *SOC1:GUS* construct, in which a 2 kb *SOC1* promoter upstream of the translational start site was fused with the GUS reporter gene (Figure 33; Liu et al., 2008). Based on this construct, we generated two reporter gene cassettes, M1 and M2, where the two CArG motifs near the number 5 genomic fragment were mutated, respectively (Figure 33). As previously reported (Liu et al., 2008), among 24 independent lines of transformants harboring *SOC1:GUS*, 20 lines displayed strong GUS staining during floral transition (Figures 35a and 36). Among 26 lines of transformants harboring the M1 mutated form, 21 lines displayed stronger GUS staining in both the shoot apex and leaf compared with *SOC1:GUS* (Figures 35a, 37b, and 36). However, among 21 lines of transformants harboring the M2 mutated form, 15 lines displayed a similar GUS staining pattern to *SOC1:GUS* (Figures 35a, 3c, and 36). A close examination of the spatial GUS staining pattern in *SOC1:GUS* and M1 revealed that M1 lines displayed notably increased GUS staining in the shoot apex (Figures 37a and 37b) and moderately increased staining in the cotyledon (Figure 38a) and rosette leaf (Figure 38b). These observations were consistent with the change of *SOC1* expression levels in wild-type and *svp-41* plants (Figures 18 and 19), indicating that SVP mainly binds to the SOC1-CArG1 to repress *SOC1* expression in the shoot apex and leaf. To further confirm this result, we crossed *SOC1:GUS* and M1 with *35S:SVP* and examined the change of GUS staining in response to the increased SVP activity. As expected, staining of *SOC1:GUS* in the

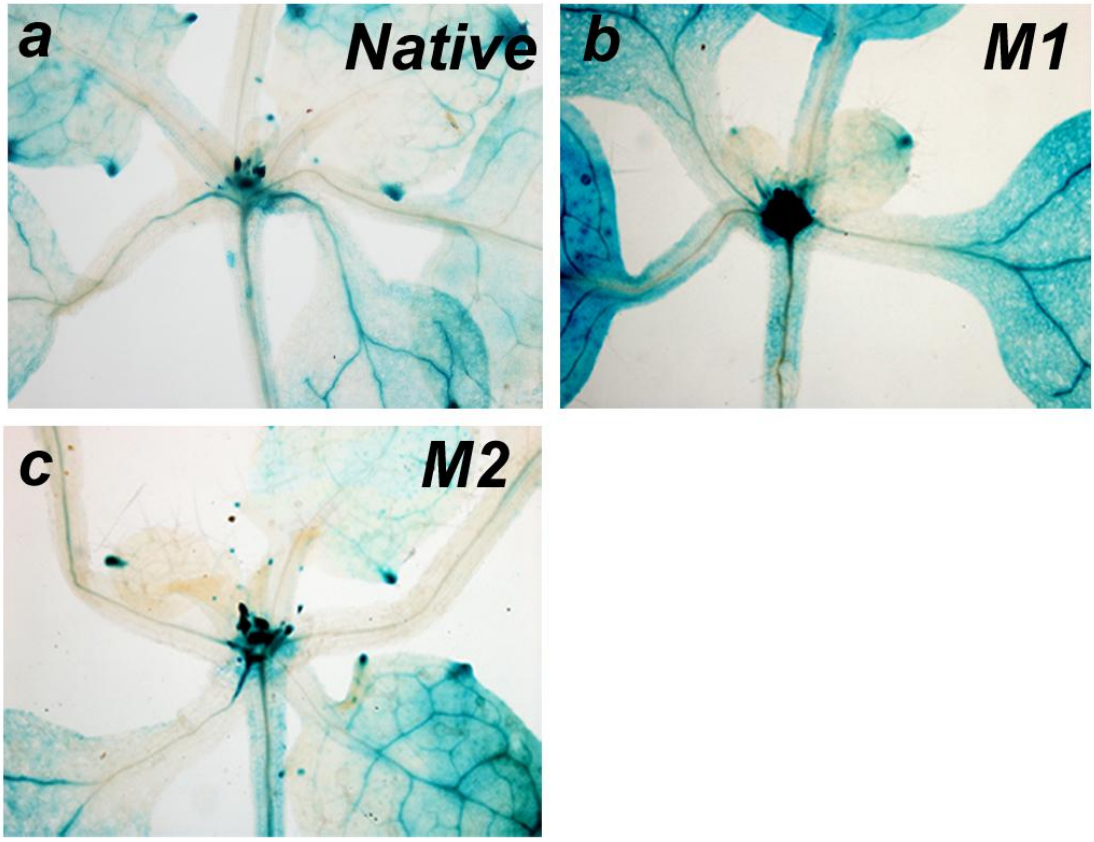

Fig 35. Representative GUS staining of 12-day-old transformants containing *SOC1:GUS* (a) and its mutated constructs M1 (b) and M2 (c).

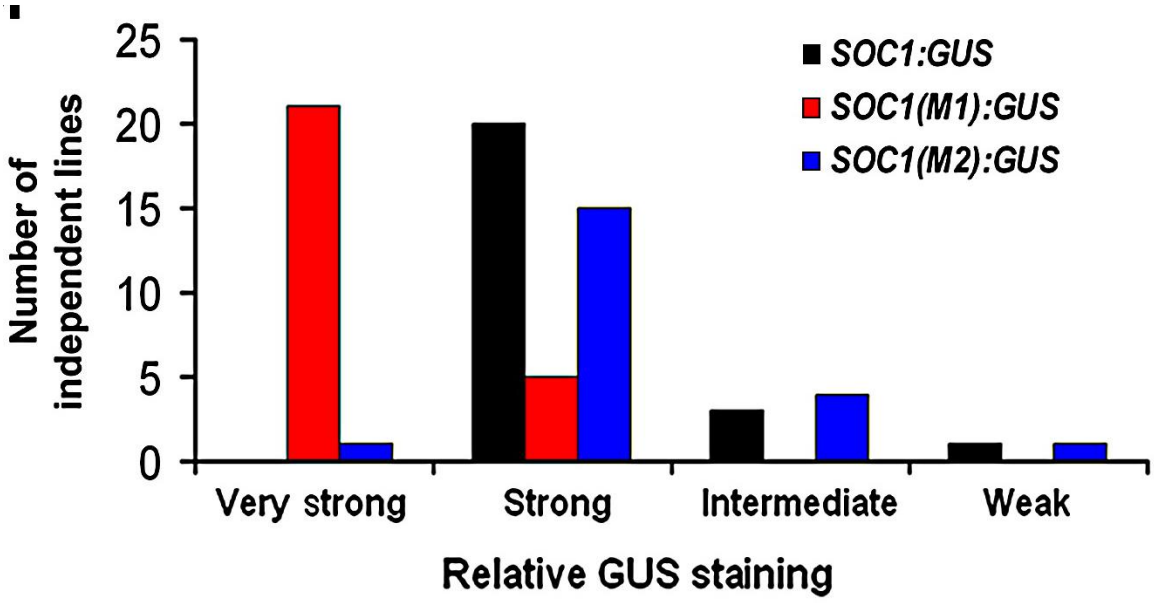

Fig 36. Distribution of relative GUS staining intensity in the transformants containing *SOC1:GUS* and its mutated forms M1 and M2. We analyzed 24 independent lines for *SOC1:GUS* (Liu et al., 2008), 26 independent lines for M1, and 21 lines for M2. The intensity of GUS staining exhibited by most *SOC1:GUS* lines was designated as "strong."

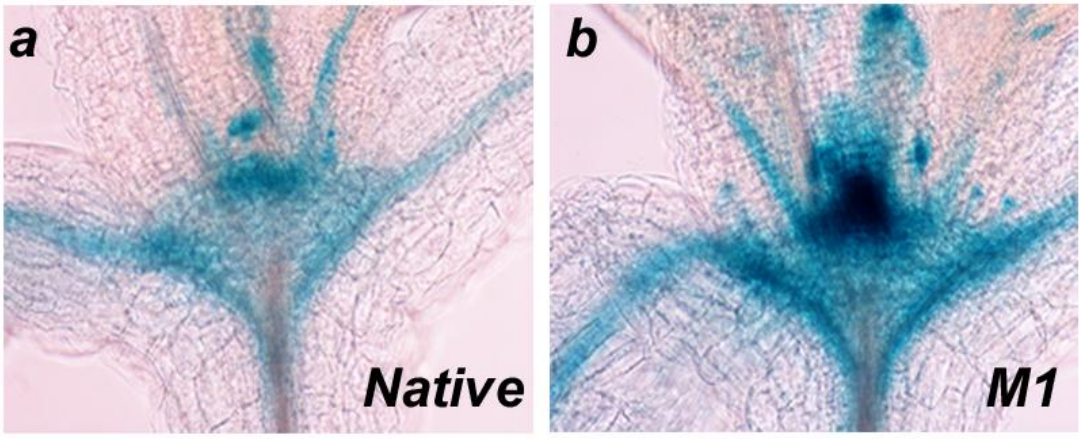

Fig 37. GUS staining of the shoot apex of 12-day-old transformants containing *SOC1:GUS* (a) and M1 (b).

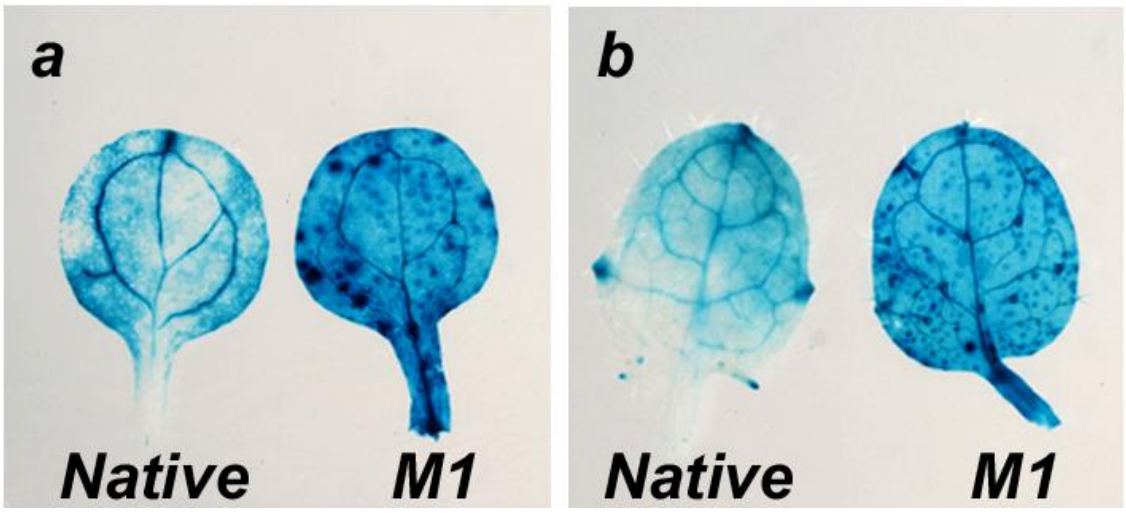

Fig 38. GUS staining of the cotyledons (a) and leaves (b) of the transformants containing SOC1:GUS and M1.

shoot apex and leaf of *35S:SVP* was reduced compared with that in wild-type background (Figures 35a and 3K), while staining of M1 plants remained almost unchanged (Figures 35b and 39b). Thus, mutation of the SOC1-CArG1 at M1 almost completely abolished repression of *SOC1* expression by SVP, confirming that SVP binds to this site to repress *SOC1* expression.

To further verify that the identified SVP binding site is essential for *SOC1* function in the control of flowering, *soc1-2* mutants were transformed with a genomic *SOC1* construct (Liu et al., 2008) or with its derived constructs with the M1 or M2 mutation. The average flowering time of T1 generation plants of *soc1-2* mutants transformed with the *SOC1* genomic construct was 15.4 total leaves (Figure 40; Liu et al., 2008). This was slightly later than the average flowering time of wild-type plants (13.2 leaves). Thus, the native *SOC1* fragment could largely rescue the late flowering of *soc1-2*, which flowered with 28 leaves under the same conditions (Figure 14). The average flowering time of *soc1-2* mutants transformed with the M2 construct was 15.2 leaves, which was comparable with that shown in *soc1-2* mutants transformed with the native *SOC1* genomic fragment (Figure 40). However, the *soc1-2* mutants transformed with the M1 construct exhibited earlier flowering (11.8 leaves) than any other plants (Figure 40). These results demonstrate that mutation of the SOC1-CArG1 box at M1 accelerates flowering, and corroborate that SVP binding site at SOC1-CArG1 is responsible for repressing *SOC1* during flowering.

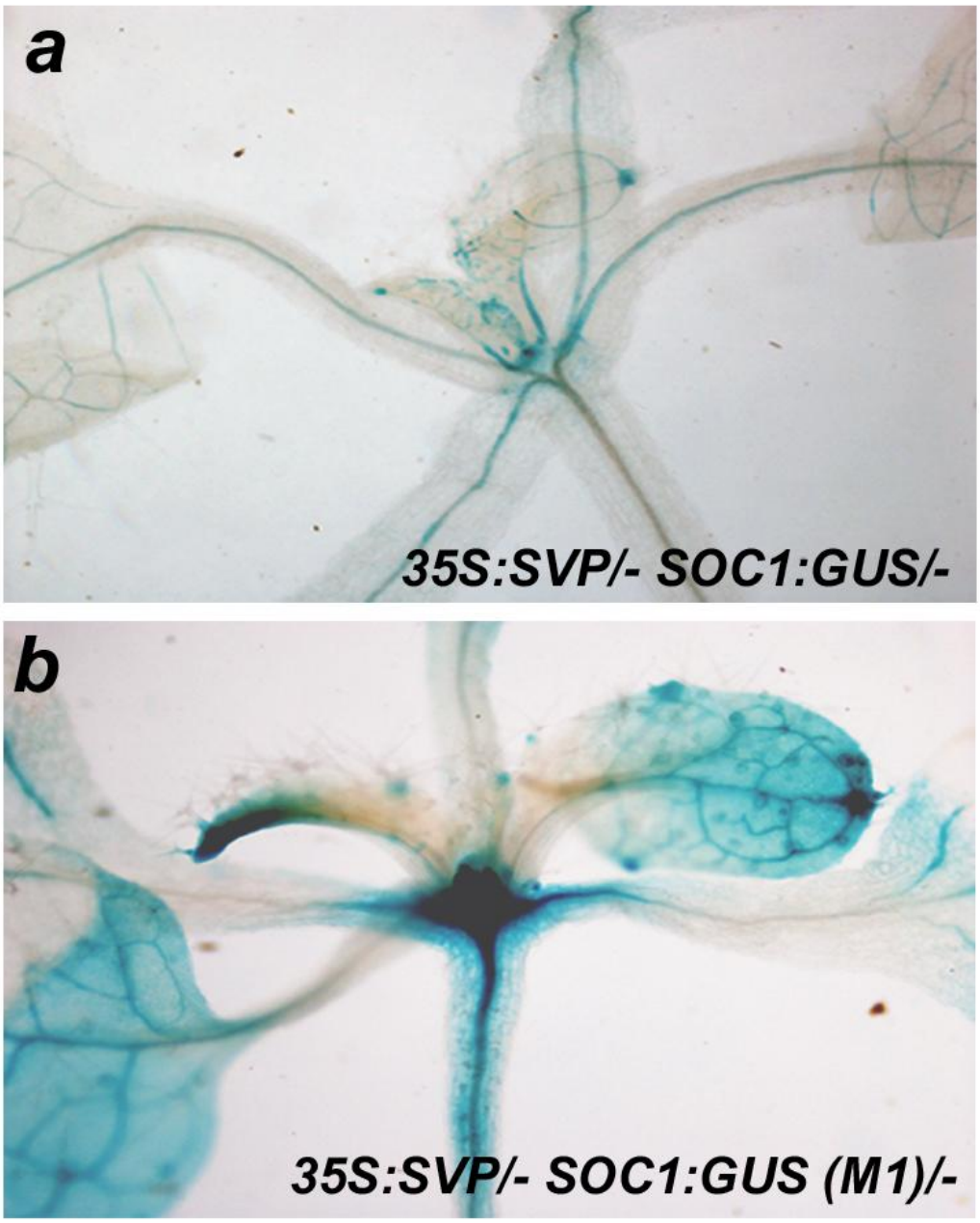

Fig 39. GUS staining of 12-day-old SOC1:GUS (a) and M1 (b) in 35S:SVP background.

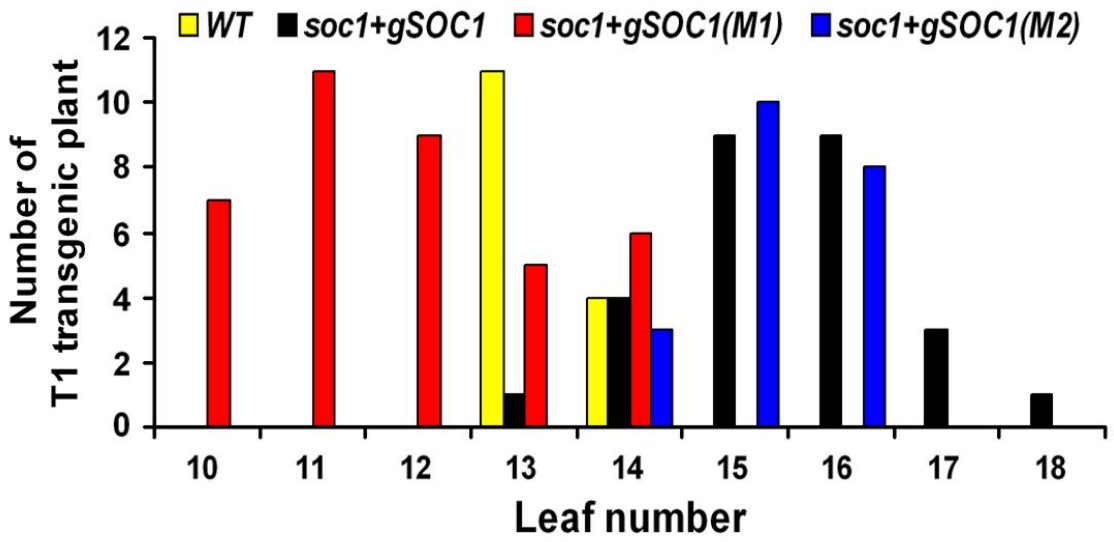

Fig 40. Distribution of flowering time in T1 transgenic plants carrying the wild-type *SOC1* gene and its mutated forms (M1 and M2) in the *soc1-2* mutant background. We analyzed 27 independent lines for *gSOC1* () 38 independent lines for *gSOC1*(M1), and 21 lines for *gSOC1*(M2). Error bars indicate standard deviation.

4.8 SVP Interacts with FLC

The SOC1-CArG1 box bound by SVP was 19 nt distant from the SOC1-CArG2 box in the *SOC1* promoter, which has previously been identified as a FLC binding site (Helliwell et al., 2006, Hepworth et al., 2002 and Searle et al., 2006). *FLC* is a potent floral repressor upon which multiple floral regulatory pathways converge. Since SVP and FLC negatively control *SOC1* expression and they exhibit a similar expression pattern in the shoot apical meristem and leaves at the vegetative phase (Figures 41a and 41b; Hartmann et al., 2000, Noh and Amasino, 2003 and Sheldon et al., 2002), their proteins may interact to control *SOC1* expression. To test this hypothesis, we performed in vitro glutathione S-transferase (GST) pull-down assays and found that GST-SVP or GST-FLC bound in vitro-translated full-length HA-FLC or Myc-SVP, respectively (Figure 42). This binding was specific because HA-FLC or Myc-SVP failed to bind to the control GST alone.

To determine whether this direct physical interaction occurs in vivo, we performed a reciprocal coimmunoprecipitation analysis using transgenic *svp41 SVP:SVP-6HA* plants in the ecotype C24, where FLC expression is high (Hartmann et al., 2000, Noh and Amasino, 2003 and Sheldon et al., 2002). Protein extracts from the *svp41 SVP:SVP-6HA* and C24 wild-type plants were immunoprecipitated with either anti-FLC conjugated to Protein G PLUS agarose or anti-HA agarose. The resulting immunoprecipitates were separated by SDS-PAGE. The precipitated proteins were analyzed by western blot using the anti-HA or anti-FLC antibody. A band with

the

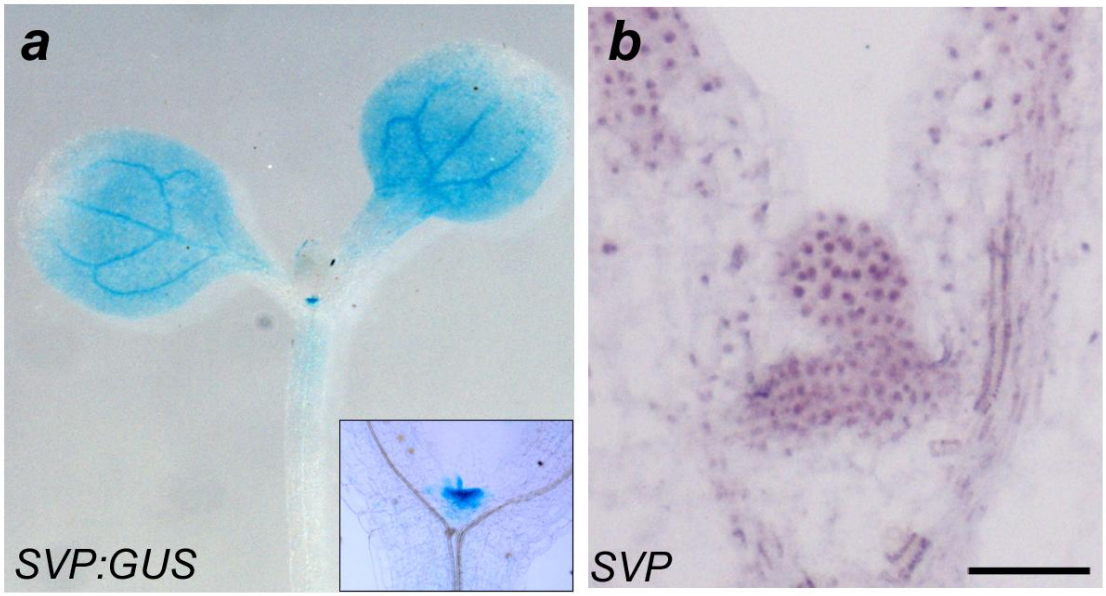

Fig 41. (a) GUS staining of 5-day-old *SVP:GUS* Col seedling. Inset shows GUS staining of the shoot apex. (b) In situ localization of *SVP* at the shoot apex of 5-day-old Col wild-type seedlings. Scale bars, 25 µm.

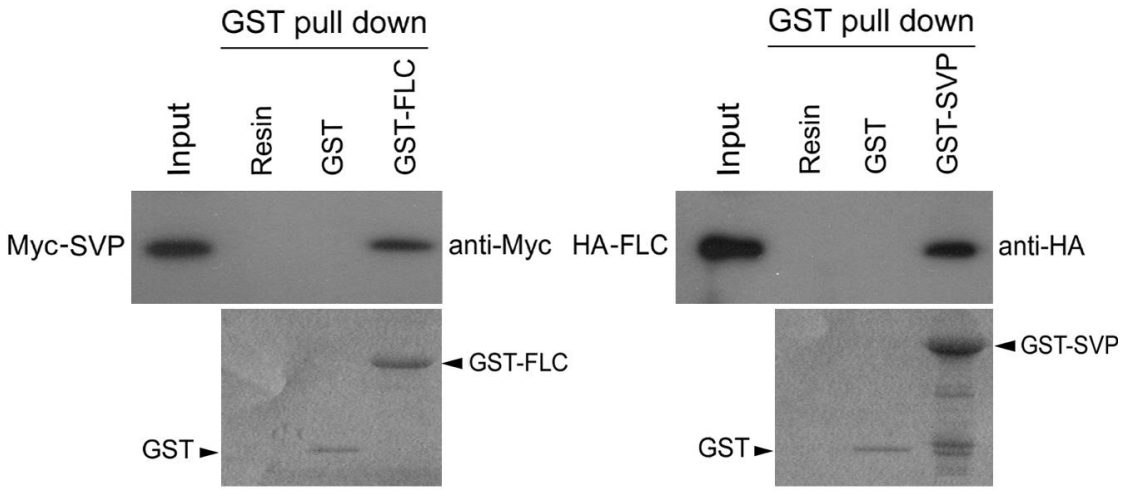

Fig 42. In vitro GST pull-down assay with SVP and FLC proteins. Precipitated GST, GST-SVP, and GST-FLC are shown by Coomassie blue staining.

expected mobility of SVP-6HA was repeatedly detected from the anti-FLC immunoprecipitates of the *svp41 SVP:SVP-6HA* plants (Figure 43). On the contrary, no band of the same mobility was detected from the immunoprecipitates of the C24 wild-type plants. The in vivo interaction of FLC and SVP was also revealed in the anti-HA immunoprecipitates (Figure 43), where FLC was only observed in the immunoprecipitates of the *svp41 SVP:SVP-6HA* plants.

Coimmunoprecipitation analysis was further carried out in developing *svp-41 SVP:SVP-6HA* Col seedlings grown in LDs (Figure 44). As *svp-41 SVP:SVP-6HA* showed comparable flowering time with wild-type Col plants, this analysis aimed to examine temporal endogenous interaction of SVP and FLC. While FLC expression is generally low in Col, its expression was detectable in 3- and 5-day-old seedlings, and reduced afterwards (Figure 44). SVP expression was consistently high in developing seedlings, with its peak in 7-day-old seedlings. Protein extracts from these seedlings were immunoprecipitated with anti-HA agarose, and the precipitated proteins were analyzed by western blot using the anti-HA or affinity-purified FLC antibody (Hartmann et al., 2000, Noh and Amasino, 2003 and Sheldon et al., 2002). The interaction between SVP-6HA and FLC proteins was clearly observed in 3- to 9-day-old seedlings, demonstrating that SVP-6HA and FLC proteins interact in vivo during vegetative growth. The weakened interaction between SVP and FLC in 11- and 15-day-old seedlings is concomitant with the upregulation of *SOC1* expression (Figure 15). To investigate the spatial interaction of SVP and FLC during seedling development, we examined their interaction in the aerial part of the seedlings (without

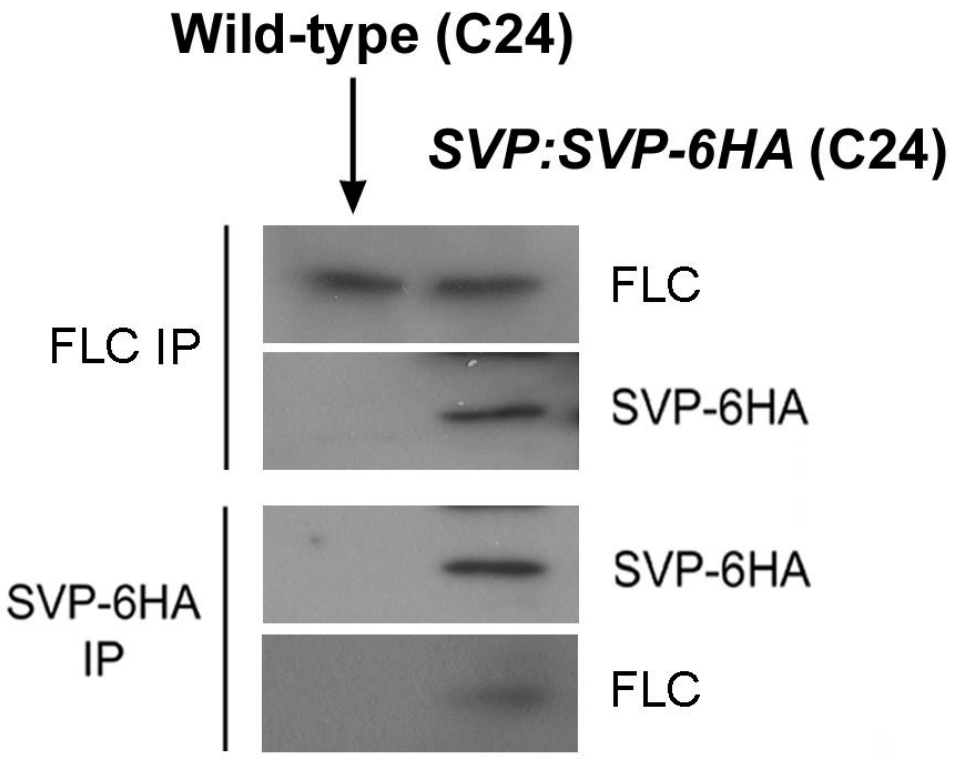

Fig 43. Interaction of SVP and FLC in SVP:SVP-6HA C24 seedlings. Protein extracts were isolated from 5-day-old SVP:SVP-6HA (C24).

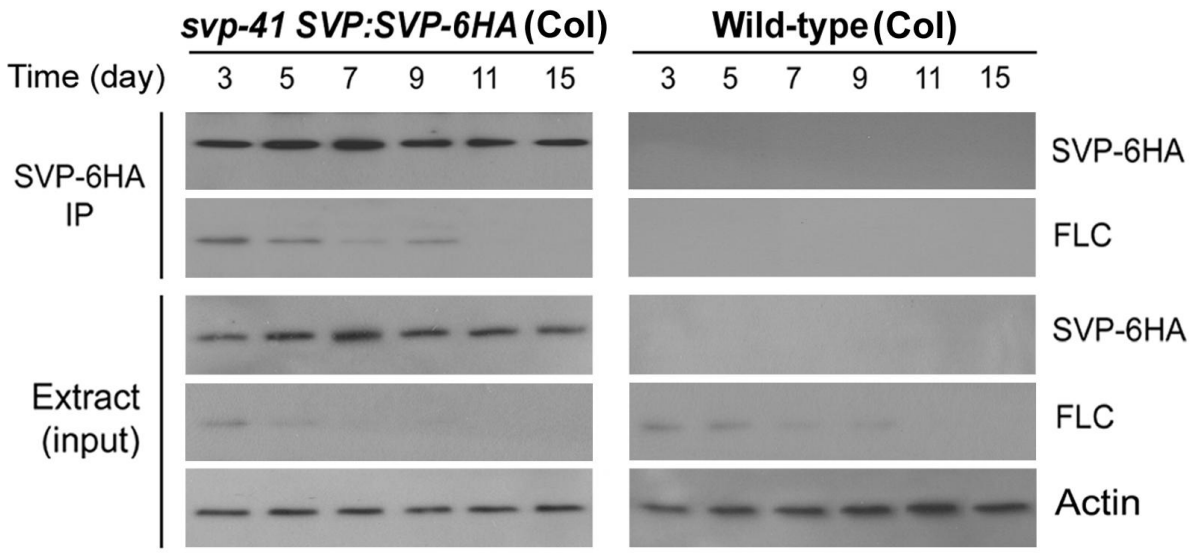

Fig 44. Interaction of SVP and FLC in *developing svp-41 SVP:SVP-6HA* (Col) seedlings grown in LDs. *svp-41 SVP:SVP-6HA* or wild-type seedlings from day 3 to day 15 were harvested for protein extraction.

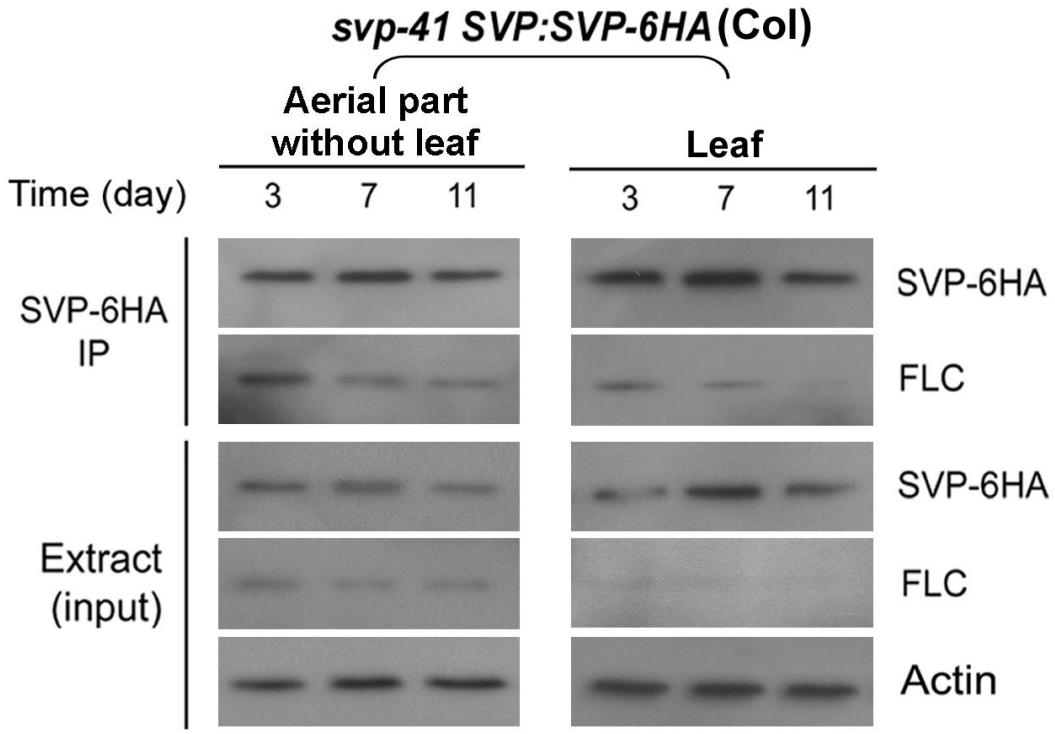

Fig 45. Interaction of SVP and FLC in the aerial part without leaves, and leaves of developing svp-41 SVP:SVP-6HA seedlings grown in LDs.

leaves) and leaves of *svp-41 SVP:SVP-6HA* (Figure 45). FLC protein expression peaked in the aerial part without leaves in 3-day-old seedlings, and was slightly reduced afterwards, while its expression in the leaf was relatively low. SVP peaked in the leaves and the remaining aerial part in 7-day-old seedlings. The interaction between SVP and FLC occurred in the aerial part without leaves of all developing seedlings examined, with the peak in 3-day-old seedlings. On the contrary, their interaction was only weakly detected in the leaves of 3- and 7-day-old seedlings.

4.9 FLC and SVP Functions Are Mutually Dependent

Since our results showed in vitro and in vivo interaction of SVP and FLC proteins, we further tested the biological significance of this interaction by genetic analysis (Figure 46). Loss of *SVP* function significantly suppressed the severe late-flowering phenotype of *FRI FLC*, in which *FLC* was highly expressed (Michaels and Amasino, 1999). On the contrary, loss of *FLC* function could moderately rescue the late-flowering of *35S:SVP*. These results indicate that *FLC* and *SVP* functions are mutually dependent, and that the former is largely dependent on the latter. The interaction of SVP and FLC was further supported by the phenotype of the double mutant *flc-3 svp-41* (Figure 46). In the Col background, *flc-3* showed slightly early flowering, while *svp-41* flowered much earlier. The double mutant *flc-3 svp-41* showed a stronger early flowering phenotype compared with either single mutant, but was much like the *svp-41* mutant.

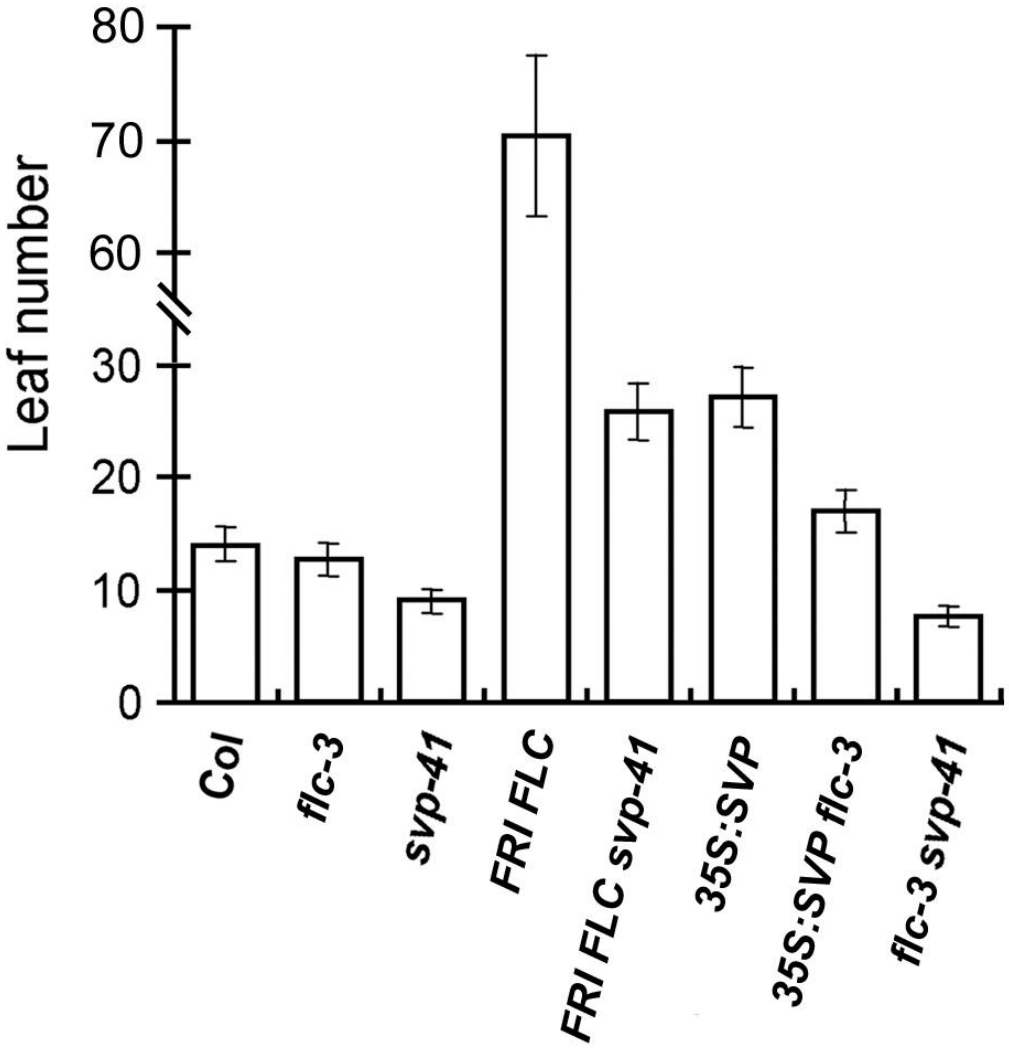

Fig 46. Flowering phenotypes of plants with different levels of FLC and SVP expression in LDs.

ChIP assays of *35S:FLC-HA* have revealed the binding of FLC to the first intron of *FT* that contains a CArG consensus sequence, suggesting that FLC directly mediates repression of *FT* in the leaf (Searle et al., 2006). The same region, together with other upstream regions, of *FT* was found to be highly associated with SVP-HA by ChIP assays using *Arabidopsis* protoplasts (Lee et al., 2007). In ChIP assays of *35S:SVP-6HA* and *svp-41 SVP:SVP-6HA* lines, we consistently found that the number 4 fragment that was close to the CArG box at the first intron of *FT* showed the highest enrichment associated with SVP-6HA by quantitative real-time PCR (Figure 47). These observations imply that FLC and SVP may bind to the same site of *FT* genomic sequence to regulate its expression, and that the interaction of FLC and SVP regulates both *SOC1* and *FT*. It is noteworthy that *FT* was only slightly upregulated in the leaves of *svp-41* in the Col background where *FLC* expression was low (Figure 18), indicating that the effect of SVP on *FT* expression in the leaves may largely rely on FLC.

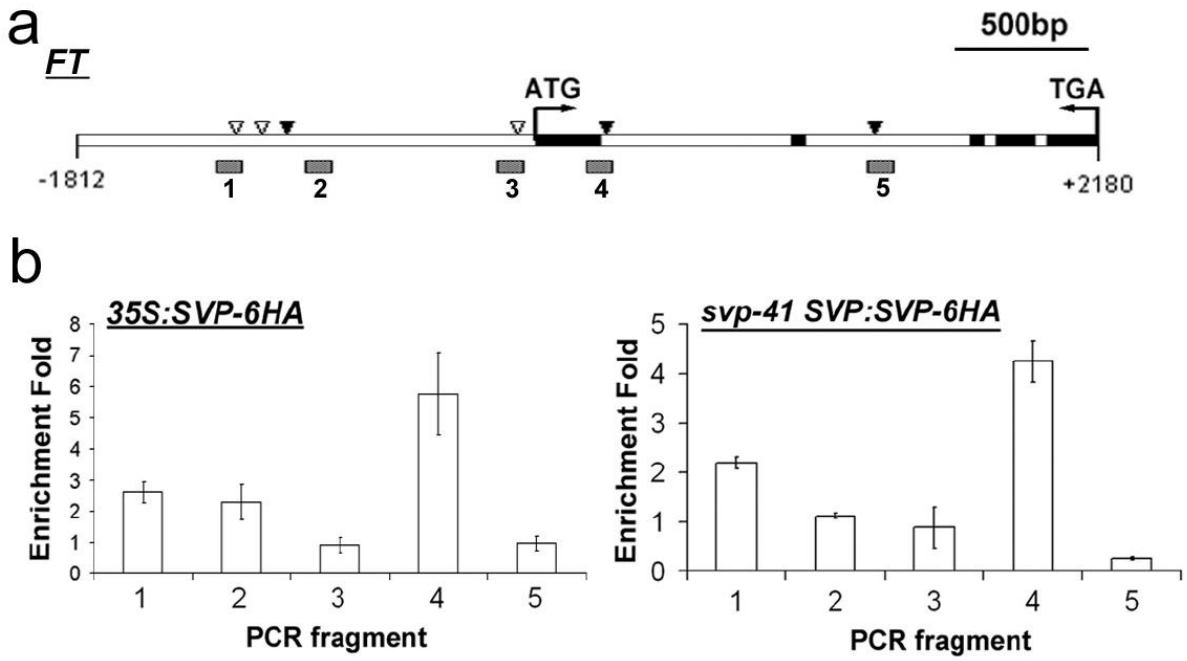

Fig 47. SVP is Associated with the *FT* Genomic Region (a) Schematic diagram of the *FT* genomic region. Exons are represented by black boxes, while introns and upstream regions are represented by white boxes. Bent arrows denote translation start sites and stop codons. Filled arrowheads indicate the sites containing either single mismatch or perfect match with the consensus binding sequence (CArG box) of MADS-domain proteins, while open arrowheads indicate the CArG sites containing two mismatches. Five DNA fragments near the above CArG sites in the *FT* genomic region were examined by ChIP enrichment test as shown in (b). (b) ChIP enrichment test shows the binding of SVP-6HA to the region near the fragment 4. Seven-day-old seedlings of *35S:SVP-6HA* and *svp-41 SVP:SVP-6HA* were harvested for ChIP analysis. Relative enrichment of each fragment was calculated first by normalizing the amount of a target DNA fragment against a genomic fragment of *ACTIN*, and then by normalizing the value for transgenic plants against the value for wild-type as a negative control.

4.10 *SVP* autoregulation

To detect if *SVP* can be self-regulated, we designed different pairs of primers that can distinguish the *SVP* transgene from its endogenous copy. The designed SVP P1/P2 primers amplified the coding and 3' untranslated regions (3'UTR) of *SVP* mRNA from 970 bp to 1,650 bp, while the primers SVP mRNA F/R only amplifies the region from 620 bp to 970 bp (Figure 11b) (Table 4). Since we only cloned the coding region (from 520 bp to 1,250 bp) into the *SVP* tagging and XVE inducible constructs, SVP P1/P2 could only amplify the expression of the endogenous *SVP* gene, while *SVP* mRNA F/R could reveal the expression of both the endogenous *SVP* and the *SVP* transgene. In *35S::SVP*, RT-PCR using the primers SVP P1/P2 showed that the endogenous *SVP* expression was down-regulated on both Day 7 and Day 13, while the analysis using the primers SVP mRNA F/R suggested that the overall *SVP* level was indeed increased. Wild-type and *svp41* plants were included as controls (Figure 11c, 11d). These results indicate the existence of a negative feedback loop leading to the self-regulation of endogenous *SVP* expression. However, the autoregulation may be direct or indirect; hence ChIP was further used to test whether *SVP* could mediate its negative feedback loop in an *in vivo* context.

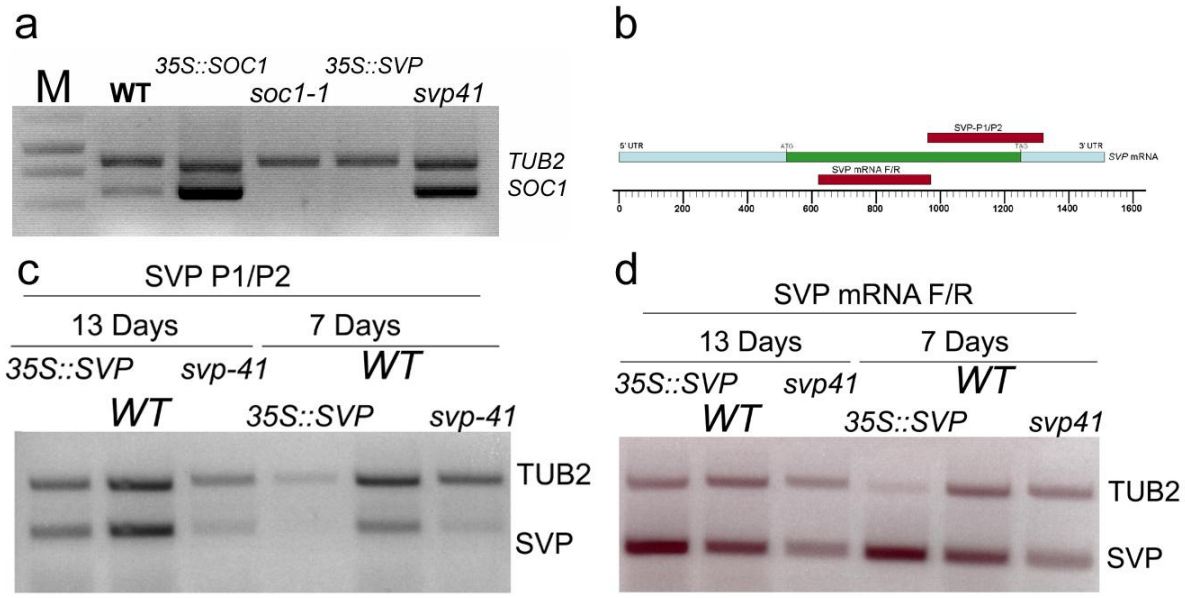

Fig 11. *SVP* over-expression leads to the down-regulation of *SOC1* and itself. (a) The *SOC1* level is dramatically decreased in the *35S::SVP* plants and significantly increased in the *SVP* loss-of-function plants. (b) SVP P1/P2 can only detect the endogenous *SVP* mRNA, but not the transcripts from *35::SVP*, which are denoted by the green region, while SVP mRNA F/R can detect both of them. (c) SVP P1/P2 detect endogenous *SVP* mRNA is decreased in *35S::SVP* on Day 7 and 13, while SVP mRNA F/R suggest *SVP* expression level is indeed increased. *TUB2* as internal control.

Table 4. Primers used for RT-PCR

Primer name	Sequence 5’-3’
AGL20-P1	GAAGATAGTTTGAGGGGCAAAACTC
AGL20-P2	GGGCTACTCTCTTCATCACCTCTTCC
TUB2-P1	ATCCGTGAAGAGTACCCAGAT
TUB2-P2	TCACCTTCTTCATCCGCAGTT
SVP-P1	GTGACAAGATTATGAAGTGAGATCAG
SVP-P2	GAATTCACTACTTAGACATTGTCTC
SVP-mRNA-F	AGTCCTAGAGAGGCATAACTTGCAG
SVP-mRNA-R	CTGATCTCACTCATAATCTTGTCAC

Chapter 5

Discussion

5.1 *SVP* and flowering time pathways

A pervious study has shown that the MADS-domain gene *SVP* is a repressor of floral transition (Hartmann *et al*., 2000). However, this study did not address the concrete functional mode of *SVP* in flowering time in *Arabidopsis*. In this study, we aimed to investigate the mechanism of *SVP* repression of flowering.

Both autonomous and vernalization pathways promote flowering by repressing the expression of *FLC* and the mutations of the genes in these pathways exhibit the late-flowering phenotype due to increased *FLC* expression. Dominant alleles of *FRI* also delay flowering by increasing *FLC* levels. The expression of *SVP* is affected in the *fve* mutant background, indicating that *SVP* is acting in the autonomous pathway. In addition, vernalization does not have any significant effect on *SVP* expression. By contrast, GA treatment causes reduced *SVP* expression, and *co* and *ft* mutants in photoperiod pathway do not show significant elevation of *SVP* expression, suggesting that GA pathways partially suppress *SVP* expression. To further validate the data, the studies on *SVP* expression in other autonomous pathway mutants (*fpe,* and *fca)* and GA pathway mutants *(ga1-3, ga1-3 rga)* are carrying out.

5.2 ChIP and *SVP* direct targets

In this study, it has been shown that SVP-6HA fusion proteins were able to regulate flowering time in a manner mimicking the endogenous *SVP*. ChIP analysis was subsequently used to identify the direct downstream target genes of *SVP*. Western blot analysis and the results from PCR enrichment test, in which the co-precipitated DNA showed an altered composition compared with input DNAs and mock DNAs, suggest that the overall ChIP process was successful.

The PCR enrichment test for *SOC1, SVP, AGL24* and *LFY* demonstrate that *SOC1* and endogenous *SVP* were bound *in vivo* by SVP in *35S::SVP-6HA* and svp41 *SVP::SVP-6HA* transgenic lines, and the amount of bound DNA correlated with the level of nuclear localized SVP-6HA protein. These results, together with RT-PCR results showing that both *SOC1* and *SVP* are in response to *SVP* expression level, strongly suggest that *SOC1* and *SVP* are the direct targets of SVP.

SOC1 is a floral integrator because it is a convergent point for several promotion pathways. *SOC1* is expressed mostly in leaves and in the shoot apex and its expression has a sharp increase occurring in the apex during floral transition (Borner *et al.*, 2000, Samach *et al.*, 2000). *In situ* hybridization has shown that during vegetative phase, *SVP* transcripts were detectable in young leaves and throughout the apical meristem. During early stages of bolting, *SVP* transcripts were absent from the main inflorescence apical meristem (Hartmann *et al.,* 2000). Our ChIP data showed that SVP protein could directly repress the expression of *SOC1* and *SVP* itself. To explain

this behaviour, it has been postulated that flowering represents a default developmental program that must be suppressed by one or more floral repressors, such as *SVP*, to allow a phase of vegetative growth. Moreover, the activity of these floral-repressing flowering time genes gradually declines during development. We have shown that *SVP* loss-of-function resulted in *SOC1* over-expression similar to *35S::SOC1* and a very early-flowering phenotype. Thus it is proposed that the repression of *SOC1* by *SVP* is a default process which allows the plant to store energy during the vegetative phase. Meanwhile, the signals from photoperiod and GA pathways accumulate and act to repress *SVP* expression throughout the plant. In addition, there may be some region specific factors that directly repress *SVP* expression, leading to *SVP* down-regulation in the shoot apical meristem (SAM). Consequently, the *SOC1* level is dramatically increased in this region, thus promoting flowering.

From this point of view, *SVP* autoregulation seems to be another default program that prevents overwhelming *SVP* expression. It causes the limited production of the full-length active *SVP* mRNA, thus limiting *SVP* activity.

It is noteworthy that although *AGL24* and *LFY* did not show any enrichment, it cannot conclude that they are not direct targets of *SVP*. This is because either the primer pairs chosen or the plant stage selected could have affected the final results. To avoid these problems, a sequence library containing the genomic loci that can potentially bind to SVP protein will be generated from the eluted DNAs. They will be the ideal candidates for further enrichment test. Moreover, a time course ChIP study

with *SVP* native expression system needs to be carried out in order to investigate whether there are interactions between *SVP* and other genes in different developmental contexts.

5.3 SVP associates with FLC to repress *SOC1* expression

Here we have shown that the flowering regulator *SVP* plays a key role in maintaining the duration of the vegetative phase by directly repressing *SOC1* transcription strongly in the shoot apex and moderately in the leaf. *SOC1* expression in whole seedlings is tightly regulated by the levels of *SVP* expression. Mutating the SVP binding site in the *SOC1* promoter in the wild-type Col background causes strong derepression of *SOC1* in the shoot apex and leaf (Figure 35). On the contrary, mutating the binding site of another *SOC1* repressor, FLC, in the *SOC1* promoter does not result in apparent derepression of *SOC1* in the wild-type Col background (Figures 35; Hepworth et al., 2002). These observations suggest that in the plants with relatively low levels of *FLC* expression (e.g., wild-type Col), *SVP* plays a major role in regulating *SOC1* expression. This is substantiated by the phenotypes of *svp-41*and *flc-3*, as the former exhibits much earlier flowering than the latter in the Col background.

SVP protein associates with the promoter region of *SOC1* where FLC binds. During vegetative growth, SVP interacts with FLC in the whole seedlings with a relatively strong affinity in the aerial part without leaf. This interaction is critical for

their function in determining flowering because loss of function of either gene compromises the ability of another gene in repressing flowering. Notably, in the plants with high levels of *FLC* expression (e.g., *FRI FLC*), the *FLC* repressive effect on flowering is significantly suppressed by *svp-41* (Figure 46), demonstrating that FLC function is highly dependent on SVP.

Interaction between FLC and SVP may also directly affect *FT* expression in the leaf, as both of them can bind to the same site of *FT* genomic sequence. It has been shown that *FLC* expression in the leaf represses flowering by mainly repressing *FT* expression (Searle et al., 2006). While SVP was suggested to negatively regulate *FT* expression in the leaf within the thermosensory pathway (Lee et al., 2007), we could only detect slightly upregulated expression of *FT* in the leaves of *svp-41* by quantitative real-time PCR (Figure 18). As the protein interaction between FLC and SVP exists in the leaf, SVP's effect on *FT* expression may be mediated by FLC. This partly explains why alteration of *FT* expression is not so significant in *svp-41* in the Col background, where *FLC* expression is relatively low. As *svp-41* more or less accelerates flowering of single or double mutants of *ft-1* and *soc1-2* (Figure 14), it is possible that SVP partially acts through other unknown factors in addition to *SOC1* and *FT*.

It has been suggested that FLC is a central regulator of the floral enabling pathways that antagonize the activation of the floral pathway integrators (Boss et al., 2004 and Reeves and Coupland, 2001). Our results suggest that SVP is another central regulator that mainly responds to the endogenous flowering signals and interacts with

FLC in the aerial part of the seedlings. Hitherto, this relationship has not been revealed in previous studies on the protein interaction among *Arabidopsis* MADS-box genes. Their combined action confers a critical control of floral induction by directly repressing the early onset of expression of floral pathway integrators at the vegetative phase. This allows plants to accumulate sufficient energy for subsequent reproductive success. During the floral transition, the flowering signals from autonomous, vernalization, and GA pathways converge on the downregulation of SVP and FLC, thus derepressing the expression of floral pathway integrators. Therefore, it is likely that the effect of these flowering genetic pathways on the floral transition is mainly mediated through a derepression mechanism. In contrast, the photoperiod pathway, which does not affect the expression of either *SVP* or *FLC*, seems to be a major pathway that activates floral pathway integrators.

Unlike another floral pathway integrator, *FT*, *SOC1* is highly expressed in the shoot apex during floral transition and has been suggested to be associated with regional specificity for initiation of floral meristems (Borner et al., 2000, Lee et al., 2000, Liu et al., 2008 and Samach et al., 2000). Complementation of *SOC1* expression in the shoot apical meristem of *soc1* mutants results in much earlier flowering than that in the phloem (Searle et al., 2006), suggesting that regulation of *SOC1* expression in the meristem has a more significant effect on the control of flowering. In addition to SVP and FLC, recent studies have revealed several other flowering regulators that are involved in the tight control of *SOC1* transcription in the meristem. FT and its cofactor FD are required for activation of *SOC1* expression in

the meristem (Abe et al., 2005, Corbesier et al., 2007, Searle et al., 2006 and Wigge et al., 2005), while AGL24 directly upregulates *SOC1* transcription in the meristem during the floral transition (Liu et al., 2008). Intriguingly, even in the absence of *FT* and *AGL24*, loss of *SVP* function results in a higher *SOC1* expression than in wild-type plants (Figure 23). This result suggests that SVP repression has a dominant effect on *SOC1* expression, and that removal of SVP activity may activate *SOC1* expression independently of those known *SOC1* activators.

A further question that arises from this study is the relationship between *SVP* and *AGL24*. While they are the closest genes among all the 107 MADS-box transcription factors found in *Arabidopsis* (Parenicova et al., 2003 and Yu et al., 2002), they exhibit completely opposite functions in directly regulating *SOC1* transcription in the meristem (Liu et al., 2008). It is possible that they regulate *SOC1* in a temporal sequence as repression of *SOC1* by SVP occurs at the vegetative phase and gets weaker during the floral transition, at which promotion of *SOC1* by AGL24 mainly happens (Liu et al., 2008). The expression level of *SVP* and *AGL24*, which is affected by various flowering genetic pathways, should be one of the important factors that contribute to the predominance of SVP or AGL24 in the *SOC1* transcription complex. It is noteworthy that *SVP* is genetically epistatic to *AGL24*, because the double mutants *agl24-1 svp-41* show a similar flowering time to *svp-41* (Figure 14). This suggests that *AGL24* may act upstream of *SVP*. In wild-type plants *AGL24* expression is upregulated at the shoot apex by *SOC1* during the floral transition (Liu et al., 2008). It is, therefore, tempting to hypothesize that *SOC1* may suppress *SVP* expression via

AGL24, thus activating its own expression in the meristem in a positive feedback loop.

Phylogenetic analysis has shown that SVP belongs to the *StMADS11*-like clade of MADS-box proteins that comprises members from gymnosperms, monocots, and eudicots (Becker and Theissen, 2003). The majority of its members are specifically expressed in vegetative tissues, and several members that repress flowering in various species have been reported (Hartmann et al., 2000, Kane et al., 2005 and Masiero et al., 2004). Whether SVP function in *Arabidopsis* flowering represents a general mechanism for members of this clade of proteins needs to be further investigated.

5.4 *SVP* and other MADS-box genes

In plants, MADS-box genes comprise a large family of transcriptional regulators that have diverse roles in development. Six MADS-box genes have been previously reported to regulate flowering in *Arabidopsis*: *FLC*, *FLM*, and *SVP* act as repressors of flowering, whereas *AGL24*, *FUL* and *SOC1* act as floral promoters. In this report, we present evidence that *SVP* represses flowering through direct down-regulation of *SOC1*.

It is interesting to note that in *Arabidopsis*, *SVP* has the highest sequence similarity to *AGL24*, which promotes flowering. The discovery that two closely related genes have opposite effects on flowering time is not unprecedented, since the floral promoter *FT* and the repressor *TFL1* are also highly similar genes with opposite

effects on flowering (Kardailsky *et al*., 1999; Kobayashi *et al*., 1999). A previous study has shown that changing a single amino acid in *FT* converts it from a flowering promoter to a repressor, with the same effect as *TFL1* (Hanzawa *et al.*, 2005). Whether the same scenario exists for *SVP* and *AGL24* remains unknown. Currently, another parallel work in our lab suggests that *AGL24* is also able to bind to *SOC1* directly (unpublished data). It will be interesting to investigate whether *SVP* and *AGL24* share the same binding site on the *SOC1* promoter. If this is true, it is possible that *SVP* and *AGL24* compete for the same binding site in a dosage dependent manner. A temporal ChIP analysis will help to reveal if *SVP* and *AGL24* show different binding capacity with *SOC1* promoter during the course of floral transition.

FLM is a MADS-domain gene, for which the mutant phenotype is similar to that of *SVP*. Although *FLM* and *SVP* are classified into different MADS domain groups on the basis of sequence similarity, they appear to act in the same flowering pathway. A previous study showed that the phenotype of *svp flm* double mutant was the same as either single mutant in LD and SD conditions (Scortecci *et al*., 2003). In the homozygous *svp* mutant background, the late-flowering effect of *35S::FLM* was suppressed, while the *flm* mutation was also able to suppress late-flowering of 35S::*SVP* (Scortecci *et al*., 2003). However, *SVP* mRNA levels were not affected by an *flm* lesion or by *FLM* over-expression. Our data also suggest that *FLM* expression is not affected by *SVP* over-expression or *SVP* loss-of-function (unpublished data). These results suggest that *FLM* and *SVP* may act in parallel with each other either as

partners or in different branches.

In the flower development, distinct MADS domain proteins can associate and bind to DNA as heterodimers or higher-order multimers. Hence it raises the possibility that *FLM* and *SVP* are part of a multimeric MADS domain complex that regulates flowering time. In order to verify this model, mass spectrometry analysis will be performed on the transgenic lines of *35S::SVP-12HA* to identify the protein partners of *SVP*.

5.5 *Cis*-regulatory elements in *SVP* promoter region

Spatial and temporal gene expression is regulated by a complex interaction of *cis*-acting DNA elements and *trans*-acting regulatory proteins. These interactions may lead to the induction or repression of gene expression with a variety of signals 'read' by the basal transcriptional machinery, either via direct interaction or through chromatin remodelling. To this end, deletion analysis is a valuable approach to identify the regulatory regions containing relevant *cis*-acting elements.

GUS staining results indicate the presence of putative positive and negative *cis*-elements regulating the expression of *SVP*. The difference in enzymatic activity between P2 and P5 shows that, although deletion of the 5' region from -1,800 bp to -1,200 bp does not alter the pattern of expression, it reduces the GUS activity. This observation supports a role of this region in enhancing *SVP* expression. The difference of GUS activity between P2 and P3 shows that a deletion from +200 bp to +1,700 bp

abolishes GUS activity, suggesting that this region is important in initiating the *SVP* expression.

It is noteworthy that the P4 construct, which contains a 3' end region 1.4 kb longer than P5, fails to show any GUS activity. This leads to the hypothesis that this region contains critical *cis*-regulatory region that is involved in the down-regulation of *SVP* expression. Our ChIP results show that *SVP* could bind to a fragment within this region, implying that this region may serve as a *SVP* binding site that mediates self-autoregulation. To provide evidence for this possibility, future studies will be performed to further dissect the regulatory elements in this region.

In addition, as there may be a *cis*-element in the region +1,700 bp to +3,100 bp that is involved in negative regulation *SVP* (Figure 13), the P2 construct may lack the essential elements required to drive endogenous spatial and temporal expression. Thus, the construct containing the *SVP* native promoter, introns and exons have to be created. In addition, to facilitate the *SVP* promoter study, more deletion constructs will be made to localize the regions respond to spatial and temporal signals. At this point, it can be concluded that the regions from -1,800 bp to -1,200 bp and +200 bp to +1,700 bp are significantly important for normal *SVP* expression: the region from -1,800 bp to -1,200 bp is required to enhance *SVP* expression; while deleting the region from +200 bp to +1,700 bp will result in complete loss of *SVP* promoter activity.

5.6 *SVP* autoregulation

Previous study suggested that *SVP* encode two detectable transcripts of about 1.7 kb and 1.3 kb long (Hartmann *et al*., 2000). The levels of both transcripts seemed to remain constant during vegetative growth regardless of photoperiodic conditions. The 1.7 kb transcript was almost absent from inflorescences of plants grown in LD, while the 1.3 kb transcript was still expressed (Hartmann *et al*., 2000). It was suggested that the 1.7 kb transcript represented the functional transcript, while the other was the product of the premature cleavage.

The alternative splicing of *SVP* is quite similar to that of *FCA*, which is another flowering time gene in the autonomous pathway. *FCA* pre-mRNA is alternatively processed, resulting in the formation of four different transcripts (Simpson *et al.,* 2003). Previous study showed that this process involved a negative feedback regulation mediated by *FCA* itself (Simpson *et al.,* 2003). The full length *FCA* protein forms a protein complex with another flowering time gene *FY*, which functions in pre-mRNA 3' end formation and promotes premature cleavage and polyadenylation at a promoter-proximal site within intron 3 of its own pre-mRNA. This results in the production of a non-functional truncated transcript (Simpson *et al.,* 2003). We have also found that *SVP* is directly mediating its down-regulation. Therefore, it is interesting to further study if *SVP* self-regulation is relevant with its alternative splicing through the use of different polyadenylation sites within the *SVP* pre-mRNA in a manner similar to that in *FCA*. Hence, a protein interaction between *SVP* and a RNA 3'

end-processing factor, such as *FY*, would be required for efficient selection of the promoter-proximal polyadenylation site. Mass spectrometry analysis will be useful to verify this model and to identify protein partners of *SVP*.

5.7 ChIP improvement and related techniques

In future ChIP studies, the fixation and immunoprecipitation conditions will be further optimized to remove contaminant molecules such as chloroplast DNA. Also, as non-specific PCR products were found during co-precipitated DNA amplification, an adjustment of PCR annealing temperature during enrichment test is necessary.

In order to localize the *SVP* binding site within *SOC1* and *SVP* genomic sequences, primer pairs would be further designed to bind regions encompassing only around 100 bp near the putative CArG boxes. Quantitative real-time PCR can be performed to detect the spatial enrichment of a specific binding site. The primer pair that shows the most significant enrichment will reveal the exact *SVP* binding site.

Although ChIP is a powerful *in vivo* method to study protein-DNA interaction, it is sometimes difficult to locate where a protein exactly binds *in vivo*. During the fixation step, the precipitated DNA-protein complexes may contain both DNA-protein and protein-protein interactions. Thus, a protein may bind to a genomic sequence via other intermediate proteins. Therefore, further investigation is necessary to confirm the interaction. Kang *et al*. (2002) developed a technique that combines ChIP and *in vivo* footprinting to identify the exact binding region of a transcription factor. Besides,

a computational algorithm has been introduced by Liu *et al.* (2002) that help to pinpoint the interaction site from ChIP-chip data down to the base-pair level. To improve specific enrichment of target sequences among the immunoprecipitated DNA, Weinmann *et al.* (2001) introduced double ChIP method, by which two rounds of immunoprecipitation were performed before obtaining co-precipitated DNA. Furthermore, Barski and Frenkel (2004) developed a novel ChIP Display (CD) strategy, where the enriched sequences were picked up from background noise by simple polyacrylamide gel resolving, thus avoiding microarray and the labour intensive sequencing protocol.

CHAPTER 6

Conclusion

In this project, we characterized *SVP*, in an attempt to localize *SVP* in specific genetic pathways, and identified *in vivo* its direct target genes in the control of flowering time. Firstly, we found that the *SVP* expression can be regulated by the photoperiod and GA pathways, suggesting that *SVP* may act downstream of these two pathways to integrate flowering time signals. Secondly, preliminary results from *SVP* promoter study showed that genomic regions from -1,800 bp to -1,200 bp and +200 bp to +1,700 bp are important for the normal expression of *SVP*. Thirdly, RT-PCR results demonstrated *SVP* delayed flowering through down-regulation of *SOC1* expression. Lastly, ChIP studies provided *in vivo* evidence showing the direct interaction between *SVP* and *SOC1*. It is noteworthy that through the results of RT-PCR and ChIP analysis, it was found that *SVP* can mediate its negative autoregulation (Figure 18).

In this study we show that by mainly responding to endogenous signals from autonomous and GA pathways, SVP plays a crucial role in directly controlling *SOC1* transcription strongly in the shoot apex and moderately in the leaf, while *FT* expression in the leaf is slightly modulated by SVP. Notably, the SVP protein consistently interacts with FLC in the seedlings during vegetative growth, and their function in regulating flowering is mutually dependent. Our findings uncover that SVP is another central flowering repressor and that its interaction with FLC determines the expression of the floral pathway integrators in response to various endogenous and environmental signals.

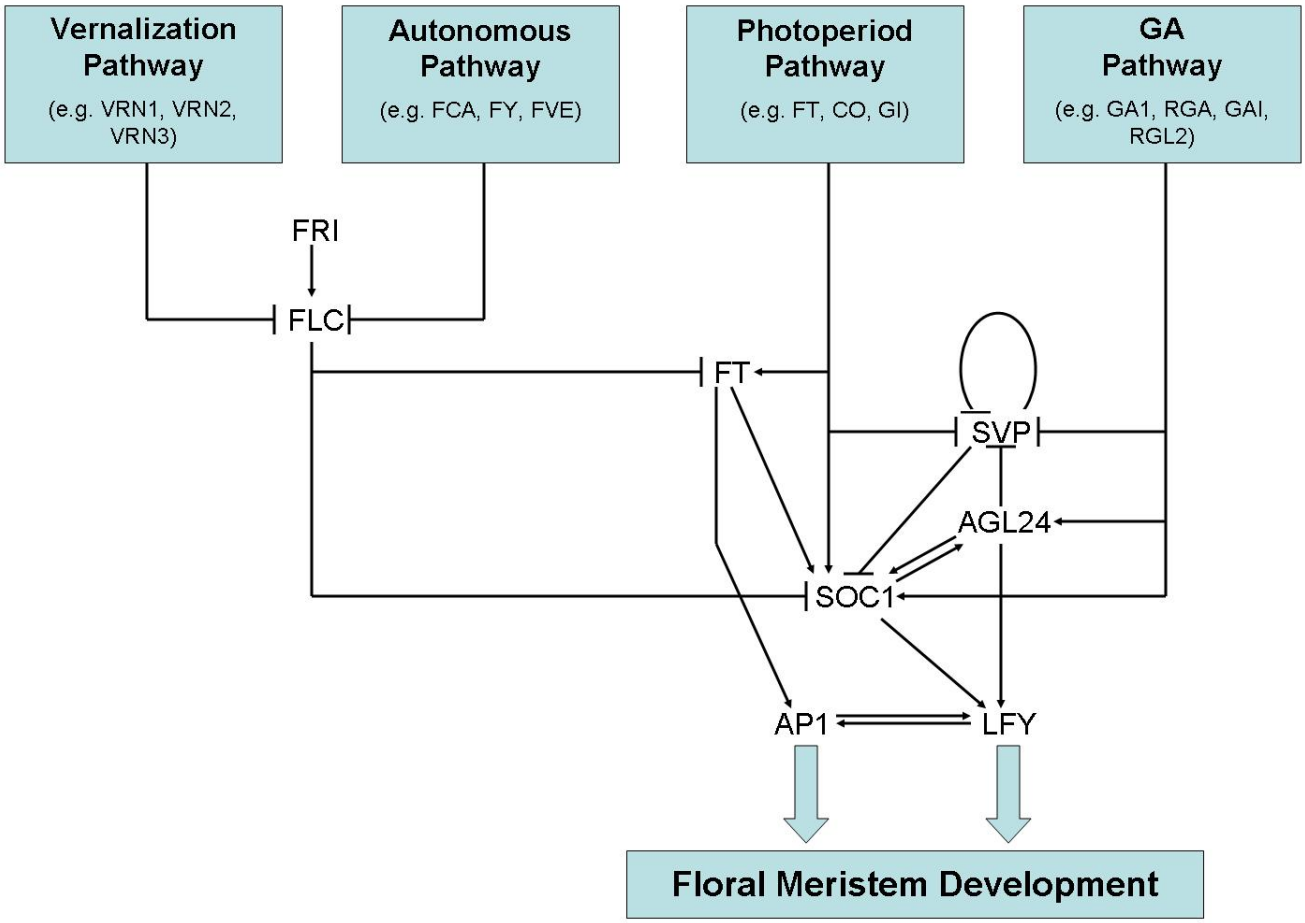

Figure 18. A current model of flowering time control. The four distinct flowering pathways in *Arabidopsis* interact through several key regulators. *SVP*, *FT*, *FLC*, *SOC1*, *AGL24* and *LFY* serve as downstream integrators in the control of flowering time. Arrows indicate promotion while T bars represent repression.

CHAPTER 7

Future Work

A further question aroused from this study is the relationship between *SVP* and *AGL24*. While they are the closest genes among all the 107 MADS-box transcription factors found in *Arabidopsis* (Yu *et al.*, 2002), they exhibit completely opposite function in directly regulating *SOC1* transcription in the meristem (Liu *et al.*, 2008). It is possible that they regulate *SOC1* in a temporal sequence as repression of *SOC1* by SVP occurs at the vegetative phase and gets weaker during floral transition, when promotion of *SOC1* by AGL24 happens (Liu *et al.*, 2008). The expression levels of *SVP* and *AGL24*, which are affected by various flowering genetic pathways, should be one of the essential factors that contribute to the predominance of SVP or AGL24 in the *SOC1* transcription complex. It is noteworthy that *SVP* is genetically epistatic to *AGL24*, because the double mutants *agl24-1 svp-41* show similar flowering time to *svp-41* (Figure 4). This suggests that *AGL24* may act upstream of *SVP*. In wild-type plants *AGL24* expression is upregulated at the shoot apex by *SOC1* during the floral transition (Liu *et al.*, 2008). It is, therefore, tempting to hypothesize that *SOC1* may suppress *SVP* expression via *AGL24*, thus activating its own expression in the meristem in a positive feedback loop.

Previous studies have suggested that FCA that belongs to autonomous pathway interact with the 3'-end RNA-processing factor FY to autoregulate its own expression post-transcriptionally, thus affecting *FLC* expression (Quesada *et al*., 2003; Simpson *et al*., 2003). Interestingly, both *FLC* and *SVP* genomic regions also generate transcript variants (Hartmann *et al*., 2000; unpublished data). This raises the

possibility that post-transcriptional control may play an important role in the control of *FLC* and *SVP* expression and flowering time. We are now further investigating the biological function of various transcripts of *SVP* and its involved regulatory mechanism.

References

Abe M, Kobayashi Y, Yamamoto S, Daimon Y, Yamaguchi A, Ikeda Y, Ichinoki H, Notaguchi M, Goto K, Araki T (2005). FD, a bZIP protein mediating signals from the floral pathway integrator FT at the shoot apex. Science **309:** 1052-1056

Ahmad M, Cashmore AR (1993) HY4 gene of A. thaliana encodes a protein with characteristics of a blue-light photoreceptor. Nature **366:** 162-166

Alvarez-Buylla ER, Liljegren SJ, Pelaz S, Gold SE, Burgeff C, Ditta GS, Vergara-Silva F, Yanofsky MF (2000) MADS-box gene evolution beyond flowers: Expression in pollen, endosperm, guard cells, roots and trichomes. Plant J **24:** 457-466

An H, Roussot C, Suarez-Lopez P, Corbesier L, Vincent C, Pineiro M, Hepworth S, Mouradov A, Justin S, Turnbull C, Coupland G (2004) CONSTANS acts in the phloem to regulate a systemic signal that induces photoperiodic flowering of *Arabidopsis*. Development **131:** 3615-3626

Ayre BG and Turgeon R (2004) Graft transmission of a floral stimulant derived from CONSTANS. Plant Physiol **135:** 2271-2278

Balasubramanian S, Sureshkumar S, Lempe J, Weigel D (2006) Potentinduction of *Arabidopsis thaliana* flowering by elevated growth temperature. PLoS Genet **2:** e106

Bannister AJ, Zegerman P, Patridge JF, Miska EA, Thomas JO, Allshire RC, Kouzarides T (2001) Selective recognition of methylated lysine 9 on histon H3 by the HP1 chromo domain. Nature **410:** 120-124

Baumann E, Lewald J, Saedler H, Schulz B, Wisman E (1998) Successful PCR-based reversed genetic screen using an En-1-mutagenised *Arabidopsis* thaliana population generated via single-seed descent. Theor Appl Genet **97:** 729-734

Baurle I and Dean C (2006) The timing of developmental transitions in plants. Cell **125:** 655-664

Blazquez MA, Green R, Nillson O, Sussman MR, Weigel D (1998) Gibberellins promotes flowering of Arabidopsis by activating the LEAFY promoter. Plant Cell **10:** 791-800

Blazquez MA, Weigel D (2000) Integration of floral inductive signals in *Arabidopsis*.

Nature **404:** 889-892

Borner R, Kampmann G, Chandler J, Gleibner R, Wisman E, Apel K, Melzer S (2000) A MADS domain gene involved in the transition to flowering in *Arabidopsis*. Plant J **24:** 519-599

Bowman JL, Alvarez J, Weigel D, Meyerowitz EM, Smyth DR (1993) Control of flower development in Arabidopsis thalianan by APETALA1 and interacting genes. Development **119:** 721-743

Briggs WR, Beck CF, Cashmore AR, Christie JM, Hughes J (2001) The phototropin family of photoreceptors. Plant Cell **13:** 993-997

Busch MA, Bomblies K, Weigel D (1999) Activation of a floral homeotic gene in *Arabidopsis*. Science **285:** 585-587

Corbesier L, Vincent C, Jang S, Fornara F, Fan QZ, Searle I, Giakountis A, Farrona S, Gissot L, Turnbull C, Coupland G (2007) FT protein movement contributes to long-distance signaling in floral induction of Arabidopsis. Science **316:** 1030-1033

Chandler J, Wilson A, Dean C (1996) *Arabidopsis* mutants showing an altered response to vernalization. Plant J **10:** 637-644

Clough, SJ, Bent AF (1998) Floral dip: a simplified method for Agrobacterium-meidated transformation of *Arabidopsis thaliana*. Plant J **16:** 735-743

de Folter S, Immink RG, Kieffer M, Parenicova L, Henz SR, Weigel D, Busscher M, Kooiker M, Colombo L, Kater MM, Davies B, Angenent GC (2005) Comprehensive interaction map of the *Arabidopsis* MADS Box transcription factors. Plant Cell **17:** 1424-1433

Dill A and Sun T (2001) Synergistic derepression of gibberellin signaling by removing RGA and GAI function in *Arabidopsis thaliana*. Genetics **159:** 777-785

Ferrandiz C, Gu Q, Martienssen R, Yanofsky MF (2000) Redundant regulation of meristem identity and plant architecture by FRUITFULL, APETALA1 and CAULIFLOWER. Development **127:** 725-734

Finkelstein RR, Zeevaart JAD (1994) Gibberellin and abscisic acid biosynthesis and response. In *Arabidopsis*, E.M. Meyerowitz and C.R. Somerville, eds (Cold Spring Harbor, NY: Cold Spring Harbor Laboratory Press), pp. 523–553

Foster TM, Lough TJ, Emerson SJ, Lee RH, Bowman JL, Foster RL, Lucas WJ (2002) A surveillance system regulates selective entry of RNA into the shoot apex. Plant Cell **14:** 1497-1508

Fowler S, Lee K, Onouchi H, Samach A, Richardson K (1999) GIGANTEA: a circadian clock-controlled gene that regulates photoperiodic flowering in *Arabidopsis* and encodes a protein with several possible membrane-spanning domains. EMBO J **18:** 4679-4688

Fujita H, Takemura M, Tani E, Nemoto K, Yokota A, Kohchi T (2003) An *Arabidopsis* MADS-Box Protein, AGL24, is Specifically Bound to and Phosphorylated by Meristematic Receptor-Like Kinase (MRLK). Plant Cell Physiol **44:** 735-742

Gendall AR, Levy YY, Wilson A, Dean C (2001) The VERNALIZATION 2 gene mediates the epigenetic regulation of vernalization in *Arabidopsis*. Cell **107:** 525-35

Gomez-Mena C, Pineiro M, Franco-Zorrilla JM, Salinas J, Coupland G, Martinez-Zapater JM (2001) early bolting in short days: an *Arabidopsis* mutation that causes early flowering and partially suppresses the floral phenotype of *leafy.* Plant Cell **13:** 1011-1024

Guo H, Yang H, Mockler TC, Lin C (1998) Regulation of flowering time by *Arabidopsis* photoreceptors. Science **279**: 1360-1363

Gustafson-Brown C, Savidge B, Yanofsky MF (1994) Regulation of the *Arabidopsis* floral homeotic gene APETALA1. Cell **76:** 131-143

Hanzawa Y, Money T, Bradley D (2005) A single amino acid converts a repressor to an activator of flowering. Proc Natl Acad Sci USA **102:** 7748-7753

Hartmann U, Hohmann S, Nettersheim K, Wisman E, Saedler H, Huijser P (2000) Molecular cloning of SVP: a negative regulator of the floral transition in *Arabidopsis*. Plant J **21:** 351-360

He Y, Michaels SD, Amasino RM (2003) Regulation of flowering time by histone acetylation in *Arabidopsis*. Science **302:** 1751-1754

Helliwell CA, Wood CC, Robertson M, peacock WJ, Dennis DS (2006) The *Arabidopsis* FLC protein interacts directly in vivo with SOC1 and FT chromatin and is a part of a high-molecular-weight protein complex. Plant J **46:** 183-192

Hempel FD, Weigel D, Mandel MA, Ditta G, Zambryski PC, Feldman LJ,

Yanofsky MF (1997) Floral determination and expression of floral regulatory genes in *Arabidopsis*. Development **124:** 3845-53

Hepworth S, Valverde F, Ravenscroft D, Mouradov A, Coupland G (2002) Antagonistic regulation of flowering-time gene SOC1 by CONSTANS and FLC via separate promoter motifs. EMBO J **21:** 4327-4337

Jefferson RA, Kavanagh TA, Bevan MW (1987) GUS fusions: beta-glucuronidase as a sensitive and versatile gene fusion marker in higher plants. EMBO J **6:** 3901-3907

Johnson L, Cao X, Jacobsen S (2002) Interplay between two epigenetic marks. DNA methylation and histone H3 lysine 9 methylation. Curr Biol **12:** 1360-1367

Kardailsky I, Shukla VK, Ahn JH, Dagenais N, Christensen SK, Nguyen JT, Chory J, Harrison MJ, Weigel D (1999) Activation tagging of the floral inducer FT. Science **286:** 1962-1965

Kobayashi Y, Yaka H, Goto K, Iwabuchi M, Araki T (1999) A pair of related genes with antagonistic roles in mediating flowering signals. Science **286:** 1960-1962

Lee H, Suh SS, Park E, Cho E, Ahn JH, Kim SG, Lee JS, Kwon YM, Lee I (2000) The AGAMOUS-LIKE 20 MADS domain protein integrates forla inductive pathways in *Arabidopsis*. Genes Dev **14:** 2366-2376

Lee I, Aukerman MJ, Gore SL, Lohman KN, Michaels SD (1994) Isolation of LUMINIDEPENDENS: A gene involved in the control of flowering time in *Arabidopsis*. Plant Cell **6:** 75-83

Lee JH, Yoo SJ, Park SH, Hwang I, Lee JS, Ahn JH (2007) Role of SVP in the control of flowering time by ambient temperature in *Arabidopsis*. Genes Dev **21:** 397-402

Levy YY, Dean C (1998) The transition to Flowering. Plant Cell **10:** 1973-1989

Levy YY, Mesnage S, Mylne JS, Gendall AR, Dean C (2002) Multiple roles of *Arabidopsis VRN1* in vernalization and flowering time control. Science **297:** 243-246

Liljegren SJ, Gustafson-Brown C, Pinyopich A, Ditta GS, Yanofsky MF (1999) Interactions among APETALA1, LEAFY, and TERMINAL FLOWER1 specify meristem fate. Plant Cell **11:** 1007-1018

Liu C, Zhou J, Bracha-Drori K, Yanovsky S, Ito T, Yu H (2007) Specification of

Arabidopsis floral meristem identity by repressing flowering time genes. Development **134:** 1901-1910

Lin C, Yang H, Guo H, Mockler T, Chen J, Cashmore AR (1998) Enhancement of the blue-light sensitivity of *Arabidopsis* young seedlings by a blue-light receptor *cry2*. Proc Natl Acad Sci USA **95:** 2686-2690

Lohmann JU, Hong RL, Hobe M, Busch MA, Parcy F, Simon R, Weigel D (2001) A molecular link between stem cell regulation and floral patterning in *Arabidopsis*. Cell **105:** 793-803

Israel A, Carlos AB, Jose AJ, Leonor RG, Jose M MZ (2004) Regulation of flowering time by FVE, a retinoblastoma-associated protein. Nat Genet **36:** 162-166

Macknight R, Bancroft I, Page T, Lister C, Schmidt R (1997) FCA, a gene controlling flowering time in *Arabidopsis* encodes a protein containing RNA-binding domains. Cell **89:** 737-745

Macknight R, Duroux M, Laurie R, Dijkwel P, Simpson G, Dean C (2002) Functional significance of the alternative transcript processing of the *Arabidopsis* floral promoter FCA. Plant Cell **14:** 877-888

Mandel MA, Gustafson-Brown C, Savidge B, Yanofsky MF (1992) Molecular characterization of the *Arabidopsis* floral homeotic gene APETALA1. Nature **360:** 273-277

Mart ínez-Zapater JM, CouplandG, Dean C, Koornneef M (1994). The transition to flowering in *Arabidopsis.* In *Arabidopsis*, E.M. Meyerowitz and C.R. Somerville, eds (Cold Spring Harbor, NY: Cold Spring Harbor Laboratory Press), pp. 403–433

Michaels SD, Amasino RM (1999) FLWERING LOCUS C encodes a novel MADS domain protein that acts as a repressor of flowering. Plant Cell **11:** 949-956

Michaels SD, Ditta G, Gustafson-Brown C, Pelaz S, Yanofsky M, Amasino RM (2003) AGL24 acts as a promoter of flowering in *Arabidopsis* and is positively regulated by vernalization. Plant J **33:** 863-874

Mizukami Y, Ma H (1992) Ectopic expression of the floral homeotic gene *AGAMOUS* in transgenic *Arabidopsis* plants alters floral organ identity. Cell **71:** 119-131

Moon J, Suh SS, Lee H, Choi KR, Hong CB, Paek NC, Kim SG, Lee I (2003) The

SOC1 MADS-box gene integrates vernalization and gibberellin signals for flowering in *Arabidopsis*. Plant J **35:** 613-623

Mouradov A, Cremer F, Coupland G (2002) Control of flowering time: interacting pathways as a basis for diversity. Plant Cell **14:** S111-130

Mylne JS, Barrett L, Tessadori F, Mesnage S, Jacobsen SE, Fransz P, Dean C (2006) *LHP1*, the *Arabidopsis* homologue of *HETEROCHROMATIN PROTEIN1* is required for epigenetic silencing of *FLC*. Proc. Natl. Acad. Sci. USA **103:** 5012-5017

Nillson O, Lee I, Blazquez MA, Weigel D (1998) Flowering-time genes modulate the response to LEAFY activity. Genetics **150:** 403-410

Parcy F (2005) Flowering: a time for integration. Int J Dev Biol **49:** 585-593

Parcy F, Nilsson O, Bush MA, Lee I, Weigel D (1998) A genetic framework for floral patterning. Nature **395:** 561-566

Parenicova L, de Folter S, Kieffer M, Horner DS, Favalli C, Busscher J, Cook HE, Ingram RM, Kater MM, Davies B, Angenent GC, Colombo L(2003) Molecular and Phylogenetic analyses of the complete MADS-box transcription factor family in *Arabidopsis*: New openings to the MADS world. Plant Cell **15:** 1538-1551

Park DH, Somers DE, Kim YS, Choy YH, Lim HK (1999) Control of circadian rhythms and photoperiodic flowering by the *Arabidopsis* GIGANTEA gene. Science **285:** 1579-1582

Pfaffl, MW (2001). A new mathematical model for relative quantification in real-time RT-PCR. Nucleic Acids Res **29:** e45

Pineiro M, Gomez-Mena C, Schaffer R, Martinez-Zapater JM, Coupland G (2003) EARLY BOLTING IN SHORT DAYS is related to chromatin remodeling factors and regulates flowering in Arabidopsis by repressing FT. Plant Cell **15:** 1552-1562

Purugganan MD, Suddith JI (1998) Molecular population genetics of the *Arabidopsis* CAULIFLOWER regulatory gene: Nonneutral evolution and naturally occurring variation in floral homeotic function. Proc Natl Acad Sci USA **95:** 8130-8134

Putterill J, Robson F, Lee K, Simon R, Coupland G (1995) The CONSTANS gene of *Arabidopsis* promoters flowering and encodes a protein showing similarities

to zinc finger transcription factors .Cell **80:** 847-857

Quail PH, Briggs WR, Chory J, Hangarter R, Harberd NP, Kendrick RE, Koorneef M, Parks B, Sharrock RA, Schäfer E, Thompson WF, Whitelam GC (1994) Spotlight on phytochrome nomenclature. Plant Cell **6**: 468-471

Ratcliffe OJ, Amaya I ,Vincent CA, Rothstein S, Carpenter R, Coen ES, Bradley DJ (1998) A common mechanism controls the life cycle and architecture of plants. Development **125:** 1609-1615

Riechmann JL, Krizek BA, Meyerowitz EM (1996b) Dimerization specificity of *Arabidopsis* MADS domain homeotic proteins APETALA1, APETALA3, PISTILLATA, and AGAMOUS. Proc Natl Acad Sci USA **93:** 4793-4798

Ruiz-Garcia L, Madueno F, Wilkinson M, Haughn G, Salinas J, Martinez-Zapater JM (1997) Different roles of flowering-time genes in the activation of floral initiation genes in *Arabidopsis*. Plant Cell **9:** 1921-1934

Samach A, Onouchi H, Gold SE, Ditta GS, Schwarz-Sommer Z, Yanofsky MF, Coupland G (2000) Distinct roles of CONSTANS target genes in reproductive development of *Arabidopsis*. Science **288:** 1613-1616

Schmid M, Uhlenhaut NH, Godard F, Demar M, Bressan R, Weigel D, Lohmann JU (2003) Dissection of floral inducation pathways using glocal expression analysis. Development **130:** 6001-6012

Schomburg FM, Patton DA, Meinke DW, Amasino RM (2001) FPA, a gene involved in floral induction in *Arabidopsis*, encodes a protein containing RNA-recognition motifs. Plant Cell **13:** 1427-1436

Schonrock N, Exner V, Probst A, Gruissem W, Hennig L (2006). Functional genomic analysis of CAF-1 mutants in *Arabidopsis thaliana*. J Biol Chem **281:** 9560-9568

Searle I, He Y, Truck F, Vincent C, Fornara F, Krober S, Amasino RA , Coupland G (2006) The transcription factor FLC confers a flowering response to vernalization by repressing meristem competence and systemic signaling in *Arabidopsis*. Genes Dev 20: 898-912

Sessions A, Yanofsky MF, Weigel D (2000) Cell-cell signaling and movement by the floral transcription factors LEAFY and APETALA1. Science **289:** 779-782

Sheldon CC, Finnegan EJ, Dennis ES, Peacock WJ (2006) Quantitative effects of vernalization on FLC and SOC1 expression. Plant J **45:** 871-883

Simpson GG, Dean C (2002) *Arabidopsis,* the Rosseta Stone of Flowering time? Science **296:** 285-289

Sung S, Amasino RM (2004) Vernalization in *Arabidopsis thaliana* is mediated by the PHD finger protein VIN3. Nature **427:** 159-164

Takada S, Goto K (2003) TERMINAL FLOWER2, an *Arabidopsis* homolog of HETEROCHROMATIN PROTEIN1, counteracts the activation of FLOWERING LOCUS T by CONSTANS in the vascular tissues of leaves to regulate flowering time. Plant Cell **15:** 2856-2865

Thomas B, Vince-Prue D (1997) Photoperiodism in Plants, 2nd ed. (San Diego, CA: Academic Press)

Wagner D, Sablowski RW, Meyerowitz EM (1999) Transcriptional activation of APETALA1 by LEAFY. Science **285:** 582-584

Wang H, Tang W, Zhu C, Perry SE (2002) A chromatin immunoprecipitation (ChIP) approach to isolate genes regulated by AGL15, a MADS domain protein that preferentially accumulates in embryos. Plant J **32:** 831-843

Weigel D, Alverez J, Smyth DR, Yanofsky MF, Meyerowitz EM (1992) LEAFY controls floral meristem identity in Arabidopsis Cell 69: 843-859

Weigel D and Meyerowitz EM (1993) LEAFY controls meristem identity in *Arabidopsis*. In Cellular Communications in Plants, Amasino R, ed (New York: Plenum Press), pp. 115-22

William DA, Su Y, Smith MR, Lu M, Baldwin DA, Wagner D (2004) Genomic identification of direct target genes of LEAFY. Proc Natl Acad Sci USA **101:** 1775-1780

Wilson RN, Heckman JW, Somerville CR (1992) Gibberellin is required for flowering in *Arabidopsis thaliana* under short days. Plant Physiol **100:** 403-408

Valverde F, Mouradov A, Soppe W, Ravenscroft D, Samach A, Coupland G (2004) Photoreceptor regulation of CONSTANS protein in photoperiodic flowering. Science **303:** 1003-1006

Yoo KS, Chung KS, Kim J, Lee JH, Hong SM, Yoo SJ, Yoo SY, Lee JS, A JH (2005) CONSTANS Activates SUPPRESSOR OF OVEREXPRESSION OF CONSTANS 1 through FLOWERING LOCUS T to promote Flowering in *Arabidopsis*. Plant Physiol **139:** 770-778

Yu H, Xu Y, Tan EL, Kumar PP (2002) AGAMOUS-LIKE 24, a dosage-dependent mediator of the flowering signals. Proc Natl Acad Sci USA **99:** 16336-16341

Yu H, Ito T, Wellmer F, Meyerowitz EM (2004) Repression of AGAMOUS-LIKE 24 is a crucial step in promoting flower development. Nat Genet **36:** 157-161

Yushibumi Komeda (2004) Genetic Regulations of Time to Flower in *Arabidopsis THALIANA*. Annu Rev Plant Biol **55:** 521-535

Zhang H and van Nocker S (2002) The VERNALIZATION 4 gene encodes a novel regulator of FLOWERING LOCUS C. Plant J **31:** 663-667

Zuo J, Niu QW, Cha NH (2000) Technical advance: An estrogen receptor-based transactivator XVE mediates highly inducible gene expression in transgenic plants. Plant J **24:** 265-273